

# Separation of solid-liquid and liquid-liquid phases using dielectrophoresis

Fei Du

Center for Environmental Research and Sustainable Technology  
Univeristy of Bremen

A thesis submitted for the degree of

*Dr. rer. nat.*

September 2010



Diese Arbeit entstand in der Zeit von Oktober 2004 bis August 2010 im Zentrum für Umweltforschung und nachhaltige Technologien der Universität Bremen unter der Leitung von Prof. Dr.-Ing Jorg Thöming.

Eingereicht am: 25.09.2010

1. Supervisor: Prof. Dr. habil. Peter J. Plath
2. Supervisor: Prof. Dr.-Ing Jorg Thöming
3. Supervisor: Dr. rer. nat. Michael Baune

## Zusammenfassung

Der Einfluss von elektrischen Feldern auf den Partikeltransport ist bereits seit vielen Jahren Gegenstand der Forschung. Speziell die Bewegung von suspendierten neutralen Partikeln unter dem Einfluss eines inhomogenen elektrischen Feldes wird als Dielektrophorese (DEP) bezeichnet und wurde erstmals von Pohl in den 70er Jahren beschrieben. Bisher wurde dieser Effekt hauptsächlich ausgenutzt um Bio-Partikel im Mikro- und Submikrometermaßstab zu trennen oder zu manipulieren und fokussieren. Allerdings konzentrieren sich nahezu alle DEP-Anwendungen auf Partikel im Mikro- und Submikrometermaßstab und Flussraten von wenigen Millilitern pro Minute. Diese Systeme sind von großem analytischem Interesse, können aber nicht einfach auf Trenntechnische Fragestellungen mit Durchsätzen von mehreren Litern oder sogar Kubikmetern pro Stunde übertragen werden. Dass dieses aber prinzipiell möglich ist, konnte durch diese Dissertation erstmalig aufgezeigt werden.

In der vorliegenden Arbeit wurden die Grundlagen des DEP-Mechanismus zusammen mit seinen Nebeneffekten und seine Anwendbarkeit für produktionstechnische Verfahren untersucht. Es wurde ein Modell entwickelt, welches den elektrothermischen Effekt (ETE) berücksichtigt, und unter Einbeziehung der dielektrophoretischen Kraft, die auf ein Partikel einwirkt, konnte die Partikelbewegung berechnet und durch Experimente verifizieren werden. Hierbei hat sich auch gezeigt, dass bei Elektrodenabständen größer 1mm der ETE Effekt dominiert und daraus eine signifikante konvektive Strömung resultiert, die bei anwendungsbezogenen Prozessen berücksichtigt werden muss.

Als Fallbeispiel im Litermaßstab wurde ein Verfahren entwickelt, mit dem die Abtrennung von sehr dünnen Goldpartikeln aus einem Mineralgemisch realisiert werden konnte. Hierbei wurde der Effekt ausgenutzt, dass unter bestimmten Bedingungen Partikel im inhomogenen elektrischen Feld dazu neigen, Ketten zu bilden. Mit diesem Verfahren konnte eine Anreicherung von Goldpartikeln auf 88% erreicht werden.

Als ein weiteres Beispiel wurde die Intensivierung der Cross-Flow Filtration im Labormaßstab unter dem Einfluss eines elektrischen Feldes experimentell untersucht. Es konnte gezeigt werden, dass der DEP Effekt eine Verdoppelung und eine gepulste Spannung sogar eine Verdreifachung der Membran-Standzeit ermöglichen kann.

## Abstract

Over 3 decades after dielectrophoresis (DEP) was explored and defined, it has already been successfully applied in separating, trapping, and handling bioparticles in micro and sub-micro scale biotechnology. However, nearly all of DEP applications are concentrated on the analysis and manipulation of particles in sub-micron and micron scaled systems with flow rates below milliliters per minute. So far, none is known in process engineering for DEP in a scaled up application at flow rates of liters or even cubic meters per minute. The research described in this Ph D thesis is the first that attempts to scale up DEP application. With the research results described in this thesis, the feasibility of the DEP technique application in separation is verified. The proved high selectivity and controllability of DEP technique in separation application grand DEP a very promising prospect in separating, trapping, handling and manipulating particles.

The whole thesis work was implemented with three main steps, basic research of DEP mechanism and its side-effect and constrains, as a proof a principle gold particle fractionation using DEP, and a lab-scaled technical application of DEP in intensifying cross-flow membrane filtration, based on four papers.

Paper No. 1 describes how the electrothermal effect influences the particle's DEP effect. The dependence of particles motions in a DEP system with a side effect of electrothermal on particle size, characteristic length of electrode configuration, medium properties, voltage and particle properties were investigated. A new model was developed to explain the interdependence of parameters and simulated with experimental tests, which employed a dc spherical electric field with Polyethylene (PE) particle and water droplet in pure water suspension.

Paper No. 2 presents a proof of DEP application in particles fractionation. In this research work, DEP was for the first time applied to fractionate ultra-thin gold particle from a mineral mixture to reach a high separation efficiency (88%) with a zero environmental risk in an ac cylindrical electric field (32 kV/m at 200 kHz). The dependence of separation efficiency on the voltage input was investigated and evaluated. The influence from the joule heating during the separation process was observed, discussed and reduced with a recirculation of liquid medium. High-pass-filter effect was found out and taken into account in designing the separation process.

Paper No. 3 described a lab-scaled technical application of DEP in separation process. In this paper, DEP was applied for the first time in cross-flow membrane filtration process to enhance the membrane performance and service life. A traction of clay particles away from

the membrane by DEP was realized to alleviate particle fouling and concentration polarization, thereby intensifying the performance of the filtration process. Due to high-pass-filter effect, a bare grid electrode and an insulated stainless steel plate on the opposite side with a distance of 1 mm was applied to produce inhomogeneous electric field with a magnitude of 160 V/mm at 200 kHz. An optimized DEP intensified cross-flow membrane filtration process demonstrated 3.3 times longer working time for membrane to have a 50% permeate flux of the initial with an energy consumption of 31.3 kJ.

Paper No. 4 overviews the theory of DEP and its potential applications with case studies, as well as the influences from side-effect (electrothermal), and constraint (high-pass-filter). In this paper, a scale-bridging approach was point out for a potential solution to the dilemma of scaling up DEP applications due to the huge gap between particle size and characteristic length of electrode configuration.

With the theoretical and experimental investigations in this thesis work, the feasibility of DEP application in separation of solid-liquid and liquid-liquid phases and the possibility of scaling up DEP applications are demonstrated.

Contents

<b>Zusammenfassung</b>	<b>I</b>
<b>Abstract</b>	<b>II</b>
<b>1. Introduction and Problems</b>	<b>1</b>
<b>1.1. Introduction</b>	<b>1</b>
<b>1.1.1. Motivation</b>	<b>1</b>
<b>1.1.2. Mechanism of DEP</b>	<b>1</b>
<b>1.1.3. Side effect – Electrothermal effect</b>	<b>4</b>
<b>1.1.4. High-pass-filter effect</b>	<b>6</b>
<b>1.2. Problems</b>	<b>7</b>
<b>2. Aims and approach</b>	<b>8</b>
<b>2.1. Aims</b>	<b>8</b>
<b>2.2. Approach</b>	<b>8</b>
<b>3. Publications</b>	<b>10</b>
<b>3.1. Paper No. 1</b>	<b>10</b>
<b>3.2. Paper No. 2</b>	<b>26</b>
<b>3.3. Paper No. 3</b>	<b>39</b>
<b>3.4. Paper No. 4</b>	<b>60</b>
<b>4. Summarized discussion</b>	<b>76</b>
<b>5. Outlook</b>	<b>80</b>
<b>6. Reference</b>	<b>83</b>
<b>7. Acknowledgement</b>	<b>87</b>
<b>8. Appendix</b>	<b>88</b>

<b>8.1. Paper No. 5</b>	<b>88</b>
<b>8.2. Curriculum Vitae</b>	<b>98</b>

## 1. Introduction and Problems

### 1.1. Introduction

#### 1.1.1. Motivation

Dielectrophoresis (DEP) is a technique to manipulate suspended neutral and/or charged particles in inhomogeneous electric field by dielectric polarization. As it was termed by Pohl, dielectro- means the dielectric polarization, and -phoresis means swim in Greek. The potential high selectivity and controllability enables DEP electrically controllably to trap, focus, separate, fractionate, translate, concentrate and characterize suspended particles in inhomogeneous electric field [Pohl 1978, Morgan & Green 2002, Gascoyne & Vykoukal 2002, Hughes 2002, Baune et al. 2008]. Due to the dependence of dielectric properties of a matter on its structure and composition, DEP accesses a much richer set of particle properties than electrophoresis (EP) [Gascoyne & Vykoukal 2002]. In addition, DEP effects can be easily controlled by the properties of electric field, which provides a very proper interface for electronics to control DEP effects. DEP is particularly well suited to applications at the small scales of microfluidic devices, and has already been recognized to offer many advantages in separation technology for laboratories-on-a-chip [Hughes 2002]. DEP can be easily and directly interfaced to conventional electronics and amenable to integrated by inexpensive fabrication methods, therefore, it reduces or eliminates the requirements for complex, expensive and potentially unreliable sample manipulation methods involving microfabricated mechanical pumps and valves [Gascoyne & Vykoukal 2002]. DEP technique has already been developed and applied mainly in micron and sub-micron scale biotechnology, although the potential for a large scaled DEP application in other industries is quite huge. The underdevelopment of large scaled DEP application for industries together with the high selectivity and controllability of DEP effect, stimulates the author to investigate DEP from its fundamental mechanism to applications.

#### 1.1.2. Mechanism of DEP

Dielectrophoresis (DEP) was firstly explored, termed and defined by Pohl in 1970s, as a translational motion of suspended neutral particle caused by dielectric polarization in an inhomogeneous electric field [Pohl 1978]. As depicted in the definition above, the effect of DEP is a motion of suspended particle superimposed by inhomogeneous electric field due to dielectric polarization. Any particle suspended in an electric field is polarized. The polarization of particles (e.g. spherical particles) with free charges on the interface presents a deformation of double layers of free charges, as shown in Figure 1 (a). Differently, to form induced dipoles by moving charges bound within the dielectrics at short distances is the



polarization of a dielectric particle under the application of an electric field (Figure 1 (b)) [Baune et al. 2008]. With the polarization of particles, dipole moment,  $P$ , is induced and is proportional to the magnitude of local electric field [Morgan & Green 2002].

$$P = \alpha E \quad (1)$$

where,  $\alpha$  is polarizability, which is a measure of the ability of a material to respond to a field (polarize), also a measure of the ability of a material to distribute charges at interface.  $E$  is the local electric field in the vicinity of the dipole [Morgan & Green 2002].

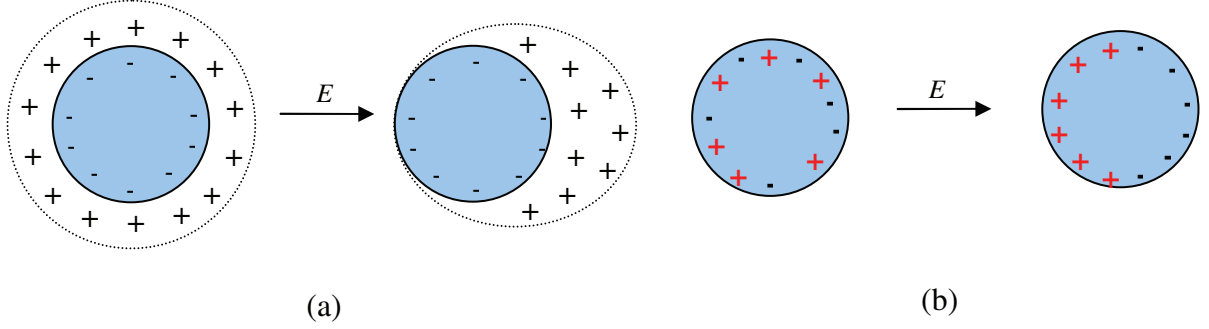


Figure 1, Polarization mechanisms of particle with free charges on interface (a) and dielectric particle (b) in a uniform electric field [Baune et al. 2008].

If the electric field is nonuniform, the local electric field and resulting forces on both sides of the particle are different, thereby a net force arising. This force is termed to be the dielectrophoretic force  $F_{DEP}$  and is given by [Baune et al. 2008],

$$F_{DEP} = (P \bullet \nabla)E \quad (2)$$

The dielectrophoretic force, as presented in Eq. 2, is dependent upon the dipole moment and the electric field. If the electric field is uniform, no DEP force exists.

When the particle is suspended in a dielectric medium and superimposed by an inhomogeneous electric field, the induced polarization refers to the effective dipole moment or induced dipole moment. The effective dipole moment is dependent upon the properties of both particle and the suspending medium, as well as the frequency of the electric field [Morgan & Green 2002]. As an example, this effective dipole moment of a spherical particle with radius  $a$  suspended in a medium is given [Morgan & Green 2002],

$$P = \frac{4}{3} \pi a^3 \tilde{\alpha} E \quad (3)$$

$$\tilde{\alpha} = 3\epsilon_M \left( \frac{\tilde{\epsilon}_P - \tilde{\epsilon}_M}{\tilde{\epsilon}_P + 2\tilde{\epsilon}_M} \right) \quad (4)$$

where,  $\tilde{\alpha}$  is effective polarizability, which is a function of permittivities of particle and medium  $\tilde{\epsilon}_P$  and  $\tilde{\epsilon}_M$  (the subscripts P and M represent particle and medium respectively).

Both permittivities of particle and medium are dependent upon the frequency ( $f$ ) of applied electric field, and can be expressed to be  $\tilde{\epsilon} = \epsilon - \frac{j\sigma}{\omega}$  ( $\epsilon$  is dielectric constant and  $\sigma$  is conductivity) with  $j = \sqrt{-1}$  and  $\omega = 2\pi f$ . This frequency dependency of effective polarizability can be described by the Clausius-Mossotti factor  $\tilde{K}$  [Morgan & Green 2002],

$$\tilde{K} = \frac{\tilde{\epsilon}_P - \tilde{\epsilon}_M}{\tilde{\epsilon}_P + 2\tilde{\epsilon}_M} \quad (5)$$

This Clausius-Mossotti factor was firstly derived by Pohl [Pohl 1978], and recently by Lorrain et al. [Morgan & Green 2002], using extrapolation for solving the potential inside and outside a dielectric sphere with boundary conditions based on Gauss's law and the divergence of electric flux density equal to the free volume charge density [Morgan & Green 2002]. It describes a relaxation in the effective permittivity (real part) or polarizability of the particle with a relaxation time of (imaginary part),

$$\tau_{MW} = \frac{\epsilon_P + 2\epsilon_M}{\sigma_P + 2\sigma_M} \quad (6)$$

where  $\tau_{MW}$  is the inverse of the angular frequency  $\omega_{MW}$ , which is often referred to as the Maxwell-Wagner relaxation frequency, since the dispersion in the dipole moment is caused by the interfacial polarization [Morgan & Green 2002], which means that the resulted separation of charges occurs in the inner dielectric boundary layers or re-distribution of surface charges on the interface.

Hence the dielectrophoretic force can be expressed by,

$$F_{DEP} = 4\pi a^3 \epsilon_0 \epsilon_M \operatorname{re}[\tilde{K}] (E \cdot \nabla) E \quad (7)$$

where  $\epsilon_0$  is the permittivity of free space with the value of  $8.854 \times 10^{-12} \text{ F m}^{-1}$ ,  $\operatorname{re}[\tilde{K}]$  is real part of Clausius-Mossotti factor. As shown in the Eq. 7, the direction of dielectrophoretic force on a suspended spherical particle in an inhomogeneous electric field is dependent on the real part of Clausius-Mossotti factor, i.e. the permittivities of particle and medium and the frequency of applied electric field. In a certain electric field (with a certain frequency), when the permittivity of particle is higher than that of suspending medium (a positive value of real part of Clausius-Mossotti factor), the direction of dielectrophoretic force on the particle is along the direction of electric field gradient, which directs from lower electric field to higher electric field. In this case, the particle is trended to be moved towards higher electric field region, presenting positive DEP effect (pDEP), as presented in Figure 2 (a). Inversely, when the real part of Clausius-Mossotti factor is negative, i.e. the permittivity of particle is lower

than that of suspending medium, the dielectrophoretic force directs oppositely to the direction of electric field gradient, which is from higher electric field to lower electric field. Therefore, the dielectrophoretic force can move the particle towards the lower electric field region, presenting negative DEP effect (nDEP), as presented in Figure 2 (b).

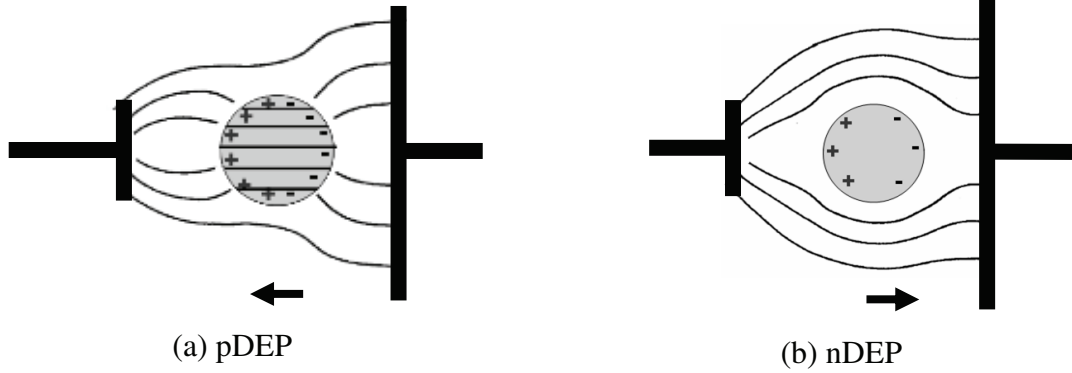


Figure 2, Two different DEP effects, positive DEP (a) and negative DEP (b).

The particle dielectric motion velocity,  $v_{DEP}$  can be given by balancing DEP force with the drag force  $F_{Drag}$  [Pohl 1978],

$$F_{DEP} = -F_{Drag} = 6\pi\eta_M a v_{DEP} \quad (8)$$

where,  $\eta_M$  is dynamic viscosity of medium. Therefore, the dielectric velocity of a spherical particle is presented as,

$$v_{DEP} = \frac{2a^2 \epsilon_0 \epsilon_M \text{re}[\tilde{K}](E \cdot \nabla)E}{3\eta_M} \quad (9)$$

In this equation, the system is assumed to be steady, the medium is assumed to be static and the Reynolds number is assumed to be low enough to remain the motion of particle in the Stokes-regime. Hence, DEP velocity is dependent upon the parameters of electric and dielectric properties of particle and medium, the particle geometry, electric field and the viscosity of medium. Besides the dependency of motion direction on the real part of Clausius-Mossotti factor, the radius of particle and the electric field play more important role in determining the magnitude of particle motion.

In comparison, the motion caused by electrophoresis  $v_{EP}$  is dependent upon the zeta-potential  $\zeta$  (the electrokinetic potential in colloidal system, which is the potential drop across diffuse double layer), electric field, electric property of medium and the fluid property of medium, as shown in Eq. 10,

$$v_{EP} = \frac{\epsilon_0 \epsilon_M \zeta E}{\eta_M} \quad (10)$$

### 1.1.3. Side effect – Electrothermal effect

The joule heating generated by the high electric field strength, always applied in DEP systems, forms temperature field due to the energy dissipation of internal friction on the medium that depends on the boundary conditions within the system, thus initiating fluid flow [Du et al. 2009]. The induced joule heating drives the fluid to flow. The fluid flow caused by joule heating is termed to be electrothermal effect (ETE). Two types of electrothermal effects, electrothermal flow (EF) and electrothermal induced buoyancy (EB), often occur simultaneously in DEP system due to different properties variation on the fluid [Baune et al. 2008];

$$\text{ETE} = \text{EF} + \text{EB} \quad (11)$$

In a considered system, the ETE gives rise to electrical forces induced by the variation in the conductivity and permittivity of the suspending medium [Castellanos et al. 2003]. The electrothermal flow is especially dominant when microelectrodes and microchannels are used, i.e. for a characteristic length below 1 mm [Du et al. 2007]. With the assumption of negligible electrode polarization due to high enough frequency, the fluid flow velocity generated by the electrothermal flow can be given to be [Castellanos et al. 2003],

$$v_{Max} = 5.28 \times 10^{-4} \frac{|M| \epsilon_M \sigma_M U^4}{T k \eta_M l} \quad (12)$$

$$|M| = \frac{\left(\frac{T}{\sigma_M}\right)\left(\frac{\partial \sigma_M}{\partial T}\right) - \left(\frac{T}{\epsilon_M}\right)\left(\frac{\partial \epsilon_M}{\partial T}\right)}{1 + \left(\frac{\omega \epsilon_M}{\sigma_M}\right)^2} + \frac{1}{2} \frac{T}{\epsilon_M} \frac{\partial \epsilon_M}{\partial T} \quad (13)$$

where  $v_{Max}$  is the fluid flow caused by electrothermal effect,  $|M|$  is a dimensionless factor (between 0.6 and 6.6 when temperature is 300 K) [Castellanos et al. 2003],  $T$  is temperature,  $U$  is the voltage,  $k$  is the thermal conductivity of the medium,  $l$  is the characteristic length of the electrode configuration. From both equations 12 and 13, the fluid flow induced by electrothermal is a function of voltage applied in the system, the characteristic length of the electrode configuration, temperature of the operation, the frequency of the electric field as well as electric, thermal and hydrodynamic properties of fluid.

When scaling up the process from micron to millimeter scale, i.e. with increasing the geometry ( $l$ ) of electrode setup, the power of joule heating increases, since joule heating is generated on the electrodes boundaries and more electric power is applied in a scaled-up DEP system. Additionally, the variation of permittivity and conductivity is much smaller compared to such largely increased magnitude of the geometry of electrode. Hence, when the order of

magnitude of the system's characteristic length is above 1 mm, the buoyancy due to joule heating always dominates the fluid flow [Castellanos et al. 2003]. The gravitational body force (meaning a force acting throughout the volume of a body) on a fluid generated by a temperature field is due to the local density change caused by the temperature difference. Hence the buoyancy force can be expressed to be [Du et al. 2007],

$$f_B = \frac{\partial \rho_M}{\partial T} \Delta T g \quad (14)$$

where  $f_B$  is the buoyancy volume force,  $\rho_M$  is the density of medium and  $g$  is the gravitational acceleration.

The fluid flow  $u$  induced by buoyancy force can be given, by balancing the buoyancy force and drag force [Du et al. 2007],

$$u = U \sqrt{\frac{\alpha g l^3}{V C_P \eta_M R}} \quad (15)$$

where  $\alpha$  is thermal volume expansion coefficient,  $V$  is volume of medium,  $C_P$  is the specific heat capacity of the medium,  $R$  is the electrical resistance of the whole system. Considering DEP and electrothermal effect (ETE) on a suspended particle, Eqs. 9 and 15 can be combined and the velocity  $v_{DEP}$  of the particles' motion can be expressed as [Du et al. 2007],

$$v_{DEP} = \frac{2a^2 \epsilon_0 \epsilon_M \text{re}[\tilde{K}]}{3\eta_M} (E \cdot \nabla) E \pm U \sqrt{\frac{\alpha g l^3}{V C_P \eta_M R}} \quad (16)$$

In this equation, the first term on the right side represents the motion caused by DEP effects, while magnitude and algebraic signs of the second term represent the speed and the direction of the fluid respectively [Du et al. 2007].

In general, the fluid flow caused by joule heating does influence the dielectrophoretic effect and always exists in a DEP system in which very strong electric field is employed. However, in most cases the electrothermal effect is not dominant compared to the DEP, it is therefore a side effect.

#### 1.1.4. High-pass-filter effect

Due to the very high electric field strength always applied in DEP systems, the electrical insulation of electrodes is necessary to avoid short circuit and electrochemical reaction on electrodes (electrode fouling), especially when a medium is used that shows electrolyte characteristics (like aqueous solutions with high electric conductivity) or contains such an electrolyte in the case of emulsion. The application of insulation causes an effect, which presents a reduced or even no DEP effect due to decreased electric field strength as the

frequency is lower than a critical value [Eow et al. 2001]. In some oil/water demulsification investigations using ac electric field, it was demonstrated that such an effect was dependent upon the properties and thickness of the insulation material [Eow et al. 2001]. It was also suggested that the effect was caused by the Maxwell-Wagner voltage decay, although some researchers pointed out that the sole theory can not fully explained the effect [Eow et al. 2001]. A high-pass-filter effect mechanism was developed and could be applied to explain such an effect perfectly [Baune et al. 2008, Du et al. 2008] as shown in the next Chapters 3.2-3.4.

## 1.2. Problems

In every DEP system, the DEP effect is not the sole drive of particle's movement. The thermo-driven effects, e.g. Brownian motion and electrothermal effect, always occur in a DEP system. The Brownian effect, which is inversely proportional to particle radius, is negligible when the particle is large enough (larger than 1  $\mu\text{m}$ ) [Baune et al. 2008]. However, the electrothermal effect, which is a fluid flow driven by temperature gradient due to high electric field strength, always exists and influence particles motion [Du et al. 2009]. The thermo-driven side effects influence on both particle's motion direction and magnitude. Besides this, in order to reduce the risk of short-circuit and electric shock and avoid electrochemical reaction on the electrodes, the insulation film is applied when a high voltage is applied in a DEP system. The insulation material together with medium and electrode configuration forms a typical high-pass filter effect. This high-pass-filter effect reduces both the DEP function scope and the DEP effect due to the limited DEP functional frequency spectrum. Further, the main reason that the DEP technique can not be scaled up for industrial application (with a volume flow over liter per minute) is the huge gap between the particle size and electrode distance of the DEP system, which augments with the increase of volume flow.

## 2. Aims and approach

### 2.1. Aims

The potentially high selectivity and controllability of DEP provide this technique a huge potential and very promising prospect in the application of separating and manipulating particles. However, the side-effect, constraint of DEP application and the dilemma in scaling up DEP system in application obstruct the DEP in much wider fields and larger scaled applications. Therefore, a deep understanding of the mechanism of DEP is very crucial.

This Ph D work is aimed to theoretically and experimentally investigate DEP effect and side effects for a better and deeper understanding of the mechanism of DEP. Based on the basic research of DEP mechanism, the DEP effect is tested to validate the feasibility of its application in separation process. With the proof of the DEP principle, the possibility of scaling-up DEP applications in separating and manipulating particles is investigated with different case-studies.

### 2.2. Approach

Three main steps, basic research of DEP effect and proof of DEP principle in application as well as an investigation of DEP application, were planned to fulfill the aims of this Ph D work.

It started with the basic research of DEP effect by modeling and simulating particles motion and investigating the influences from the side-effect (electrothermal) [Du et al. 2007] and the constraint (high-pass-filter effect) [Baune et al. 2008]. As presented in the definition of DEP, the DEP effect is a translational motion of particle suspended in medium caused by dielectric polarization in an inhomogeneous electric field. In order to understand the DEP effect better and more deeply, different particle suspensions (e.g. polyethylene particle in silicone oil, and water droplet in silicone oil) were tested using a typical spherical electrode configuration [Du et al. 2007]. In such a DEP system, the particles performed two different DEP effects, nDEP and pDEP. By measuring particles' motions in such a system with different parameters such as voltage and particle size, the DEP effect and its side-effect, electrothermal effect, could be modeled and simulated [Du et al. 2007]. In addition, the high-pass-filter effect limits the DEP effect by both reducing the electric field strength and the DEP working spectrum. The constraint of the high-pass-filter effect can be simulated to investigate the influences from two important parameters, thickness of insulation material and the electrical properties of the insulation material [Baune et al. 2008].

As a proof of DEP principle in the application of separation processes, two lab-scaled separation processes are investigated, which are dielectrophoretic gold particle fractionation

[Du et al. 2008] and enhancement of sedimentation using DEP [Baune et al. 2008]. In the case of dielectrophoretic gold particle fractionation, the gold particle is aimed to be fractionated from a raw mineral mixture due to different DEP effects (gold particle presents positive DEP and others present negative DEP). The opposite motion directions of gold particle and the rest particles in the mixture allow gold particle to be fractionated from the mixture [Du et al. 2007]. In the case of enhancement of sedimentation using DEP, the DEP force works as an additional force to increase particle's settling speed thereby increasing the sedimentation efficiency. In a simply designed lab-scale lamella separator, the DEP enhancement function was tested with PE particles suspended in silicone oil [Baune et al. 2008].

Based on a better understanding of DEP mechanism and proved DEP principal in application, the feasibility of DEP application in separation can be further validated with a real DEP application in a lab-scaled separation process. In this case, the scaling approach is also proposed to test whether DEP could be possibly applied in industry. Therefore, a DEP intensified cross-flow membrane filtration process is designed to examine the DEP effect on enhancing permeate flow by reducing the fouling problem in the membrane filtration process [Du et al. 2009]. In such a DEP intensified membrane filtration process, DEP force works as an additional force to move clay particle suspended in pure water away from the membrane for an anti-fouling function so as to extend the membrane working time [Du et al. 2009]. With this investigation, the millimeter range as a scaling-bridge is tested for the feasibility of scaling up the DEP application in industry.



### 3. Publications

The following papers were published in the Journal of Electrostatics (3.1.), Separation of Science and Technology (3.2.), Journal of Membrane Science (3.3.) and in book Vernetzte Wissenschaften edited by P.J. Plath and E. Hass (3.4), respectively.

#### 3.1. Paper No. 1

##### Insulator-based dielectrophoresis in viscous media – Simulation of particle and droplet velocity

F. Du, M. Baune, J. Thöming

UFT, Section of Process Integrated Waste Minimization, University of Bremen,  
Leobener Str., D 28359 Bremen, Germany

*This paper was published in the Journal of Electrostatics in 2007. The Journal of Electrostatics is aimed to disseminate knowledge of static electricity in its fundamental aspects, its useful applications and in its hazardous nature with a 5-year Impact Factor of 1.4.*

##### Abstract

The velocity of micro-particles in a nonuniform electric field was examined as a function of electrical potential and particle size to illustrate the possible application of dielectrophoresis (DEP) as a new separation technique in viscous media. A new comprehensive model is presented that combines the effects of DEP and electrohydrodynamic forces on particle motion. The current model simulation takes into account the possible significant influence of electrohydrodynamic effects depending on the particle size, electrode distance, and voltage applied during DEP particle separation. The heat generated as a consequence of high electric-field strength leads to density gradients in the liquid, thus inducing buoyancy forces that cause fluid convective motion.

Experimental velocity measurements using two materials having extreme properties, i.e. polyethylene (PE) particles (diameter range 100  $\mu\text{m}$  to 2000  $\mu\text{m}$ ) and water droplets (diameter range 25  $\mu\text{m}$  to 275  $\mu\text{m}$ ), both suspended in a viscous medium (silicone oil), correspond with the proposed theoretical predictions. The comprehensive model presented was applied to insulator-based dielectrophoresis in a direct current electric field, but it is expected to allow predictions of various similar systems.

**Keywords:** Nonuniform electric field, particle separation, DC dielectrophoresis, electrohydrodynamics

## 1. Introduction

Dielectrophoresis (DEP) is a technique that has been used in separating [Pohl 1978, Jones 1995, Li & Kaler 2004, Wakizaka et al. 2004, Arnold 2001, Lapizco-Encinas et al. 2004] and trapping [Green et al. 1997, Muller et al. 1996, Chou et al. 2002] particles principally in biotechnological applications. The theory of dielectrophoresis was firstly defined by Pohl to describe the translational motion of neutral matter caused by polarization effects in a nonuniform electric field [Pohl 1978]. DEP must be carefully distinguished from electrophoresis, which is motion caused by the response to free charge on a body in an electric field (uniform or nonuniform).

The dipole moment induced in the particle can be represented by two equal and opposite charges at the particle boundary. However, when the two induced charges are not uniformly distributed over the surface of the particle, a macroscopic dipole will be created. When the dipole is positioned in a nonuniform electric field, the local field strength on each side of the particle will be different, causing a net force referred to as the *dielectrophoretic force* [Pohl 1978]. When a particle is suspended in a medium, depending upon the different polarizations of particle and medium, the particle will be induced to move either towards the stronger electric field region (positive DEP) or towards the weaker electric field region (negative DEP). In the case of a spherical particle of radius  $a$  suspended in a medium having relative dielectric constant (permittivity)  $\epsilon_M$ , the dielectrophoretic force can be expressed by,

$$F_{DEP} = 4\pi a^3 \epsilon_0 \epsilon_M \operatorname{re}[K] (E \cdot \nabla) E \quad (1)$$

where  $\epsilon_0 = 8.854 \times 10^{-12}$  F m<sup>-1</sup> is the permittivity of free space,  $\operatorname{re}[K]$  is real part of the Clausius-Mossotti factor  $K$ , a parameter defining the effective dielectric polarizability of the particle, and  $E$  is electric field intensity. The Clausius-Mossotti factor depends upon the dielectric properties of the particle and the medium as described in detail in books by H. A. Pohl [Pohl 1978] and T. B. Jones [Jones 1995].

The motion of a particle suspended in an aqueous medium is often simply assumed to be the steady state value obtained by balancing the dielectrophoretic and viscous drag forces. Thus, the velocity of particle  $v$  is obtained as

$$v = \frac{2a^2 \epsilon_0 \epsilon_M \operatorname{re}[K] (E \cdot \nabla) E}{3\eta_M} \quad (2)$$

where  $\eta_M$  is the dynamic viscosity of the medium. In Eq. 2, either the aqueous medium is assumed to be static, or the particle velocity is assumed to be independent of fluid motion [Li & Kaler 2004, Wakizaka et al. 2004]. In contrast to these assumptions, the high electric field strength that is often necessary in DEP applications usually initiates fluid motion

[Castellanos et al. 2003]. As a consequence of joule heating, which is a function of the electric field, electrothermal forces are induced by the variation in the conductivity, permittivity and density of the suspending medium [Muller et al. 1996]. By increasing the dimensions of the electrodes used from the micrometer scale to the millimeter scale, joule heating has been observed to give rise to buoyancy forces [Castellanos et al. 2003]. Although there have been many previous investigations on the effects of electrothermal fluid flow on the particle's motion caused by DEP [Arnold 2001, Muller et al. 1996, Castellanos et al. 2003], these research works focused mainly on the micro- (larger than  $10^{-6}$  m) or/and sub-micro- (smaller than  $10^{-6}$  m) electrodes for micro- or/and sub-micro-particle operation, so that diffusion heat transport was dominant in the energy balance. In addition, the reported DEP investigations focused on particles suspended in a medium of relative *high* conductivity in alternating current (ac) electric fields. Furthermore, a number of studies with focus on the application of DEP using bare electrodes were also performed. However, bare electrodes generally produce problems such as short-circuits and electrochemical reactions on the electrodes (e.g. electrode fouling). The potential for a human electric shock is higher in bare electrode configurations, especially given the high electric field strengths used in DEP. Cummings and Singh [Cummings and Singh 2003] introduced the concept and initial characterization of a so-called insulator-based dielectrophoresis (iDEP) device. With the exception of the studies of Cummings and Singh, as well as those of Lapizco-Encinas *et al.* [Lapizco-Encinas et al. 2004], who performed iDEP experiments using micro-particles in a medium with a relative high conductivity [Lapizco-Encinas et al. 2004, Chou et al. 2002, Cummings and Singh 2003], most of the applications of iDEP used ac electric fields [Chou et al. 2002, Cummings and Singh 2003]. In Chou *et al.* [Chou et al. 2002] experiments showed iDEP trapping of DNA molecules using insulating structures and ac electric fields.

In the present work, the motion of both micro-particles and the medium is investigated in a low conductivity medium in a nonuniform direct current (DC) electric field with an insulated electrode configuration (characteristic length 6 mm). Results are discussed to validate the feasibility of separating larger particles (25 - 2000  $\mu\text{m}$  diameter) using DEP.

## 2. Materials and methods

In this investigation, an electrode configuration of spherical geometry, shown in Fig. 1, was used in the experiments. The two electrodes were made of platinum and insulated by a thin layer of glass and integrated into a glass reservoir. The radius of the central, spherical electrode was 1.4 mm, while that of the outer concentric shell was 6 mm.

The high resistances of the entire system, as well as that of the glass and the silicone oil, were determined via impedance spectroscopy using EG&G Instruments Model 398 and EG&G Electrochemical Impedance Software EIS. The impedance data were evaluated using Bode diagrams identifying the best fit horizontal line (least squares method) in the frequency range from 0.1 to 10 Hz. By this means, the dc resistances were received as offset values at 0 Hz.

Spherical polyethylene (PE) particles and droplets of demineralized water were dispersed in 0.223 cm<sup>3</sup> silicone oil DC200 (Fluka) having a viscosity of 20 mPas. The diameter range of the PE particles varied from 100 μm to 2000 μm, while the water droplets ranged in size from 25 μm to 275 μm.

The electrodes were powered using a High Stability Power Supply (KNOTT ELECTRONIK), which could provide voltages from 0.2 kV to 2.4 kV DC. By means of a microscope with a scaled lens (CARL ZEISS) both particle diameter and displacement of the particles were recorded. A cold light source (KL2500LCD, SCHOTT) was used to decrease the external heat influence.

Additionally, two thermal sensors were positioned in the system, as shown in the A-A sectional view of Fig. 1, to measure the medium increment of temperature.

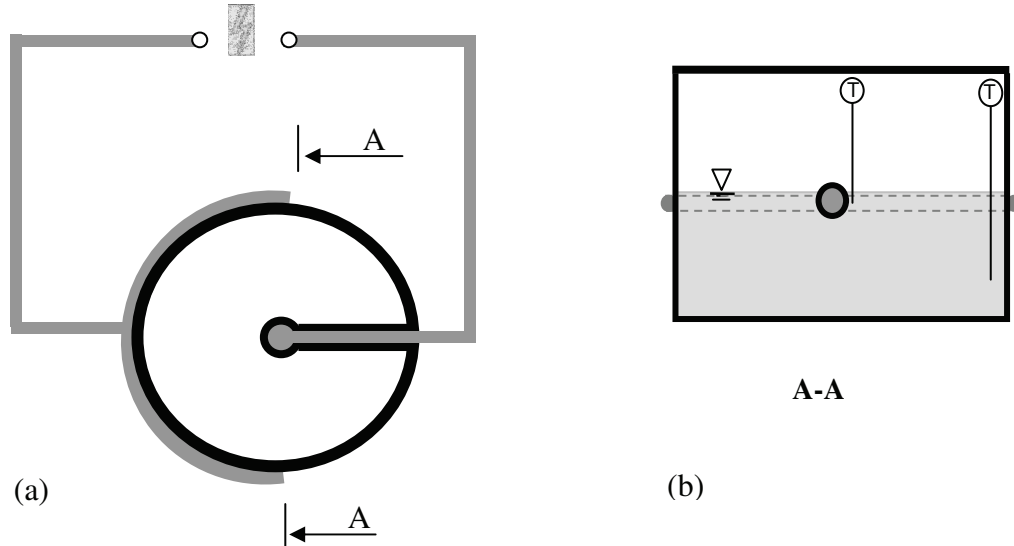


**Figure 1.** Top view (a) and sectional view (b) of experimental cell system including the two points of temperature measurement. The indicated surface of the liquid is identical to the plane, at which the particle velocity was measured.

### 3. Theoretical Model

#### 3.1. Electric field calculation

The spherical electrode configuration used in the theoretical model as well as in the experimental setup (Figure 1) can be approximately described mathematically by a spherical

capacitor having a central sphere of radius  $r_i$ , and an outer concentric shell of radius  $r_o$ . The gradient of the square of the applied field at any point  $s$  between these spherical shells, for a voltage  $U$  applied from the DC power supply, is given by,

$$E = \frac{r_o r_i U}{s^2 (r_o - r_i)} \hat{r} \quad (3)$$

$$2(E \cdot \nabla)E = \nabla |E|^2 = \frac{-2r_i^2 r_o^2 U^2}{s^5 (r_o - r_i)^2} \hat{r} \quad (4)$$

where  $s$  is the distance between the central electrode and the observed particle,  $\hat{r}$  is the unit radius vector. The quantity,  $\nabla |E|^2$  is the (geometric) gradient of the square of the field intensity, which is defined by Pohl [Pohl 1978] and generally applied in DEP with the assumption that the materials are linear, isotropic dielectrics [Pohl 1978].

### 3.2. Forces

With reference to the experimental setup, the motion of a particle suspended in a viscous medium will generally be influenced by the following forces: gravitational, buoyancy, drag, dielectrophoretic, and Brownian. Because the directions of the gravitational and buoyancy forces are vertical, and the velocity of particles horizontal in the case of our experiments, the effects from both these forces were assumed to be negligible. The effects of the Brownian force decrease with increasing particle size. The diameter of particles used was mainly greater than 100  $\mu\text{m}$ , hence the influence of Brownian effects could be neglected. Therefore, with respect to forces in the horizontal direction, the dielectrophoretic and drag forces only were considered in developing our theoretical model. As shown in Eq. 1, the dielectrophoretic force is dependent upon the Clausius-Mossotti factor (dielectric properties of the particle and the medium), the electric field, and the size of particle.

In this theoretical model, the drag force is assumed to lie in the Stokes-regime, because the size and velocity of particles investigated are small. Hence the resulting Reynolds numbers are lower than 0.5. According to Stokes' law [Sommerfeld 2000], the drag force  $F_D$  is given as,

$$F_D = \frac{1}{2} C_D \rho_M (u - v)^2 A \quad (5)$$

where,

$$C_D = \frac{24}{\text{Re}} \quad (5a)$$

and

$$\text{Re} = \frac{\rho_M d (u - v)}{\eta_M} \quad (5b)$$

where,  $C_D$  is the drag coefficient,  $\rho_M$  is the density of medium,  $u$  is the medium flow velocity,  $v$  is the velocity of the particle,  $A$  is the cross-sectional area of particle,  $\text{Re}$  is the Reynolds number,  $\eta_M$  is the dynamic viscosity of medium, and  $d$  is the diameter of particle. By balancing drag and dielectrophoretic forces in the horizontal direction, the velocity of a large particle can be calculated theoretically by combining Eqs. (1) and (5).

### 3.3. Energy balance

An analogy can be made between the dielectrophoretic system considered here and an electrical circuit having parallel resistance and capacitance. In the latter model, the “capacitance” drives the dielectrophoresis, while electrical energy is transformed into heat across the “resistance”. In the actual DEP system, this effect leads to a buoyancy-driven flow, because the Boussinesq approximation [Boussinesq 1903] holds. The Navier-Stokes equation then becomes,

$$\rho_M C_P \left( \frac{\partial T}{\partial t} + (u \bullet \nabla) T \right) = k \nabla^2 T + q_{gen} \quad (6)$$

where  $C_P$  is the specific heat capacity,  $T$  is the temperature,  $k$  the thermal conductivity of the fluid, and  $q_{gen}$  the heat generation of the model. In this equation, it is assumed that all of the heat generated from resistance heats the fluid within the balanced segment around the central electrode. Furthermore, the temperature-field distribution is assumed to rapidly reach steady state after the application of the electric field, hence the cell is cooled down sufficiently at its outer shell.

For the model used in the experiments, the convective heat transport was higher than diffusive heat transport, as indicated by the large value of the Peclet number, which was much higher than unity for  $u = 1$  mm/s, and  $l = 6$  mm,

$$Pe = \frac{\rho_M C_P u l}{k} \approx 57.6 \quad (7)$$

Here  $l$  is the characteristic length of system. Thus Eq. 6 can be reduced to

$$\rho_M C_P u \nabla T = q_{gen} \quad (8)$$

In contrast to the energy balance equation for microsystems [Chou et al. 2002], in which heat transport via diffusion is dominant, heat transport via convection was considered dominant.

The experimental cell system shown in Fig.1, having a certain volume  $V$  of medium, is heated by electrical power  $q_{gen}$ , which is a function of applied voltage  $U$  and the resistance  $R$  of the entire system -- in our case the experimental cell system, shown in Fig. 1.

Hence, the Eq. 8 can be expressed as

$$\rho_M C_p V u \nabla T = \frac{U^2}{R} \quad (9)$$

As a consequence of the application of the spherical electrode configuration in the system investigated, the electric field is assumed to be radial. The temperature gradient in the radial direction can be approximated using the relation

$$\nabla T \approx \frac{\Delta T}{l} \quad (10)$$

Therefore, the temperature increment can be described by

$$\Delta T = \frac{U^2 l}{R \rho_M C_p V u} \quad (11)$$

In our system, the characteristic length is the radius of the outer concentric shell  $r_o$ .

### 3.4. Joule heating induced fluid flow

The use of a high electric field in DEP usually implies that there will be a large power density in the fluid surrounding the electrode. The joule heating generated in the system causes a temperature field that depends on the boundary conditions. There are generally two types of joule heating induced fluid flows: electrothermal and buoyancy. When the order of magnitude of the system's characteristic length is above about 1 mm, the buoyancy due to joule heating always dominates the fluid flow [Chou et al. 2002]. In general, the gravitational body force on a fluid generated by a temperature field is due to the local density change caused by the temperature difference. In a closed system, this leads to a convective circulation, in which the fluid flows from the higher to the lower temperature region in the upper plane of the liquid and recirculates back on the lower plane of the liquid at the lowest temperature level. In our experimental setup, the fluid flows from the central electrode region to the outer concentric shell region and back in the lower plan to the central electrode, as shown in Fig. 2, because the higher electric field region generates higher temperature.

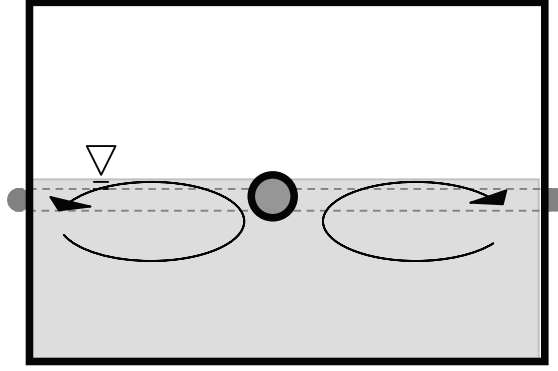


**Figure 2.** Convective fluid flow caused by joule heating.

Hence the buoyancy force which results from the joule heating can be expressed as

$$f_B = \frac{\partial \rho_M}{\partial T} \Delta T g \quad (12)$$

where  $f_B$  is the buoyancy volume force, and  $g$  is the gravitational acceleration.

Considering an incompressible fluid, the medium flow can be assumed to be predominantly influenced by both the buoyancy force generated by joule heating, and drag force. For a steady state situation, the two forces are equal and the volume-force balance equation can be given as

$$\frac{\partial \rho_M}{\partial T} \Delta T g = \eta_M \nabla^2 u \quad (13)$$

The density change generated by the temperature field, which is dependent upon the thermal expansion coefficient, is given by

$$\alpha = \frac{1}{\rho_M} \frac{\partial \rho_M}{\partial T} \quad (14)$$

where  $\alpha$  is volume expansion coefficient. By combining Eqs. 11, 12, 13 and 14, the medium motion can be expressed as

$$u = U \sqrt{\frac{\alpha g r_0^3}{V C_p \eta_M R}} \quad (15)$$

The latter follows if the motion is unhindered, i.e. occurs at a certain distance apart from the electrodes. From Eq. 15, it can be seen that the medium motion is dependent upon the following parameters: electric conductivity of the medium, the voltage applied between the electrodes, electrode geometry, as well as the specific heat, thermal expansion coefficient, and the viscosity of the liquid.

### 3.5. Modeling of the particle velocity

Considering DEP and electrothermal (ETE) effects on a suspended particle, Eqs. 2, 4, and 15 can be combined, and the velocity  $v$  of the particle's motion can be expressed as



$$v = \frac{d^2 \varepsilon_0 \varepsilon_M \operatorname{re}[K]}{6\eta_M} \frac{r_0^2 r_i^2}{s^5 (r_0 - r_i)^2} U^2 \pm U \sqrt{\frac{\alpha g r_0^3}{VC_P \eta_M R}} \quad (16)$$

In this equation, the first term on the right-hand side represents the motion caused by DEP effects, while magnitude and algebraic signs of the second term represent the speed and the direction of the fluid, respectively. This direction of the fluid motion is given relative to the direction of DEP, i.e. the sign of Clausius-Mossotti factor. Since joule heating-induced fluid flow points from higher to lower electric field regions, the algebraic sign of the second term is positive in the case of negative DEP, and negative in the case of positive DEP. The motion of the medium will thus increase the particle velocity in the case of negative DEP (e.g. PE in silicone oil), where particle movement is also towards lower electric field regions. Similarly, the fluid motion will thus decrease particle velocity in the case of positive DEP (e.g. water droplets in silicone oil). From Eq. 16, one can show that the particle velocity is dependent on electric field strength, electrode geometry, particle size, the dielectric constants of the medium and particle, and the viscosity and thermal properties of the liquid.

The properties of the particle, medium, and electrode configuration are independent of the electric field strength, hence the velocity  $v$  of particle is a linear function of the square of the particle diameter  $d$ :

$$v = kd^2 + b \quad (17)$$

where

$$k = \frac{\varepsilon_0 \varepsilon_M \operatorname{re}[K]}{6\eta_m} \frac{r_0^2 r_i^2}{s^5 (r_0 - r_i)^2} U^2 \quad (17a)$$

and

$$b = \pm U \sqrt{\frac{\alpha g r_0^3}{VC_P \eta_M R}} \quad (17b)$$

Here the slope  $k$  represents the properties of DEP, and the intercept  $b$  represents the effect of electrothermal fluid flow. For an assumed particle size, the velocity  $v$  of the particle is a function of voltage  $U$ ,

$$v = mU^2 + nU \quad (18)$$

where

$$m = \frac{d^2 \varepsilon_0 \varepsilon_M \operatorname{re}[K]}{6\eta_M} \frac{r_0^2 r_i^2}{s^5 (r_0 - r_i)^2} \quad (18a)$$

and

$$n = \pm \sqrt{\frac{\alpha g r_0^3}{V C_p \eta_M R}} \quad (18b)$$

For the case of positive DEP, where the direction of particle motion is opposite that of fluid flow, it follows that ETE will cause particle velocity to decrease and may even move the particle in the opposite direction, as shown in Fig. 3. From this theoretical model, the relationship between particle velocity and the square of the applied voltage is not linear, and the particle movement velocity is decreased by the ETE effect.

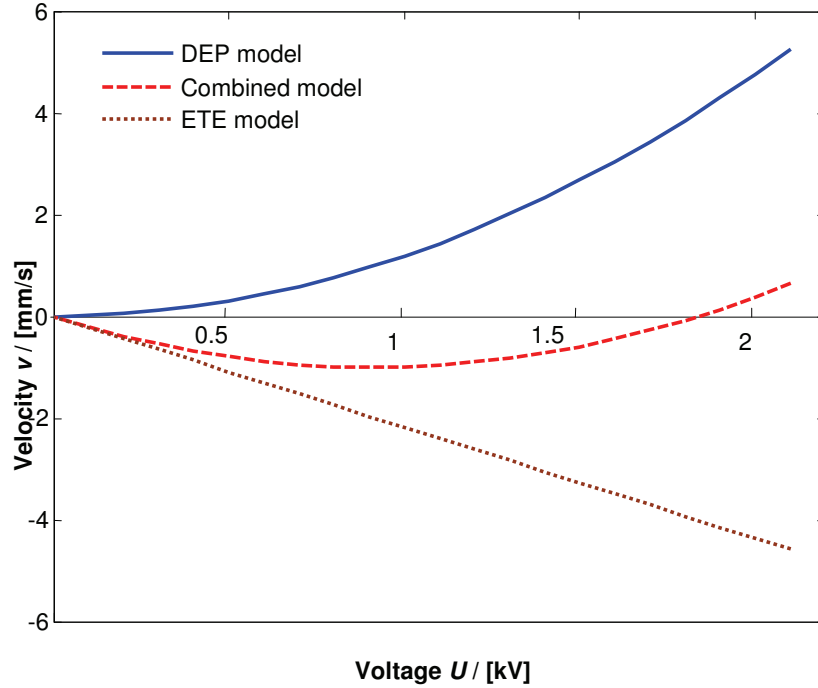


**Figure 3.** Theoretical comparison of relationship between velocity and voltage due to positive dielectrophoresis (DEP), electrothermal effect (ETE), and a combination of the two forces (combined model) according to Eqs.1, 15, and 18, respectively. The calculations were performed for 0.1 mm diameter water droplets in silicone oil ( $\eta = 20$  mPas,  $C_p = 1.4$  J/(K g),  $\rho_M = 0.96$  g/mL,  $\varepsilon_M = 2.9$ ) at  $s = 1.4$  mm in the experimental cell system shown in Fig. 1.

#### 4. Results and discussion

By means of impedance spectroscopy, the resistance of the entire experimental cell was measured for silicone oil containing water droplets. The total resistance for this case was determined to be  $1.10 \times 10^8 \Omega$ . In addition, the measured conductivities of glass and the pure silicone oil were found to be  $7.04 \times 10^{-8}$  S/m and  $5.42 \times 10^{-8}$  S/m respectively. The resistance of the system can be assumed to be equivalent to three resistors connected in series, of which one is the silicone oil and two are the glass walls at the inner surface of the outer electrodes and around the inner electrode. By using the measured conductivities of silicone oil and glass, the approximate field across the silicone oil is calculated to be about 91.2% of the total field.

By this approach, the theoretical total resistance of the pure, water-free system is calculated to be  $10.12 \times 10^8 \Omega$ .

With application of a dc electric field, the PE particles in silicone oil moved immediately towards the outer concentric shell, where the electric field strength was weaker (negative DEP), since the polarizability of PE (relative dielectric constant 2.25) is lower than that of silicone oil (relative dielectric constant 2.9). The PE particle motion could be sped up or slowed down by increasing or decreasing the applied voltage. Once the particles reached the outer concentric shell, they remained there.

However, the induced electrothermal fluid movement could be observed in the experiment as shown in Fig. 2 and was a function of the applied voltage. The velocity of PE particle in motion was measured and calculated by dividing the observed distance traveled by measured time. The experimental results were compared with theoretical model calculation results at different applied electric fields, as shown in Fig. 4(a). In addition, the particle's motion was not influenced by the change in polarity, as shown in Fig. 4(b), with which the DEP effect was confirmed. Furthermore, for an applied dc voltage of 0.7 kV, the medium increment of temperature was found to be  $0.22625 \pm 0.00875$  K over a measurement period of 5-minutes. According to Eq. 13, the measurement result is reasonable when the fluid flow is on the order of over 1 mm/s.

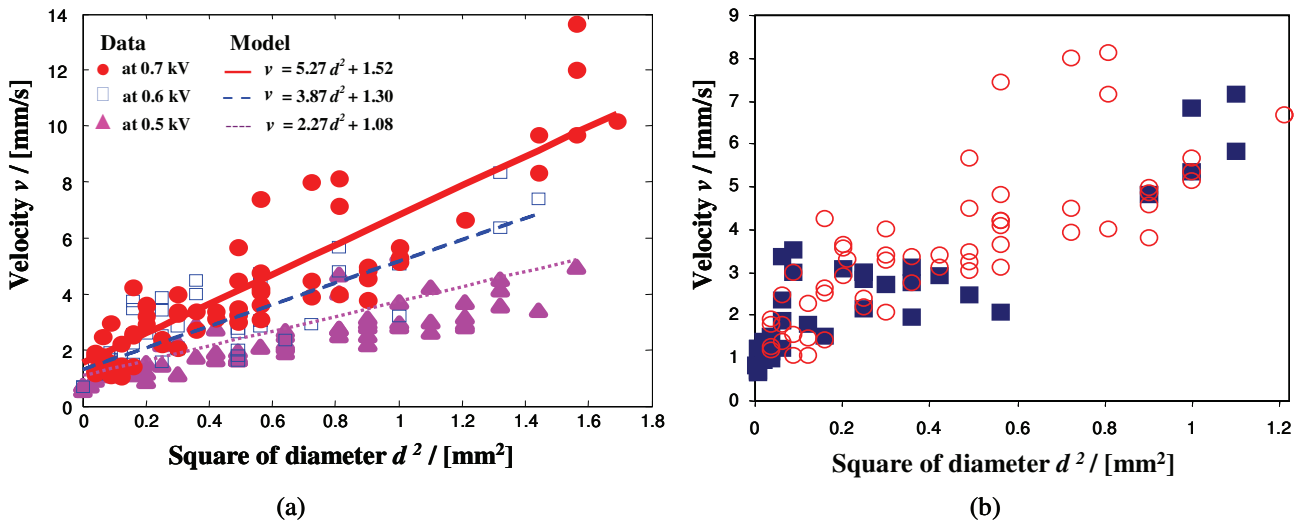


**Figure 4.** Comparison of experimental results and combined DEP-EDE model for PE particles in silicone oil. (a) Influence of electric field intensities on the velocity with model lines according to Eq. 17; (b) Comparison of particle velocity for positive (circle) and negative (square) outer electrode. A comparison of the theoretically calculated model and least-square-fit of the experimental data is provided in Table 1.

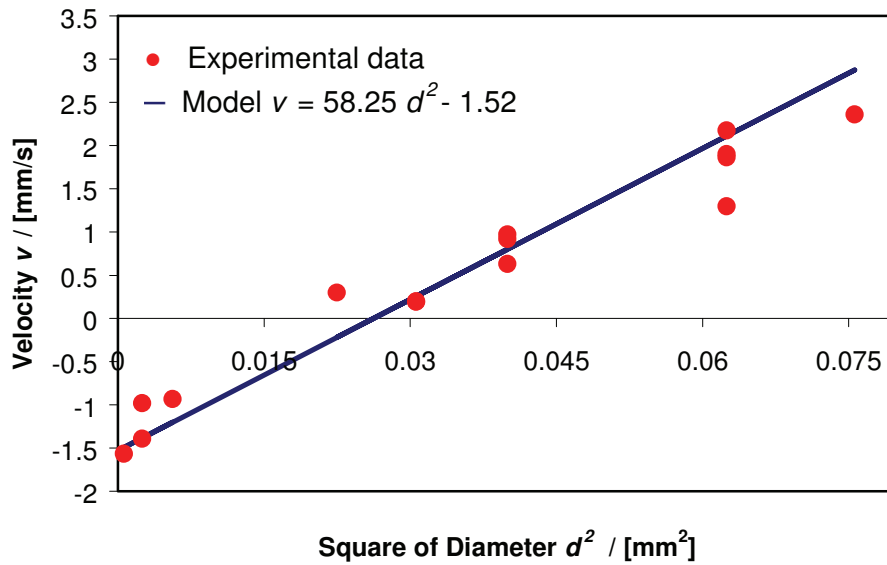


**Figure 5.** Velocity of water droplets in silicone oil as a function of the square of the diameter for experimental data and theoretical model calculations at 0.7 kV. The simulation was performed according to Eq. 17. A comparison of the theoretically calculated model and least-squares-fit of the experimental data is provided in Table 1.

In contrast to the PE particles, water droplets (diameter above 150  $\mu\text{m}$ ) in the same silicone oil moved immediately towards the central electrode (positive DEP). This was due to the higher polarizability and conductivity of pure water (relative dielectric constant 78, conductivity  $1 \times 10^{-4}$  S/m) compared to that of silicone oil. In the same electric field, the smaller water droplets (diameter below 150  $\mu\text{m}$ ) moved immediately towards the outer concentric shell (i.e. opposite the motion of larger particles), as shown in Fig. 5. The velocity of droplet motion varied with changes in voltages (Fig. 6). However, unlike the linear relationships between velocity and squared voltage as described in the prior literature [Li & Kaler 2004], a nonlinear relationship was found in the experiments summarized in Fig. 6. A certain sized droplet, (100  $\mu\text{m}$  diameter, for example), sped up with increasing voltage until the voltage reached a critical value (region a in Fig. 6), at which point the particle's speed was reduced again even down to a net velocity of zero (region b in Fig. 6). With further voltage increase in voltage, the direction of the droplets' motion became inverted (region c in Fig. 6).

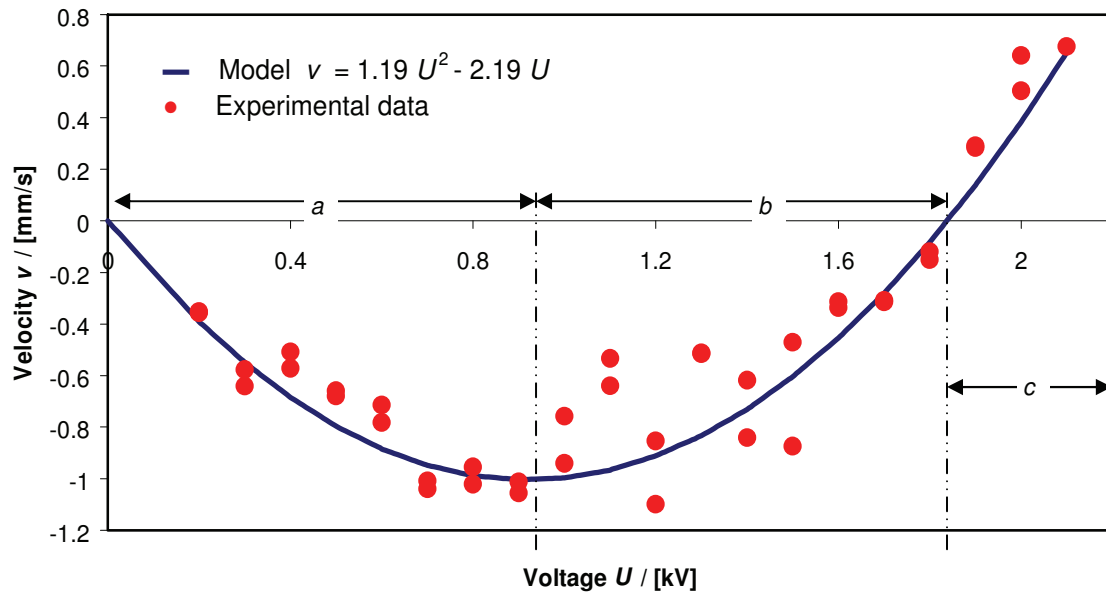


**Figure 6.** Dependence of velocity of water droplet (diameter 0.1mm) in silicone oil with voltage for experimental data (dots) and simulation (line). The simulation was performed according to the combined model given by Eq. 18 and illustrated in Figure 3. A comparison of the theoretically calculated model and least-square-fit of the experimental data is provided in Table 1. Regions a and b: motion towards outer electrode; region c: motion towards central electrode.

The theoretical model presented in Eq. 17 provides an intercept value which can be interpreted as the medium flow speed of an infinitesimally small particle (i.e. one of negligible particle speed due to DEP). This interpretation is strengthened by the fact that for both types of particles (PE and water) the same magnitude was found for the intercept, as shown in Figs. 4 and 5. The different arithmetic sign in these two cases is related to the different types of DEP, negative DEP in the case of PE, and positive DEP for water.

In addition to our theoretical model calculations, a least-squares-fit of the experimental data was performed. The model equations were used as regression functions. For each chosen electric-field strength, the slopes ( $k$ ) of the linear regression functions of both experimental results and theoretical model functions were nearly identical (Table 1). The slopes can be determined by the characteristics of DEP and the hydrodynamic properties of medium. Although the square of the correlation coefficients  $r^2$  of all linear regression functions are not above 0.79 in the case of PE in silicone oil, the differences of slopes  $k$  between the experimental regression and the theoretical model function have very low variation between 0.44% and 2.07%. Furthermore, despite the low value of  $r^2$ , the graphical presentation of the regression lines indicates that they can sufficiently represent the experimental data.

Additionally, both intercepts  $b$ , which represent the velocity of the medium flow, vary only slightly.

**Table 1.** Theoretically, calculated parameters using Eqs. 17 and 18 compared to linear regressions of experimental data for PE particles (100 $\mu\text{m}$  to 2000  $\mu\text{m}$ ) and water droplets (25  $\mu\text{m}$  to 275  $\mu\text{m}$ ) in silicone oil (viscosity 20 mPas).

	Voltage $U / \text{kV}$	Eq.	Regression of experimental data			Theoretical model	
			Fitted Parameters		Correlation coefficient squared	Calculated Parameters	
PE		17	$k$ $/ \text{m}^{-1} \text{s}^{-1}$	$b$ $/ \text{m} \text{s}^{-1}$	$r^2$	$k$ $/ \text{m}^{-1} \text{s}^{-1}$	$b$ $/ \text{m} \text{s}^{-1}$
	0.5		2.28	0.89	0.70	2.27	1.08
	0.6		3.79	1.41	0.69	3.87	1.30
	0.7		5.37	1.36	0.79	5.27	1.52
Water	0.7	17	49.79	-1.27	0.96	58.25	-1.52
		18	$m$ $/ \text{m} \text{s}^{-1} \text{V}^{-2}$	$n$ $/ \text{m} \text{s}^{-1} \text{V}^{-1}$	$r^2$	$m$ $/ \text{m} \text{s}^{-1} \text{V}^{-2}$	$n$ $/ \text{m} \text{s}^{-1} \text{V}^{-1}$
	0.2-2.1*		1.14	-2.05	0.90	1.19	-2.19

\* This case is illustrated in Figs. 3 and 6

In the case of water, the velocity is also determined as a function of the two factors  $m$  and  $n$  which represent DEP and ETE, respectively. Here, the difference between theoretical model and experimental results is small (4.20% for  $m$  and 6.39% for  $n$ ) for a squared correlation coefficient  $r^2$  of experimental regression function of 0.90.

## 5. Conclusion

Separation of micro-particles can be achieved in nonuniform electric fields with velocities high enough even for continuous separation processes at voltages below 1 kV dc. According to our theoretical model, the thermal fluid flow generated from a high electric-field intensity can increase (in the case of negative dielectrophoresis) or decrease (in the case of positive dielectrophoresis) the particle velocity. The adapted energy balance function for our experimental system indicates a decreasing influence of the electrothermal effect during continuous separation. Due to the relatively large characteristic length compared to

microscale systems for our electrode setup, which was in the millimeter range, heat convection, rather than heat diffusion, is dominant in our system. The experimental velocity data for PE particles and water droplets in silicone oil are in good agreement with the theoretical velocity models and confirm the proposed influence of the electrothermal effect.

## 6. Acknowledgements

The authors wish to acknowledge Prof. Dr. P. J. Plath and his group at the University of Bremen for fruitful discussions, as well as for his support of the cold light source apparatus. We are also grateful to George Okoth for help in improving the English of the original manuscript.

## References

- Arnold, W.M., Positioning and levitation media for the separation of biological cells *IEEE Trans. Ind. Appl.* 37 (2001)1468-75.
- Boussinesq, J., *Theorie analytique de la chaleur*, Vol.2, Gauthier-Villars, Paris, 1903.
- Castellanos, A., Ramos, A., González, A., Green, N.G. and Morgan, H., Electrohydrodynamics and dielectrophoresis in microsystems: scaling laws, *J. Phys. D: Appl. Phys.* 36 (2003) 2584-2597.
- Chou, C., Tegenfeldt, J., Bakajin, O., Chan, S., Cox, E., Darnton, N., Duke and Austin, T.R., Electrodeless dielectrophoresis of single- and double-stranded DNA, *Biophys. J.* 83 (2002) 2170-2179.
- Cummings, E. and Singh, A., Dielectrophoresis in Microchips Containing Arrays of Insulating Posts: Theoretical and Experimental Results, *Anal. Chem.* 75 (2003) 4724-4731.
- Green, N.G., Morgan, H. and Milner, J.J., Manipulation and trapping of sub-micron bioparticles using dielectrophoresis, *J. Biochem. Biophys. Methods* 35 (1997) 89-102.
- Jones, T.B., *Electromechanics of particles*, Cambridge University Press, USA, 1995.
- Lapizco-Encinas, B.H., Simmons, A.B., Cummings, B.E. and Fintschenko, Y., Insulator-based dielectrophoresis for the selective concentration and separation of live bacteria in water, *Electrophoresis*, 25 (2004) 1695-1704.
- Li, Y., Kaler, K.V.I.S., Dielectrophoretic fluidic cell fractionation system, *Analytic Chimica Acta.* 507 (2004) 151-161.
- Muller, T., Gerardino, A., Schnelle, T., Shirley, S.G., Bordoni, F., DeGasparis, G., Leoni R. and Fuhr, G., Trapping of micrometer and sub-micrometer particles by high-frequency electric fields and hydrodynamic forces, *J.Phys.D: Appl. Phys.* 29 (1996) 340-349.
- Pohl, H.A., *Dielectrophoresis*, Cambridge University Press, Cambridge, 1978.

Sommerfeld, M., Theoretical and experimental modeling of particulate flows, Martin-Luther University Halle-Wittenberg, Germany, 2000.

Wakizaka, Y., Hakoda, M. and Shiragami, N., Effect of electrode geometry on dielectrophoretic separation of cells, *Biochem. J.* 20 (2004) 13-19.



### 3.2. Paper No. 2

#### Dielectrophoretic gold particle separation

F. Du, M. Baune, A. Kück, J. Thöming

Center of Environmental Research and Sustainable Technology,  
University of Bremen, Leobener Str., D 28359 Bremen, Germany

*This paper was published in the journal of Separation Science and Technology in 2008. The journal of Separation Science and Technology is an international journal dealing with fundamental and applied aspects of separation processes related to a wide variety of fields with a 5-year Impact Factor of 1.150.*

#### Abstract

We present a novel process for gold particle separation from aqueous setup with high separation efficiency and without any environmental risk. Dielectrophoresis (DEP), as the main mechanism of this separation process, is applied for the first time to separate gold even continuously from a raw mineral mixture. Electrothermal and high-pass-filter effects, occurring in DEP with water as liquid phase, were investigated and considered during the design of the separation process. The experimental results demonstrate that even ultra thin gold particles can be separated from a raw mineral mixture with an efficiency of up to 88 % at an electric field of 32 kV/m and 200 kHz in continuous operation with specific fluid flow of about 400 m<sup>3</sup>/(m h).

**Keywords:** Dielectrophoresis, electric field flow fractionation, gold leaf, non-uniform electric field, pearl chain, thermal effect

#### 1. Introduction

In nature, gold occurs as a pure free metal, typically associated with oxides of other metals. In gold mining, techniques like manual panning or continuous sluicing are used to produce mineral concentrates. For separating gold particles from such mixtures, typically cyanidation or amalgamation is applied, however both methods pose a considerable operational and environmental danger [Hylander et al. 2007]. As a non-chemical method, magnetism has been suggested in recovery of gold particle from ore, however, the separation efficiency is low [Hylander et al. 2007]. Another non-chemical method was reported for the separation of colloidal gold particle from gold laden material in water by using an oppositely charged collecting material to capture colloidal gold particle from gold laden material [Loewen 2006]. Although this method is environmentally friendly, it appears not to be suitable in mining due to the small size of particles. This is also true for a dielectrophoretic

method (DEP), which has been proved by Kumar et al., who reported a bridging effect of 20 nm gold nanoparticles between two electrodes by DEP [Kumar et al. 2008].

In this work, we focus on a non-chemical separation of gold particles of  $\mu\text{m}$ - scale that is based on the movement of pure gold particle in aqueous medium by DEP.

## 1.1 Dielectrophoresis

Dielectrophoresis, which has been employed in trapping particles mainly in biological industries [Ramadan et al. 2006, Jones 1995, Pohl 1978, Pethig & Mark 1997, Morgan & Green 2002], is defined by Pohl to describe the translational motion of neutral matter caused by polarization effects in a nonuniform electric field [Pohl 1978]. The dipole moment induced in the particle can be represented by two equal and opposite charges at the particle boundary, however when they are not uniformly distributed over the particle surface a macroscopic dipole will be created [Pethig & Mark 1997]. When the dipole is positioned in a nonuniform electric field, the local field strength on each side of the particle will be different, causing a net force referred to as dielectrophoretic force. Therefore, a suspended particle in a liquid medium will be induced to move either towards stronger electric field region (positive DEP) or towards a weaker electric field region (negative DEP), depending upon the different polarizations of particle and liquid medium.

When a spherical particle (radius  $a$ ) suspended in a medium, whose relative dielectric constant (permittivity) is  $\epsilon_M$ , the dielectrophoretic force can be given as [Ramadan et al. 2006],

$$F_{DEP} = 4\pi a^3 \epsilon_0 \epsilon_M \text{re}[K](E \cdot \nabla)E \quad (1)$$

where  $\epsilon_0$  is the permittivity of free space with the value of  $8.854 \times 10^{-12} \text{ F m}^{-1}$ ,  $\text{re}[K]$  is the real part of Clausius-Mossotti factor  $K$ , a parameter defining the effective dielectric polarizability of the particle, and  $E$  is electric field intensity. The Clausius-Mossotti factor is a function of frequency of the electric field, depending upon the particle and medium's dielectric properties and is expressed as,

$$\text{re}[K] = \text{re}\left(\frac{\tilde{\epsilon}_p - \tilde{\epsilon}_M}{\tilde{\epsilon}_p + 2\tilde{\epsilon}_M}\right) \quad (1a)$$

$$\tilde{\epsilon} = \epsilon - \frac{i\sigma}{\omega} \quad (1b)$$

where  $\tilde{\epsilon}$  is the complex permittivity of the particle ( $\tilde{\epsilon}_p$ ) and the medium ( $\tilde{\epsilon}_M$ ),  $\sigma$  the conductivity,  $\omega$  the angular frequency of the applied electric field ( $\omega = 2\pi f$ ) in which  $f$  is frequency,  $i = \sqrt{-1}$ .  $\nabla|E|^2$ , the (geometric) gradient of the square of the field intensity, is

defined by Pohl and generally applied in DEP to calculate  $(E \cdot \nabla)E = |E|\nabla|E| \approx \frac{1}{2}\nabla|E|^2$  with the assumption that the materials are linear isotropic dielectrics [Pohl 1978].

The motion of a particle suspended in aqueous medium is often simply assumed to be a steady state by balancing the dielectrophoretic force and drag force. Thus, the velocity of particle  $v$  is obtained by,

$$v = \frac{2a^2 \varepsilon_0 \varepsilon_M \text{re}[K](E \cdot \nabla)E}{3\eta_M} \quad (2)$$

where  $\eta_M$  is dynamic viscosity of medium.

The DEP gold-separation is a unique case because gold is chemically inert and exists as a free and pure metal in nature. Gold, which is characterized by an infinitely huge permittivity [Pohl 1978], will consequently always move towards stronger electric field when suspended in any liquid, depicting a positive DEP. Therefore, the principal concept is to move and trap gold particle at the stronger electric field regions, which concurrently repel other particles in the mixture away from gold particles.

Nevertheless, due to the high electric field strength necessarily applied in a DEP system, a side-effect, which often occurs in a DEP system and is termed to be electrothermal effect, presents a temperature gradient caused by the energy dissipation of internal friction on the medium [Du et al. 2007]. Joule-heating from the temperature gradient in the DEP system will drive medium to flow. The driven fluid flow influences particle's motion. Especially when the order of magnitude of the system's characteristic length is above 1 mm, the buoyancy due to joule heating always dominates the fluid flow [Du et al. 2007]. The gravitational body force on a fluid generated by a temperature field, which directed from higher electric field region to lower electric field region, is due to the local density change caused by the temperature difference. The temperature difference can be given as [Du et al. 2007]

$$\Delta T = \frac{U^2 l}{R \rho_M C_P V u} \quad (3)$$

where,  $\Delta T$  is the temperature difference,  $U$  is applied voltage,  $l$  is characteristic length,  $\rho_M$  is the density of medium,  $C_P$  is the specific heat capacity,  $V$  is volume of medium, and  $u$  represents the fluid flow speed.

In addition, a constraint in the application of DEP is caused by high-pass-filter effect. The insulated electrodes applied in a DEP system together with the medium could be represented as a high-pass-filter circuit. Such a high-pass-filter circuit will require much higher voltage to satisfy the high electric field requirement for DEP system in a low

frequency region. Therefore, the high-pass-filter effect not only limits the DEP application in low frequency region, but increases the energy requirement in a DEP system.

Therefore, in order to increase separation efficiency by preventing the disadvantage from the side effect and constraint caused by electrothermal and high-pass-filter effect respectively, a continuous separation process with a specific electrode configuration for high frequency electric field application is designed and examined in this work and compared with batch operation. The separation phenomena and efficiency are recorded and discussed to optimize and demonstrate the feasibility of gold separation using dielectrophoresis.

## 2. Experimental setup and procedures

### 2.1. Electrode configuration design

With insulated electrodes configuration, the setup could be modeled to be a high-pass filter circuit with two serially connected capacitors (the two insulated electrodes  $C_{E1}$  and  $C_{E2}$ ) in series with a resistor  $R_M$  paralleled by a capacitor (the medium and insulation material  $C_M$ ), as shown in Figure 1.

The frequency-dependent voltage fraction of voltage across the medium  $U_M$  to voltage applied  $U_0$  is simulated as shown in Figure 2, from which, it is deduced that at low frequency the electric field in the medium tends to zero, meaning that the dielectrophoretic force on particles will tend to zero and no movement will occur. When both electrodes are insulated, the critical frequency,  $f_{cr}$  for electric field to be able to develop across the medium is about 300 kHz.

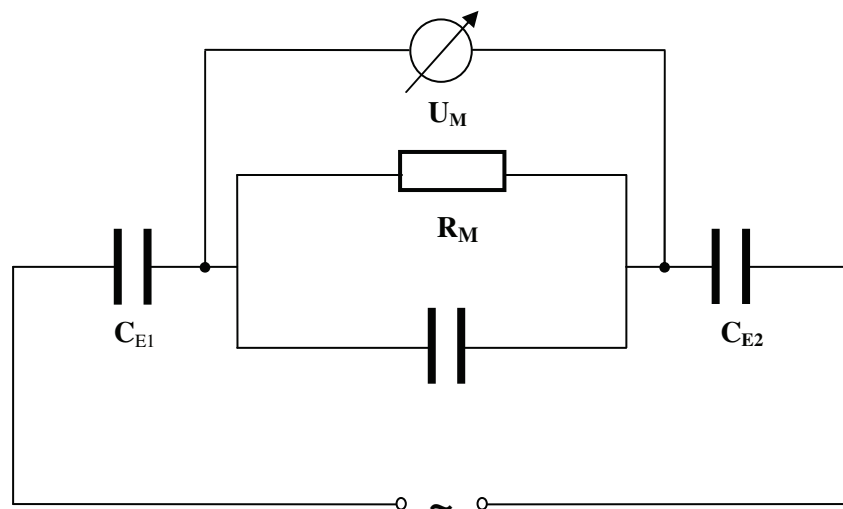


**Figure 1.** Electrical analogy of the setup including two electrodes E1 and E 2 as well as medium M.

But, when one bare electrode and one insulated electrode are used in the setup, the critical frequency  $f_{cr}$  is comparatively reduced to approximately 150 kHz, at which the voltage

fraction of insulated electrodes is less than 0.5. This implies that the insulated electrodes could decrease the danger of electrical shock and provide electrode fouling protection. However, the energy cost from much higher frequency and output voltage requirements will also be proportionally higher. With one bare electrode together with one insulated electrode, the energy cost can be effectively decreased and some advantages of insulated electrodes setup can be reserved. Therefore, the electrode configuration is designed with an insulated wire together with a bare plate to form a cylindrical electric field across the medium. The inhomogeneous electric field around the wire presents much higher electric field strength compared with the electric field near the plate when the voltage of output from the power supply is  $200\text{ V}_{\text{rms}}$  at  $200\text{ kHz}$ .

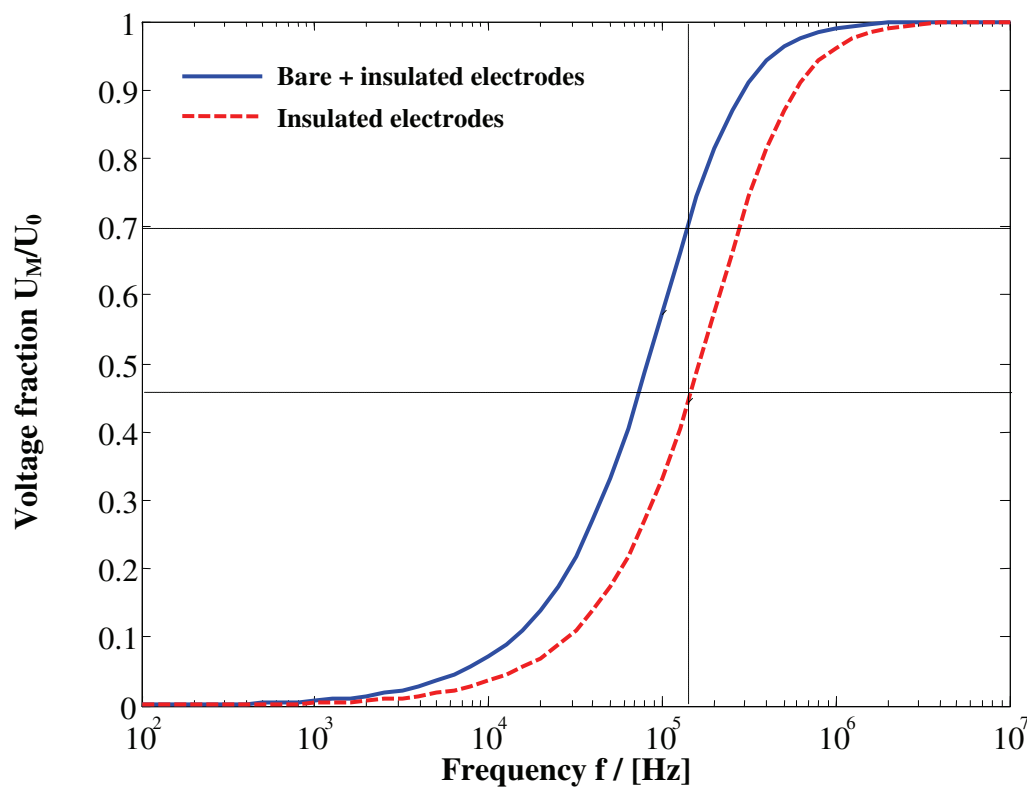


**Figure 2.** Frequency dependency of voltage fraction of voltage across medium  $U_M$  to output voltage  $U_0$ .

## 2.2. Experimental setup and procedures

The experimental setup, shown in Figure 3, was composed of a PC (1), a camera (2) (SONY MODEL XCD-X710), a lens (3) (RODENSTOCK, TELECENTRIC LENS with 114 mm focal length), a power amplifier (4) (FM1290, FM ELEKTRONIK BERLIN), a function generator (5) (VOLTcraft® 7202), the separation chamber (acrylic glass, channel length 200 mm) (6) with two opposite electrodes installed, one bare stainless steel plate (thickness 0.5 mm) (7) and an insulated wire (diameter 0.5 mm) (8) with a 6 mm distance between, as

well as two collectors for collecting gold particle (9) and residual particle (10). Both ends of two electrodes were connected and fixed with adjustments for electrodes distance (12). The whole experimental setup was fastened with fixations (13).

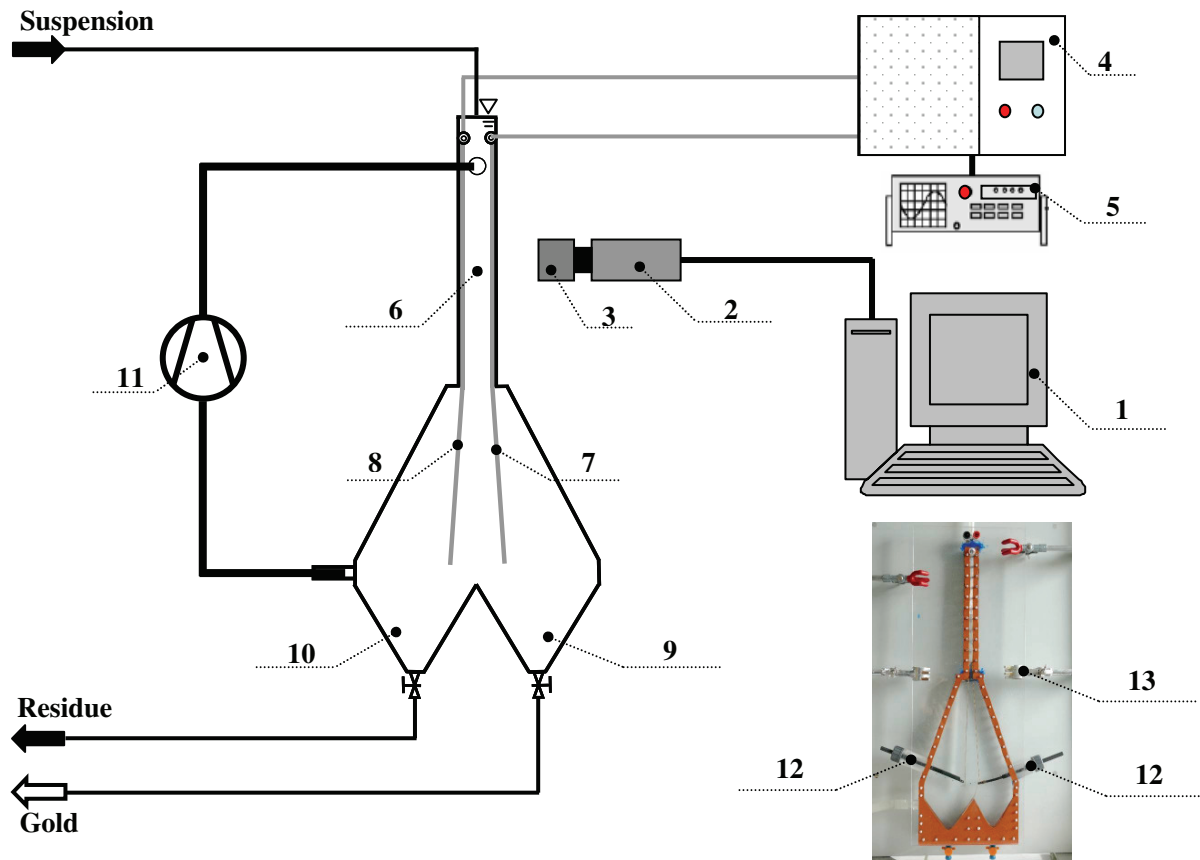


**Figure 3.** Experimental setup.

The power amplifier (4) and the function generator (5) together provided alternating effective voltage approximately from 0 to 280 V, and frequency from 0 to  $10^6$  Hz. The particles mixture investigated was a sample from sand classification. It mainly consists of gold, zircon, and quartz of unknown fractions (Figure 4). The gold particles are ultrathin plates of about  $227.3 \pm 39.7$   $\mu\text{m}$  diameter and  $30.3 \pm 3.5$   $\mu\text{m}$  thickness, i.e. an aspect rate of a 7:1. In each experiment a certain mass ( $0.02 \pm 0.005$  g) was introduced into the separation chamber with a volume of 4.2 mL (6), which was completely filled with demineralized water (i.e. a solid to liquid ration of  $4.8 \pm 1.2$  g/L). Only in “batch operation mode with recirculation” this water was continuously cycled by a pump (DC15/5 HARTON) (11). Using the lens (3) and camera (2), the introduced particles’ motion was simultaneously projected on the monitor and recorded into computer (1). The treatment time, which is constrained by the particle’s settling time, can be estimated to be 10 seconds. Particles settled in the collectors were collected and dried. The gold particles gathered from the samples were counted. The numbers from counted gold particles samples in both collectors were recorded and compared.

As shown in Figure 3 this experimental setup allows a continuous feeding of particles (“continuous operation mode”) applying two independent mass flows. One is recirculated flow of operating liquid, the other is particle suspension feed flow. However, only discontinuous feeding of particles suspension is reported here.

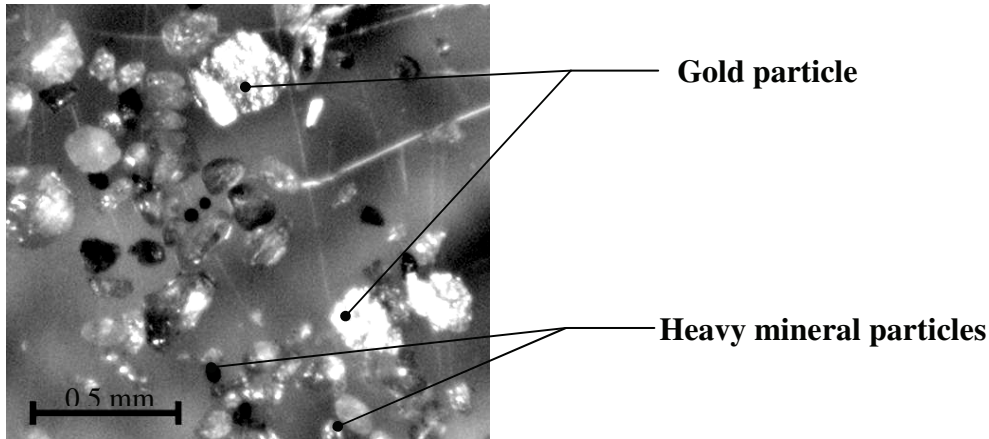


**Figure 4.** Particle mixture, with gold particles (bright plate), and heavy mineral particles (zircon and quartz).

### 3. Results and discussion

Theoretically, in the case of the mineral mixture composing of gold, zircon and quartz particles suspended in distilled water, the simulation of real part of Clausius-Mossotti factors as a function of frequency from Eq (1a) is shown in Figure 5. From Figure 5, the real part of Clausius-Mossotti factor for gold particle in distilled water is always positive and independent of frequency (the magnitude is 1) due to the much higher conductivity and relative dielectric constant of gold compared to distilled water; instead, those of zircon and quartz particles in distilled water are negative (-0.4 for zircon and -0.45 for quartz) and dependent on frequency (when frequency is over 10 kHz). Therefore, the gold particles will alone move towards the stronger electric field (positive DEP), rather the zircon and quartz particles will move towards weaker electric field regions (negative DEP), although the movement speed will be different between these two particles as the frequency is larger than 10 kHz, thereby the gold particles are separated from the mixture. In a designed dielectrophoretic gold separator, according to Eq. 2, the gold particle’s motion velocity will be increased with the increment of electric field. A batch process was examined to verify the reasonability of gold particle separation in the designed system and predict the influences from side effect and constraint. The particles mixture was introduced from the upper inlet of the separation chamber, in which pure water had already been filled. Due to much higher density compared to water, heavy particles mixture settled very fast, while gold plates were attracted to the wire, where the electric field strength is highest. The enhancement of the nonuniformity of electric field around a trapped

single particle will attract other particles to move towards it and form a “pearl-chain”, which is always along the direction of electric field because only like particles could form a pearl chain directed along the electric field [Morgan & Green 2002].

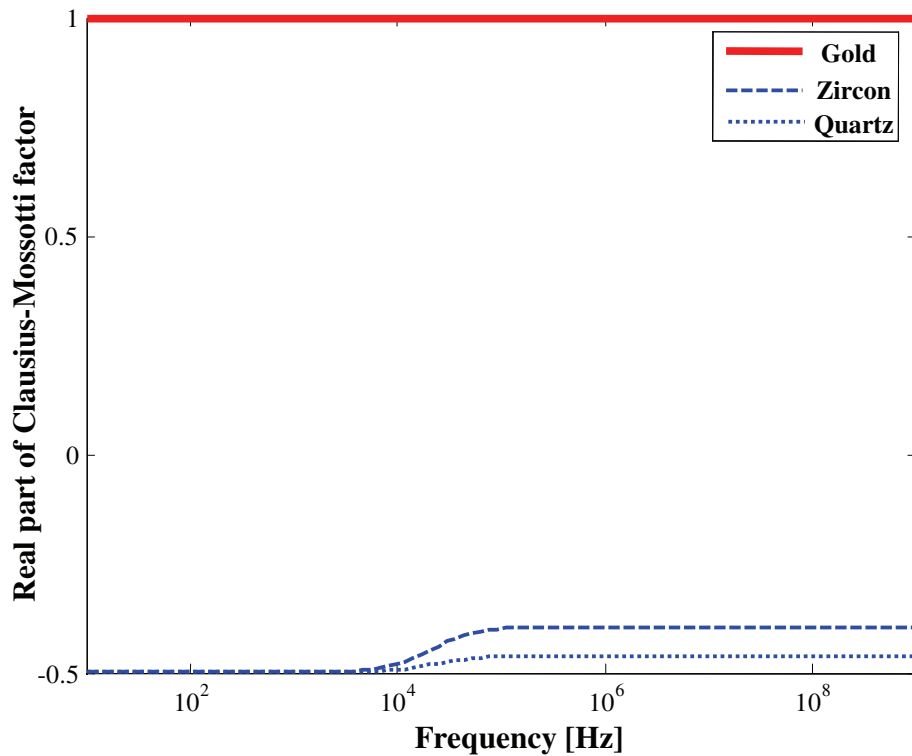


**Figure 5.** Theoretical simulation of the real part of Clausius-Mossotti factor as a function of frequency

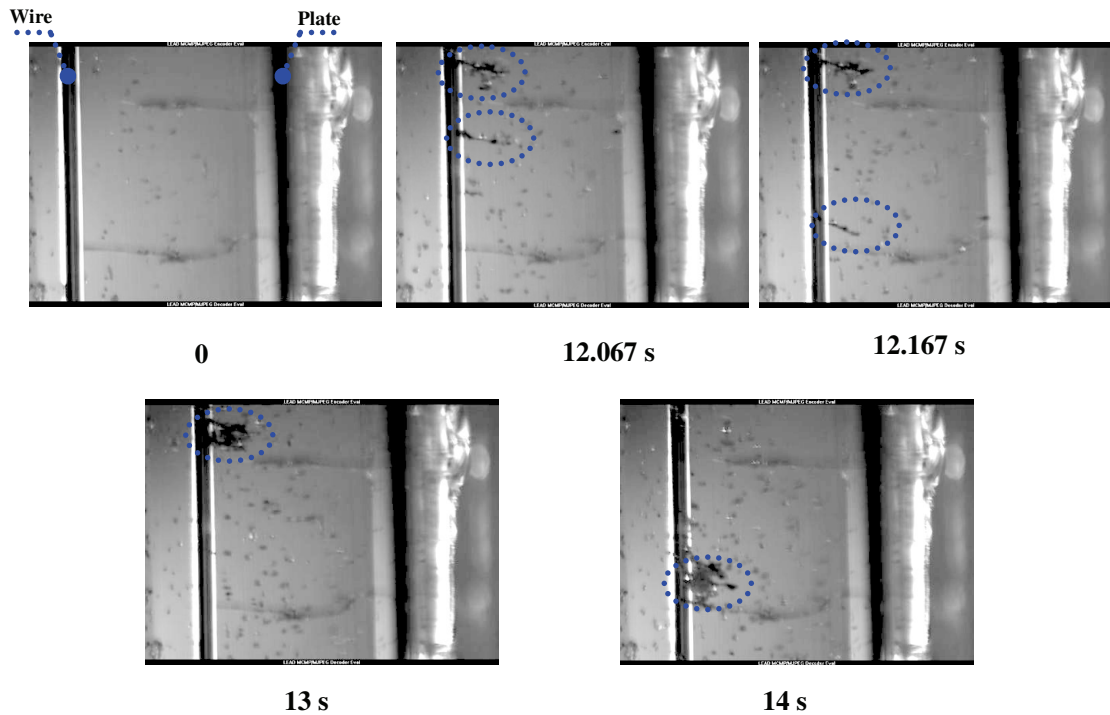




**Figure 6.** Experimental phenomena for particles mixture of gold (dark chained big particles in blue circles), zircon and quartz (gray separated particles) in distilled water with and without electric field (AC voltage output 200 V<sub>rms</sub>, frequency 200 kHz).

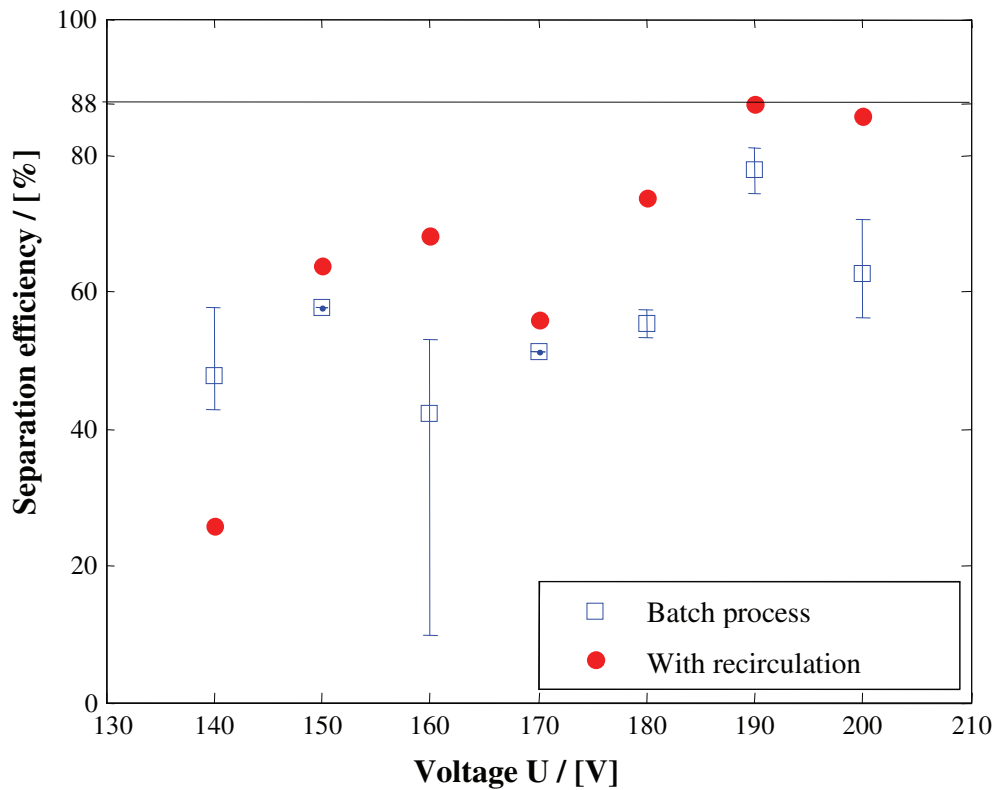


**Figure 7.** Particle separation efficiency comparison between batch (3 repeated experiments) and batch separation process with recirculation (one experiment) as a function of voltage.

The enhancement of the nonuniformity of electric field around a trapped single particle will attract other particles to move towards it and form a “pearl-chain”, which is always along the direction of electric field because only like particles could form a pearl chain directed along the electric field [Morgan & Green 2002]. This pearl-chain formation effect turns out to increase the rate, at which the gold particle is separated from mixture and concentrated. As more gold particles were attracted to close to the wire, they formed chains, which directed along the electric field line, as shown in Figure 6. These gold particles chains settled downwards along the wire into the gold particle collector, thereby being fractionated from the mixture. By counting gold particles in the samples gathered from two collectors, the separation efficiency could be given by comparing the gold particle number in gold collector with the sum of gold particles collected in both collectors. The experimental results are shown in Figure 7 in triplicate in an electric field. The maximum separation efficiency (78 %) was reached when the voltage was 190 V, while the separation efficiency decreased to 63 % (max: 71 %, min: 56 %) at the voltage of 200 V. This phenomenon does not follow theoretical prediction, in which more gold particles will be trapped on the wire of a certain length thereby

being separated from the mixture as higher voltage is applied. This is due to Eq. 2, which gives the velocity of spherical particles that increases quadratically with electric field strength. Accordingly, this is equal to a quadratic shortening of deposition length of the collecting electrode or an increase of separation particles at a certain critical length. The reason of the lowered efficiency could be explained with the electrothermal effect. With the increase of voltage, more gold particles indeed were trapped and formed longer pearl chains. The formed gold particle pearl chain shortened the distance between the opposite electrode (plate) and the chain, which replaces wire as an electrode. This shortened distance together with increased voltage causes much higher temperature difference. Especially in such a closed channel in our experimental system, the heat caused by electricity can not be transferred out of the system. Therefore, in a certain experimental time  $t$  the temperature increment  $\Delta T_t$  of the bulk medium in the channel could be estimated by balancing the inputted electric energy and the internal heat increment

$$\frac{U^2}{R}t = C_p V \rho_M \Delta T_t \quad (4)$$

The temperature increments of the bulk medium modeled as a function of voltage in a 5 minutes experiment were compared within different distance between electrodes, as shown in Figure 8. It is clear that the increment of voltage and decrease of length of gold particle pearl chain will increase the medium temperature so high as to boil the medium from room temperature (20 °C) in an about 5 minutes experiment. As an example, when voltage is 200 V with a 1 mm long pearl chain formed (5 mm distance between tip of pearl chain and the opposite electrode), the temperature of the medium is increased about 95 K, thereby the medium is boiled. Compared with voltage 190 V and about 6 mm distance between tip of pearl chain and the opposite electrode, the medium temperature is increased about 71 K, which could not boil the medium. The bubbles produced by boiled medium will not only retard particles motion towards wire but bring particle upwards by attaching particles on the bubbles. Therefore, when the voltage is much higher and the distance between the pearl chain and opposite electrode is shorter, the medium will be heated much faster, thus the particles motion is influenced. When the voltage is lower than 190 V, number of gold particles trapped on the wire was fewer. Therefore, although the lower heat produced by lower voltage applied, the separation efficiency can not achieve so high efficiency as that with voltage 190 V. In addition, gold separation process can not last longer time caused by the electrothermal effect. As shown in Figure 8, if the experiment lasts longer than 5 minutes with voltage 190 V, the medium will be boiled and gas bubbles will be produced in the channel. In order to solve the

problem caused by the electrothermal effect, a cycling medium system was designed as shown in Figure 3. This separation process with a cycling medium system is named to be batch separation process with recirculation. The medium was cycled with a pump at the volume rate of 2.36 mL/s, resulting in a specific flow rate (cross sectional velocity) of 408.78  $\text{m}^3/(\text{m h})$ , to keep temperature in a moderate range. The volume flow was controlled constant so as to keep the influence from volume flow on the particle motion equally. With this cycling medium system, the heat could be transferred to out of the channel so that the boiling effect was eliminated, while the increased particle settle speed by fluid flow decreased the trapped gold particle number on the wire thereby shortening the length of the pearl chain.

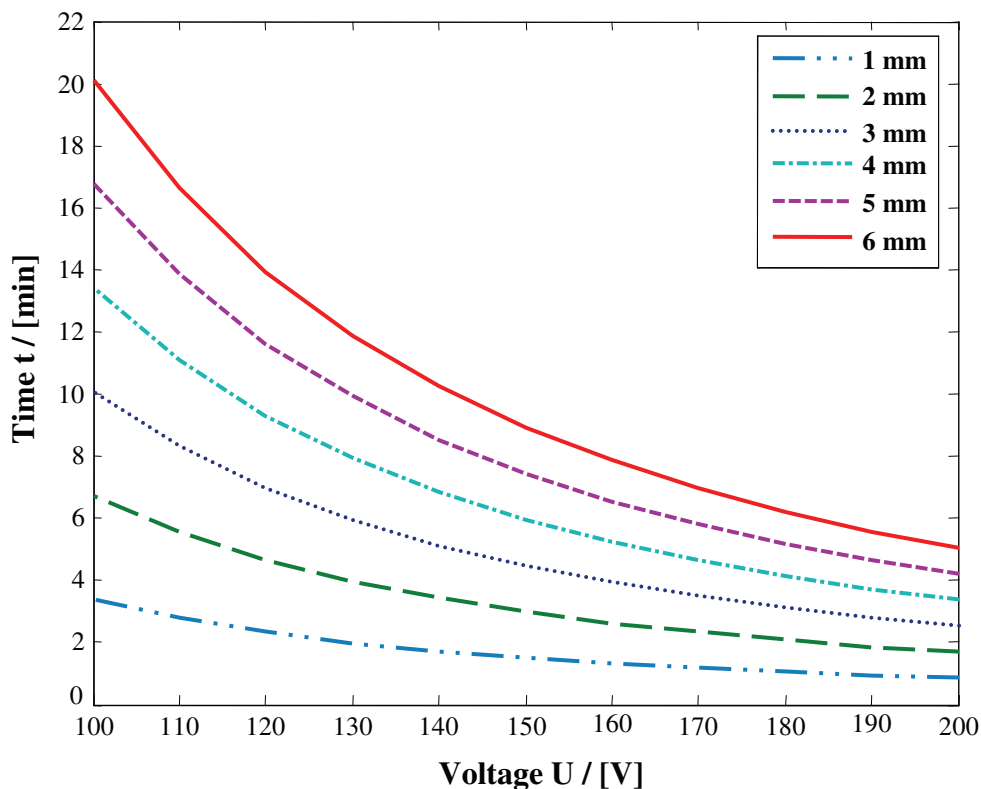


**Figure 8.** Time for heat from electricity to boil (100 °C) the medium from room temperature (20 °C) as calculated from Eq. 4 at different electrode distances.

It can be seen in Figure 7, that the separation efficiencies with voltages 190 V and 200 V are very close. In addition, the separation efficiency at 140 V in the batch separation process with recirculation is lower than that in the batch process. It is caused by the higher settling speed of gold particles increased by fluid flow by cycling medium system compared to the batch process, while the electric field is not strong enough to attract particles to reach the wire before particles sediment into particles collectors. When the applied voltage is between 150 V and 200 V, the separation efficiency of process with cycling medium is higher than that without cycling medium, although the increased particle sedimentation speed could attenuate particle number attached to the wire. As shown in Figure 7, the separation efficiency

of the process with cycling system is increased with the increment of voltage, which fits the theoretical prediction. The maximum separation efficiency reached 88% at the applied voltage of 190 V, which equals to an electric field of 31666.67 V/m.

## Conclusion

In this work, we present a novel separation method without a further pretreatment to fractionate gold particle from a mineral mixture that decreases the possibility of environmental pollution through toxic substances down to zero. Dielectrophoresis (DEP) as the main separation technology in the gold separation was verified to be reasonable.

The test of the lab-scale DEP separation process, which was investigated in batch operation mode with and without recirculation of liquid and with discontinuous feeding, shows the possibility to achieve 88% gold particle fractionated from the mixture. The separation efficiency depends also on voltage, which showed an optimal range (140 V – 200 V). Recirculation improved the separation efficiency significantly due to cooling. The investigated set-up allows also for continuous separation mode.

In terms of separation efficiency, this new DEP method is comparable to cyanidation, which has been the most efficient gold recovery process so far [Bahrami et al. 2007]. But in contrary to cyanidation, DEP separation is free of hazardous effluents.

In general DEP is constrained by side-effects such as electrothermal and high-pass-filter effect. However in its current set-up DEP separation is limited by Joule heating, which interferes with separation and wastes energy and costs. The presence of other elemental metals would also reduce the separation efficiency. A solution for a low cost and high efficient process would be a high-throughput dielectrophoretic particle separator. Therefore, the channels can easily be numbered up as long as temperature control is considered. An application in pilot scale is intended by the authors.

## Acknowledgement

The authors wish to acknowledge Max-Buchner Forschungsstiftung Deutschland for the financial support in this project work, and Prof. Dr.-Ing. Hermann Wotruba, AMR, RWTH Aachen, for providing with the solid sample.

## Reference

- Bahrami A., Hosseini M.R., Razmi K., An investigation on reusing process water in gold cyanidation. *Mine water environ.*, 2007, 26:191.
- Du, F., Baune, M. and Thöming, J., Insulator-based dielectrophoresis in viscous media – Simulation of particle and droplet velocity. *J. Electrostat.* 2007, 65:452.

Hylander, D.L., Plath, D., Miranda, R.C., Lücke, S., Öhlander, J. and Rivera, A.T.F., Comparison of different gold recovery methods with regards to pollution control and efficiency. *Clean*, 2007, 35 (1):52.

Jones, T.B., *Electromechanics of Particles*, Cambridge University Press: U.S.A., 1995.

Kumar, S, Yoon, S.H., Kim, G.H., Bridging the nanogap electrodes with gold nanoparticles using dielectrophoresis technique. *Current Applied Physics*, 2008, doi:10.1010/j.cap.2007.12.001.

Loewen, W.W., Method of gold separation and gold separation device. U.S. Patent 7,012,209 B2, March 14, 2006.

Morgan, H. and Green, N.G., *AC Electrokinetics: colloids and nanoparticles*. Research Studies Press Ltd: U.K., 2002.

Pethig, R. and Markx, G.H., Applications of dielectrophoresis in biotechnology. *TIBTECH*, 1997, 15, 426.

Pohl, H.A., *Dielectrophoresis*; Cambridge University Press: Cambridge, U.K., 1978.

Ramadan, Q., Samper, V., Poenar, D., Liang, Z., Yu, C., and Lim, T.M., Simultaneous cell lysis and bead trapping in a continuous flow microfluidic device. *Sensors and Actuators*, 2006, B 113-944.

### 3.3. Paper No. 3

#### Dielectrophoretically intensified cross-flow membrane filtration

F. Du<sup>a</sup>, A. Hawari<sup>b</sup>, M. Baune<sup>a</sup>, J. Thöming<sup>a\*</sup>

a, Center of Environmental Research and Sustainable Technology, University of Bremen, Leobener Str., D 28359 Bremen, Germany

b, Dept. of Water Management & Environment, College of Natural Resources & Environment, Hashemite University, P.O.Box 150459, Zarqa, 13115, Jordan

\* Corresponding author, Tel.: +49 421 218-63300 /-63371 Fax.: +49 421 218 8297, Email: thoeming@uni-bremen.de

*This paper was published in the Journal of Membrane Science. The Journal of Membrane Science provides a focal point for “membranologists” and a vehicle for publication of significant contributions that advance the science and technology of membrane processes and phenomena. Its primary emphasis is on the structure and function of non-biological membranes, but papers bridging the gap between non-biological and biological membranes are sought. The 5-year Impact Factor of the Journal of Membrane Science is 3.673.*

#### Abstract

Dielectrophoresis (DEP) is applied for the first time in cross-flow membrane filtration process to enhance the membrane performance and service life. The DEP force allows moving particles independently of their charge in an inhomogeneous electric field. Here a traction of particles opposite to the permeate flow direction was realized alleviating particle fouling and concentration polarization, thereby intensifying the filtration process. The inhomogeneity of the electric field needed was realized using a bare grid electrode as membrane supporter and an insulated plate electrode on the opposite side. An optimized DEP intensified cross-flow membrane filtration process with an applied electric field of 160  $V_{\text{eff}}/\text{mm}$  (ac) and 200 kHz demonstrated 3.3 times longer working time for membrane to have a 50% permeate flux of the initial ( $470 \text{ mL}/(\text{min m}^2)$ ) and an energy consumption of 31.3 kJ.

**Keywords:** Dielectrophoresis, inhomogeneous electric field, intensification of cross-flow membrane filtration, anti-fouling, thermal effect.

#### 1. Introduction

In membrane filtration processes, the permeate flux may decrease significantly and rapidly until a final steady state mainly caused by two phenomena: concentration polarization and fouling [Kyllönen et al. 2005]. Although cross-flow membrane filtration can minimize contact between solid and membrane so as to prolong the service time, fouling is inevitable [Lin et al 2007, Belfort et al. 1994]. Membrane fouling can be minimized by the pretreatment,

the membrane geometry and stacking structure, surface feed-flow velocities, turbulent pulses, sponge balls, backwashes, air splurges, and chemical and biological cleaning protocols [Li et al. 2003, Maatens et al. 1999, Kennedy et al. 1998, Redkar & Davis 1995]. For example, backwashing or backpulsing, often used in industry to reduce fouling and thus enhancing permeate flux for conventional membrane filtration processes, will have to stop the filtration process and need an additional pump to backwash particles sticking on the surface of the membrane [Srijaroonrat et al. 1999, Sondhi et al. 2000, Chai et al. 1999, Crozes et al. 1997]. In addition, chemicals such as detergents and acids or alkalis are often used to clean fouled membranes [Chai et al. 1999]. The chemical cleaning should be minimized or avoided, because the chemicals sometimes damage the membrane materials and cause secondary pollution [Koh et al. 2008]. Although these techniques may somewhat recover the permeate flux, they have drawbacks: stopped process, additional equipment cost, additional energy, and usage of chemicals [Lamminen et al. 2006].

The application of additional force in anti-fouling has been gaining more attentions recently [Kyllönen et al. 2005]. Ultrasonic field as one of anti-fouling methods was used to clean membrane with two primary phenomena: cavitation and acoustical streaming [Kyllönen et al. 2005]. However, the control of erosion and possible damage to the membrane caused by high ultrasonic intensity hinder the application of ultrasound [Kyllönen et al. 2005]. Besides, the bulky ultrasound system together with its difficulty in introducing into a cross-flow membrane filtration caused by the stagnated development of transducer technology is another obstacle for the anti-fouling function of ultrasonic field [Kyllönen et al. 2005].

Manegold [Manegold 1937] as one among the first to study the electrostatic anti-fouling method combined the conventional pressure filtration and electrophoresis (EP). The mechanism of this electrical cross-flow filtration system (ECFF) or cross-flow electrofiltration analyzed by Henry in 1977 [Henry et al. 1977] is based on the EP, which is the movement of a particle with a non-zero net charge produced by the Coulomb force [Morgan & Green 2002]. With the assumption of that most particles suspended in water are charged negatively, the particles can be moved towards an anode electrophoretically, the direction away from membrane. However, the high ion-complexity of feed suspensions prevents its use in many cases and causes too high energy consumption [Kyllönen et al. 2005]. In addition, the application of bare electrodes required by EP will result in an electrochemical reaction, leading e.g. to pH shifts or even worse to toxic by-products, and increase the risks of short circuit and human electric shock [Du et al. 2007]. Particles' dielectrophoretic motion was simulated by Molla and Bhattacharjee to present the opportunity

of dielectrophoresis (DEP) in avoiding fouling effect in cross-flow membrane filtration process [Molla & Bhattacharjee 2005]. With this simulation result, Molla and Bhattacharjee experimentally examined particles levitation in a laboratory setup [Molla & Bhattacharjee 2007]. Although there was no membrane involved in their experiments, the particles trajectory simulated with the experimental setup implicated the potential of DEP in both anti-fouling function and increment of permeate flux [Molla & Bhattacharjee 2005].

The combination of the ultrasonic field and ECFF was examined by Wakeman and Tarleton [Wakeman & Tarleton 1991]. They reported that the permeate flux gained an order of magnitude higher enhancement than the corresponding flux without additional forces [Wakeman & Tarleton 1991]. The effect of EP reported by Sora et al. was presented to be dominant compared to that of the ultrasonic field [Kyllönen et al. 2005]. Although the combined model was proved to give much better result in anti-fouling, this process also combined the drawbacks of both methods as described above. In addition, the inherent hydraulic resistance of clean membrane already commented decreases with increasing temperature, due to lower values of the viscosity of the liquid and the increase of the mass-transfer coefficient according to the film [Benítez 2009]. On the contrary, the fouling resistance increases linearly with temperature, indicating a more severe fouling phenomenon at higher temperature [Benítez 2009].

In this work, we present a novel method to intensify cross-flow membrane filtration that is based on dielectrophoretic motion of particles in inhomogeneous electric field. A lab-scaled dielectrophoretic cross-flow membrane filtration process was designed and experimentally examined for the first time with two different types of membranes: ultrafiltration and microfiltration membranes.

## **2. Dielectrophoresis**

Dielectrophoresis, which has been employed in separating particles mainly in biological industries [Morgan & Green 2002, Du et al. 2007, Pohl 1978, Pethig & Markx 1997], was firstly defined by Pohl as a translational motion of neutral particles caused by dielectric polarization in inhomogeneous electric field [Pohl 1978]. The dipole moment induced in the particle can be represented by two equal and opposite charges at the particle boundary, however when they are not uniformly distributed on the particle surface a macroscopic dipole will be created [Du et al. 2008]. When the dipole is posed in an inhomogeneous electric field, the local electric field strength on each side of the particle will be different, arising a net force referred to as dielectrophoretic force. Thus, a suspended particle in a liquid medium will be induced to move either toward stronger electric field region (positive DEP) or weaker electric



field region (negative DEP), depending upon the different polarizations of particle and liquid medium.

When a spherical particle (radius  $a$ ) suspended in a medium, whose relative dielectric constant (permittivity) is  $\epsilon_M$ , the dielectrophoretic force can be given as [Du et al. 2007],

$$F_{\text{DEP}} = 4\pi a^3 \epsilon_0 \epsilon_M \text{re}[K] (\mathbf{E} \cdot \nabla) \mathbf{E} \quad (1)$$

Where  $\epsilon_0$  is the permittivity of free space with the value of  $8.854 \times 10^{-12} \text{ Fm}^{-1}$ ,  $\text{re}[K]$  is the real part of Clausius-Mossotti factor  $K$ , a parameter defining the effective dielectric polarizability of the particle, and  $E$  is electric field intensity. The Clausius-Mossotti factor is a function of frequency of the electric field, depending upon the particle and medium's dielectric properties and is expressed as,

$$\text{re}[K] = \text{re} \left( \frac{\tilde{\epsilon}_p - \tilde{\epsilon}_M}{\tilde{\epsilon}_p + 2\tilde{\epsilon}_M} \right) \quad (1a)$$

$$\tilde{\epsilon} = \epsilon - \frac{j\sigma}{\omega} \quad (1b)$$

where  $\tilde{\epsilon}$  is the complex permittivity of the particle ( $\tilde{\epsilon}_p$ ) and the medium ( $\tilde{\epsilon}_M$ ), which is a physical quantity to describe the polarisability of a material [Pohl 2002],  $\sigma$  the conductivity,  $\omega$  the angular frequency of the applied electric field ( $\omega = 2\pi f$ ) in which  $f$  is frequency,  $j = \sqrt{-1}$ .  $\nabla|\mathbf{E}|^2$ , the (geometric) gradient of the square of the field intensity, is defined by Pohl and generally applied in DEP to calculate  $(\mathbf{E} \cdot \nabla)\mathbf{E} = |\mathbf{E}|\nabla|\mathbf{E}| \approx \frac{1}{2}\nabla|\mathbf{E}|^2$  with the assumption that the materials are linear isotropic dielectrics [Pohl 2002].

As shown in Eqs. 1 and 1a, the direction of DEP force is dependent upon the difference of permittivities between particle and medium. In other words, if the permittivity of particle is smaller than that of medium, the dielectric motion of particle will direct toward lower electric field region, presenting negative DEP. In aquatic dispersions, the permittivities of particles, except for pure metal, are significantly smaller than the permittivity of water. It means that such particles suspended in aqueous medium will be repelled from the higher electric field. Therefore, with appropriately designed electrode configuration, these particles can be moved away from membrane, and flushed out by the fluid flow in a cross-flow membrane filtration, thereby avoiding fouling. With this method based on DEP, nearly all of particles in suspension can be prevented from depositing on the membrane no matter whether particles are charged or uncharged. In addition, as shown in Eq. (1), the DEP force is more dependent upon the electric field gradient than the voltage applied. When the applied voltages in DEP

and EP systems are identical, the dielectrophoretic motion of particle presents much higher speed than electrophoretic movement [Thöming et al. 2006].

A side-effect often occurs in a DEP system, termed as electrothermal effect, caused by a temperature gradient due to the energy dissipation of internal friction on the medium [Du et al. 2007]. This temperature gradient, which is induced by joule-heating, drives medium to flow in the DEP system, which in turn influences particle's movement [Du et al. 2007]. Especially when the order of magnitude of the characteristic length is above 1 mm, the buoyancy due to joule heating always dominates the fluid flow [Du et al. 2007]. Due to the local density variety caused by the temperature difference, the gravitational body force will drive the fluid flows from higher electric field region to lower electric field region, the identical direction of particle's negative dielectrophoretic movement. This would result in an increased motion speed of particle [Du et al. 2007]. Nevertheless, if the increment of temperature due to joule heating is so high to boil the liquid medium the joule heating in a closed system could interfere with particle's movement and waste energy and costs [Du et al. 2008].

Further, in order to avoid problems often occurring in bare electrode configuration such as electrochemical reactions on electrodes, and risks of short circuit in conductive aqueous medium and human electric shock, an electric insulation system is necessarily installed in the electrode configuration of DEP system. However, the insulation on electrodes together with liquid medium will result in a high-pass-filter effect, which not only limits the DEP application in low frequency region, but increases the energy requirement in a DEP system [Baune et al. 2008]. Therefore, in order to maximize the particle's DEP effect to prevent fouling in cross-flow membrane filtration by minimizing the constraint caused by high-pass-filter effect, a specific electrode configuration for high frequency electric field application was carefully designed. The permeate flux as the main parameter was measured, recorded and evaluated by comparing the permeate fluxes between without and with DEP as an additional process intensification method. A pulsed DEP application is improved to minimize the interference caused by the aggregate of particles on the membrane. The experimental results demonstrate a significant improvement of permeate flux in an optimized dielectrophoretically intensified cross-flow membrane filtration process.

### **3. Experimental setup and procedure**

#### **3.1 Electrode configuration design**

In order to avoid the occurrence of electrochemical reaction, short circuit and electric shock in bare electrodes configuration, one insulated electrode combined with one bare

electrode configuration was applied. It is because an electrode configuration with both electrodes insulated will present a high-pass-filter effect [Du et al. 2008], which only allows high frequency signal pass through the system. The frequency-dependent voltage fraction of voltage across the medium  $U_M$  to applied voltage  $U_0$  is simulated as shown in Figure 1, from which, it is deduced that at low frequency the electric field in the medium tends to zero, meaning that the dielectrophoretic force on particles will tend to zero and no movement will occur. When both electrodes are insulated, the critical frequency,  $f_{cr}$  for electric field to be able to develop across the medium is about 300 kHz. But, when one bare electrode and one insulated electrode are used in the setup, the critical frequency  $f_{cr}$  is comparatively reduced to approximately 150 kHz, at which the voltage fraction of insulated electrodes is less than 0.5. This implies that the insulated electrodes could decrease the danger of electrical shock and provide electrode fouling protection. However, the energy cost from much higher frequency and output voltage requirements will also be proportionally higher. With one bare electrode together with one insulated electrode, the energy cost can be effectively decreased and some advantages of insulated electrodes setup can be reserved. Therefore, the electrode configuration is designed with a stainless steel plate insulated with plastic film (thickness 0.25 mm) together with a bare grid to form a nonuniform electric field across the medium, as shown in Figure 2. When the voltage of output from the power supply is 200 V<sub>rms</sub> at 200 kHz, the inhomogeneous electric field around the bare grid presents much higher electric field strength compared with the electric field near the insulated plate, which can be calculated to be 160 V/mm with 80% voltage developed across the medium, as presented in Figure 1. However, the thickness of insulation film, as one of important parameters, influences the high-pass-filter effect much. The high-pass-filter effect with a doubled thickness of insulation film in an electrode configuration with one bare and one insulated electrodes are identical to that in an electrode with both insulated electrodes. When the thickness of insulation film is reduced to half of original, the voltage developed across the medium can reach 94%, which is much higher than the insulation film used in this experiment. Therefore, further optimization of the electrode configuration to pursue a better performance of electric field by alleviating the influence from high-pass-filter effect is required.

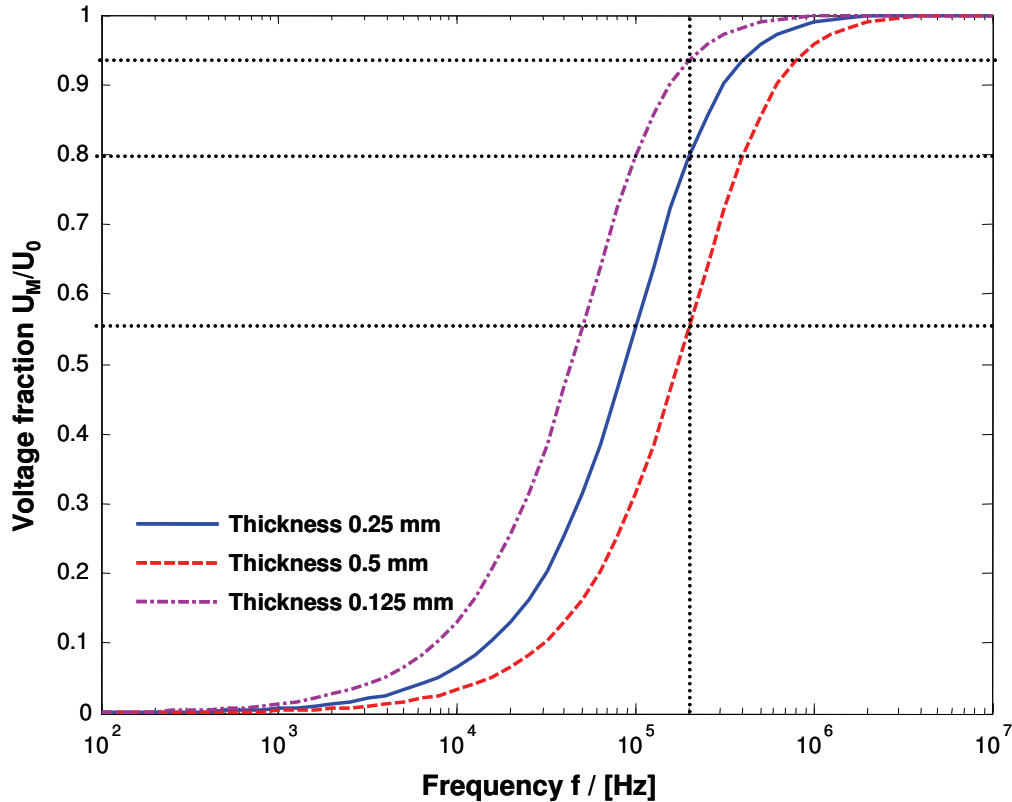


**Figure 1.** Influence of thickness of electrode insulation on the high pass filter effect of the aqueous body in the feed chamber, illustrated as frequency dependency of voltage fraction, i.e. ratio of voltage across medium ( $U_M$ ) and applied voltage ( $U_0$ ) for three cases: (a) one bare and one insulated electrodes with insulation thickness 0.25 mm, (b) both electrodes insulated (with insulation thickness 0.25 mm) or one bare and one insulated electrode with insulation thickness 0.5 mm, and (c) one bare and one insulated electrode with insulation thickness 0.125 mm.

### 3.2 Materials and setup

The experimental setup, shown in Figure 2, was composed of a cross-flow membrane filtration cell (1) (acrylic glass, area of the filtration:  $2.838 \times 10^{-3} \text{ m}^2$ ) and a pump (2) (DC 15/5 HARTON). In the cross-flow membrane filtration cell, a flat membrane (3) (NADIR) was mounted in between one bare grid stainless steel electrode (4) (wire diameter 0.5 mm and opening area  $34 \text{ mm}^2$ ) and one stainless steel plate electrode (5) (thickness 0.5 mm) electrically insulated with a plastic film (6) (thickness 0.25 mm). The distance between the isolation film and the grid electrode was 1 mm. The two electrodes were connected to a power amplifier (FM 1290, FM ELEKTRONIK BERLIN) integrated with a function generator (VOLT CRAFT<sup>®</sup> 7202), which can provide ac effective voltage ranging from 0 to 280 V, and frequency from 0 to  $10^6$  Hz. In the experiments, two different types of membranes were used:

ultrafiltration membrane (FM UC030, 30 kDa, Cellulose, NADIR<sup>®</sup>), and microfiltration membrane (FM MV020, 0.2 $\mu$ m, PVDF, NADIR<sup>®</sup>), respectively.

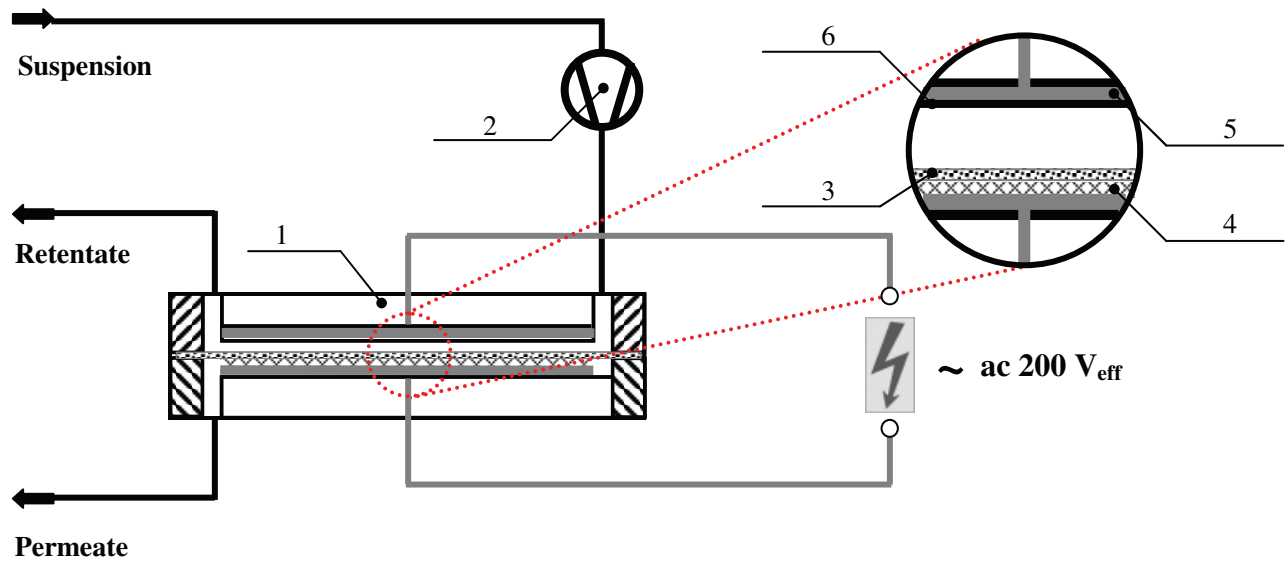


**Figure 2.** Sketch of dielectrophoretically intensified cross-flow membrane filtration process used in experiment. It consists of a filtration cell (1), pump (2), membrane (3), bare grid electrode (4), plate electrode (5), and plastic insulation film (6).

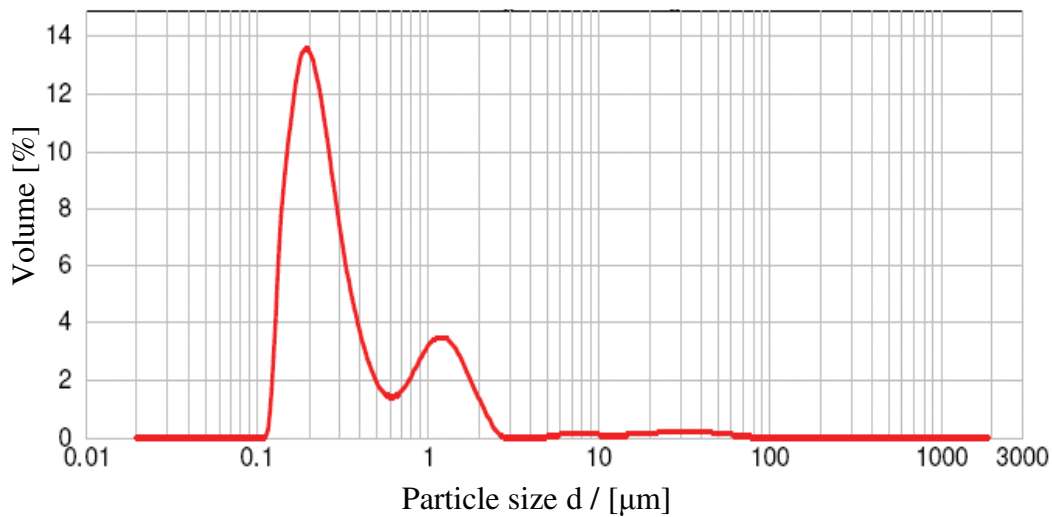


**Figure 3.** Particle size distribution of clay supernatant measured with laser diffraction system.

Clay was mixed with demineralized water to make a clay suspension with a particle concentration of 5 g/L. The supernatant was collected from the original clay suspension after overnight particle sedimentation. The particle size distribution in the supernatant was analyzed with a laser diffraction system, Mastersizer 2000 (MALVERN). The sizes of particles in the supernatant, as shown in Figure 3, are between 100 and 3000 nm. Most of particles in the supernatant have the size of around 200 nm.

The experiments were performed both with and without electric field to compare the function of DEP in ultra- and micro- membrane filtration processes. In the case of with DEP, the clay supernatant was introduced into the cross-flow membrane filtration cell by pump with a specific feed velocity of 40 L/(min m<sup>2</sup>), while the electric field was turned on. Particles were levitated by DEP and drifted away with the medium flow, thus pure water was separated from the suspension by membrane and outputted out of the membrane filtration process as permeate. The permeate and the retentate were collected and volumetrically measured in a certain process time. The time-average fluxes of permeate and retentate were calculated by dividing the recorded volumes of permeate and retentate by the process time.

The processes with continuously applied DEP (continuous DEP) and intervallic application of DEP (pulsed DEP) with two different pulse frequencies: 10 min DEP with electric field after 10 min without DEP (pulsed DEP 10 -10), and 5 min with DEP after 15 min without (pulsed DEP 5 -15), were examined and compared.

In addition, the operational temperatures were measured with thermometer and compared between the feed flow and retentate. The temperature increase was about zero °C when no electric field was applied, which is negligible compared with the 11 °C temperature increase with electric field.

The additional temperature increase, which is caused by electric field, was used to estimate energy consumption. A direct measurement of electric energy input is limited, because both voltage and frequency of the electricity input were too high for a precise measurement.

#### 4. Theoretical simulation of particle trajectories

The theoretical particle trajectory allows for predicting particles motion in the channel of filtration cell (see Figure 2, (1)). The motion of single particles motion was tracked and modeled by combining DEP and hydrodynamic effects,

$$h_i = \left( \frac{C}{h_{i-1}^3} - v_p \right) \Delta t + h_{i-1} \quad (2)$$

$$S = v_F \cdot i \cdot \Delta t \quad (3)$$

where,  $h_i$  is particle motion height orthogonal to the membrane (in the vertical direction) at any a time interval  $\Delta t$ ;  $i = (1, n)$  is an integer that presents particle's transient position during its migration;  $v_p$  is permeate flow velocity;  $S$  is particle's displacement in the horizontal direction;  $v_F$  is feed flow velocity; and  $\frac{C}{h_i^3}$  presents particle's DEP velocity calculated by balancing DEP force (Eq. 1) and drag force with

$$C = \frac{a^2 \epsilon_0 \epsilon_m \text{re}\{K\} \nabla |E|^2}{3\eta} h_i^3 \quad (4)$$

where,  $\eta$  is dynamic viscosity of liquid medium. The (geometric) gradient of the square of the field intensity in our case can be estimated to be,

$$\nabla |E|^2 = \frac{-2U_M^2}{h_i^3 \left( \ln \left( \frac{r_1}{r_2} \right) \right)^2} \quad (5)$$

where,  $r_1$  is the thickness of grid electrode,  $r_2$  is the distance between the grid electrode and the plate electrode. The inhomogeneity of applied electric field can be presented by the unequal electric field strength between grid electrode and plate electrode. The electric field strength around the wires of the grid electrode is higher than that around the plate electrode.

In the inhomogeneous electric field provided by two opposite electrodes, as shown in Figure 2, the particle's migration in the vertical direction (distance to the electrode) can be presented as a function of particle's horizontal displacement caused by feed fluid flow, as shown in Figure 4. When the permeate volume flow  $\dot{V}_p$  is assumed to be constant over entire height yielding 1.3 mL/min, the particles with sizes of 1  $\mu\text{m}$  and 200 nm are levitated by DEP and drifted out of the filtration cell by the feed flow, as presented in Figure 4 (a). The DEP effect decreases with an increase of height  $h_i$  until the DEP velocity is identical to the permeate speed, when the particle reaches the maximum height  $h_n$ , as shown in the 200 nm particle trajectory in Figure 4 (a). Afterwards, particle will move along with the feed fluid flow in the horizontal direction without change of height. The maximum height presented with an equilibrated line in the particle trajectory is dependent upon the particle size and the permeate flow. It increases with particle size and decreases with permeate flow rate, as shown in Figure 4 (b). In addition, if the permeate velocity is identical or larger than that induced by DEP, the particle can not be moved away from membrane but stay on the membrane surface, as shown in Figure 4 (b). With cumulative formation of a particle cake on the surface of membrane permeate flow is reduced. When it falls below a threshold value (which is equal to that induced by DEP) the particle starts to levitate again.

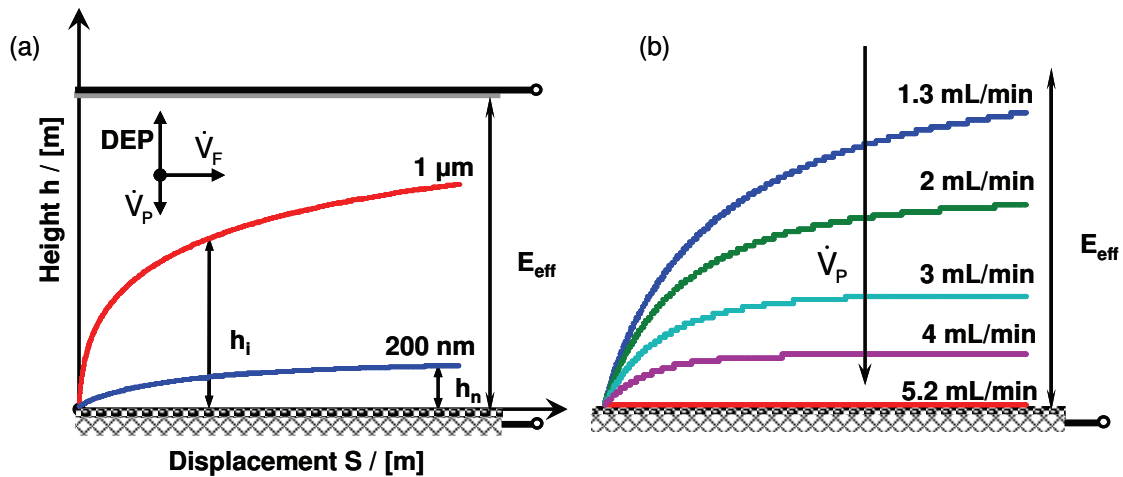


**Figure 4.** Simulation of particle trajectory inside the filtration cell in an inhomogeneous electric field of 160 kV/m at 200 kHz. (a) 200 nm and 1  $\mu\text{m}$  particles migration simulation with permeate flow rate 1.3 mL/min; (b) enlarged 200 nm particle trajectories with different permeate flow rates.

The distribution of DEP force across the membrane corresponds necessarily with electric field. Due to its inevitable inhomogeneity also DEP force is not equally distributed but showing a pattern similar to the grid. The highest strength of the field, for which the calculation was done, is located directly above the wires of the grid. This means that small particles in DEP assisted membrane filtration can be expected to show – under certain conditions – a distribution pattern that looks like a negative image of the grid.

## 5. Experimental results and discussion

The function of DEP in intensifying cross-flow membrane filtration was examined firstly with ultrafiltration membrane. Here fouling is caused by cake forming particles that are about one order or even two orders of magnitude larger compared to pore size. Without DEP, the ultrafiltration membrane was nearly fully covered by deposited clay particles in a process time  $t$  of 80 min, as shown in Figure 5 (a). In the same process time, the coverage of particle on the membrane surface was significantly reduced when DEP was applied, as shown in Figure 5 (b).



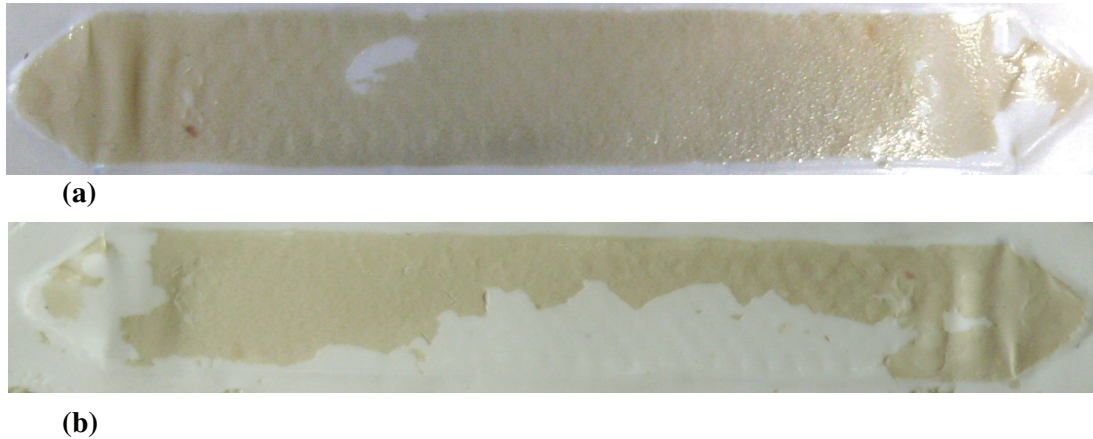


**Figure 5.** Comparison of clay particle cake on the surface of ultrafiltration membrane (30 kDa) after a process time of 80 min without (a) and with (b) DEP. The latter reveals that smithereens of particle cake were removed by DEP force.

When the microfiltration membrane was used in the experimental setup, again there was a formation of particle cake on the membrane. But here, in contrary to the ultrafiltration membrane, the main hindrance effect was the blockage of membrane pores, which were now of nearly the same size as that of particles. This resulted in a further strong reduction of permeate flux and shorter membrane service time. The normalized permeate flux without the intensification from DEP, by comparing with the initial permeate flux measured at 30 min, was reduced very fast in the first 180-minutes process time, then tend to be constant, as shown in Figure 6. When the electric field was continuously applied in the process to drive particles' dielectrophoretic motion, the normalized permeate flux was increased about 35%, and decreased more slowly. Nevertheless, the improvement from DEP was decreased after 330 minutes. The permeate flux with DEP dropped down at the 360 min process time and was getting closer to the steady state permeate flux without DEP, as shown in Figure 6.

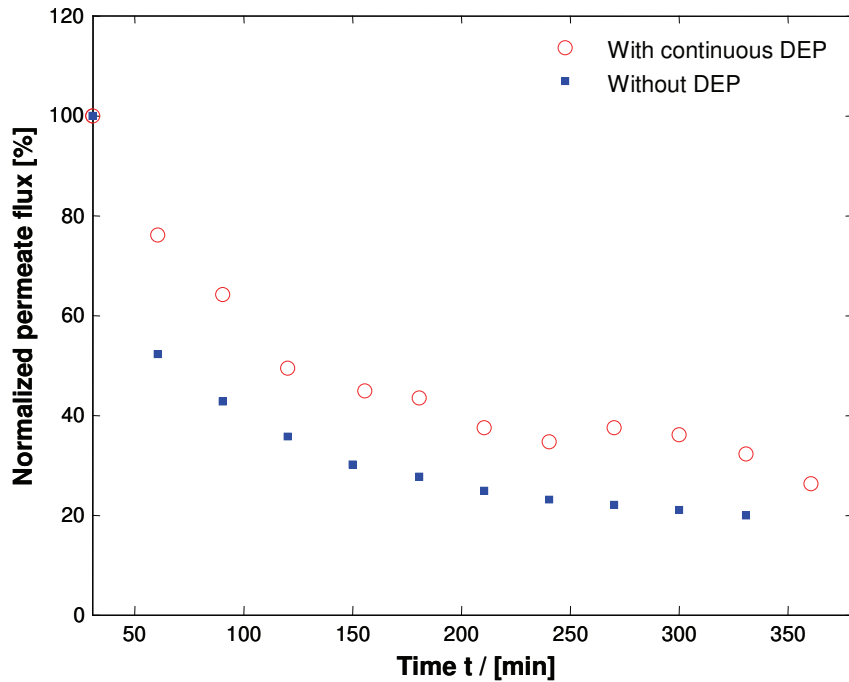


**Figure 6.** Normalized permeate flux with and without continuous DEP in microfiltration (0.2  $\mu\text{m}$ ) process with supernatant of 5 g/L suspension (after overnight sedimentation).

This is because an electrostatic force or van der Waals binding between particles and membrane attracts particles to move towards and adheres them to the membrane when particles are close enough to the membrane. Due to higher permeate flow compared to small particles' DEP velocity, the small particles are moved towards membrane, while big particles are moved away from membrane by DEP, as shown in Figure 7 (a). The electrostatic or van der Waals force arises when particle is very close to the membrane. The force holds small particles on the surface of membrane; therefore, particle adheres on the membrane (see Figure 7 (b)). When additional particle is close enough to the adhered particle on the membrane, the pearl-chain effect occurs by aligning the particles along the electric field thereby forming an agglomerate of particles in the inhomogeneous electric field, as presented in Figure 7 (b). The formed particle agglomerate together with the membrane and grid electrode works as an opposite electrode to the plate electrode, therefore, these particles on the membrane are not in the working region of DEP effect and can not be removed by DEP. Thus particles adhered on the membrane are agglomerated and moved in the direction of feed flow (see Figure 7 (b)) due to surface diffusion or viscous drag of feed flow. The electrostatic force or the van der Waals binding disappears when the electric field is off. Therefore, the agglomerate of small particles keeps its moving direction along the feed flow, while big particle settle down to the agglomerate due to the permeate flow (see Figure 7 (c)). In this period, the agglomerates are

less strongly bound to the membrane and thereby can be scoured more easily by the permeate flow.

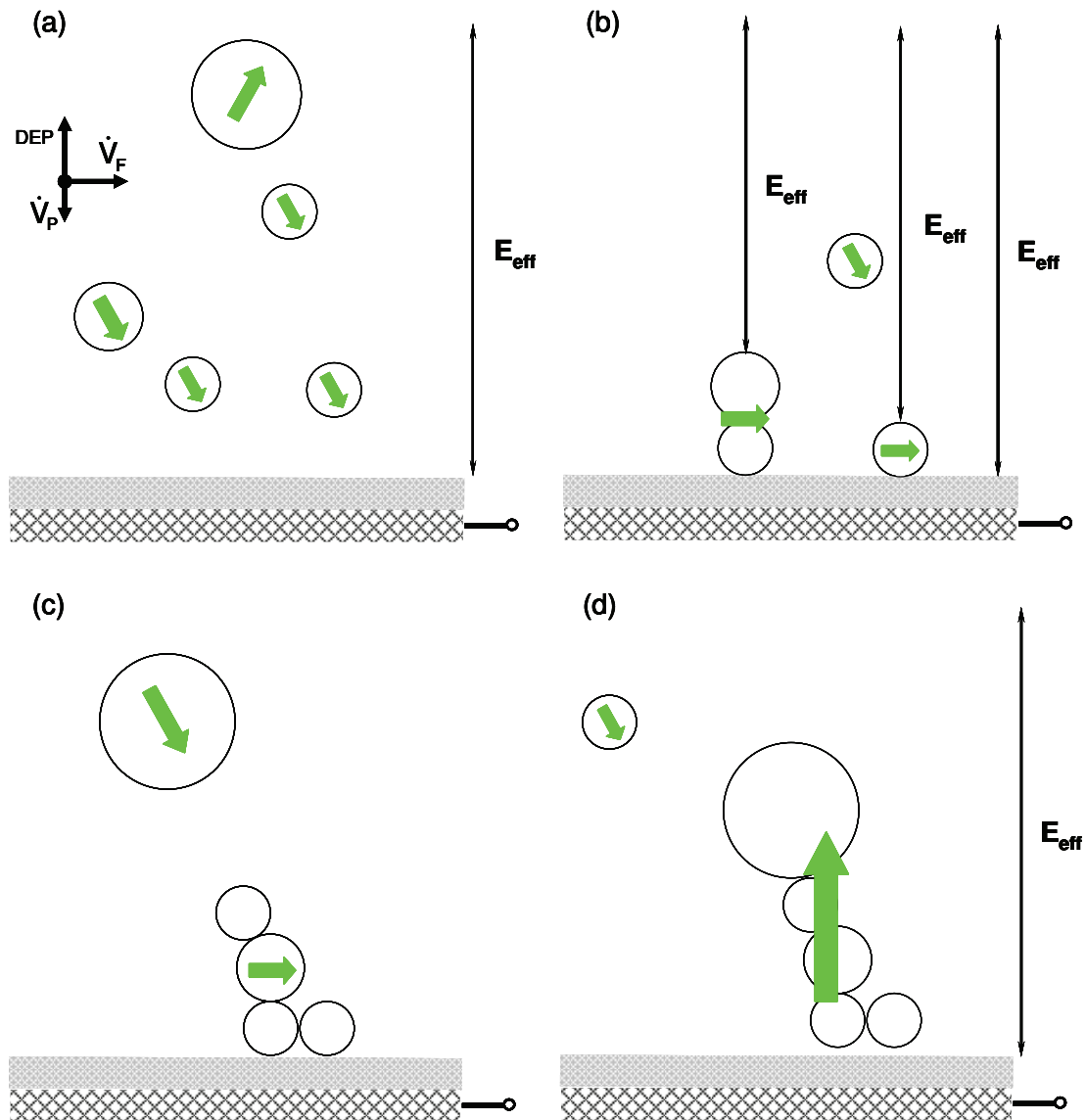


**Figure 7.** Proposed mechanism of particle deposition on membrane-electrode assembly and removal in a pulsed operation mode. (a) Small particles are moved towards the membrane due to permeate flow; for big particle DEP is dominating. Green arrows indicate particle motion directions. (b) Particles which adhere to the membrane become part of the electrode as such they preferentially attract other particles forming pearl-chain. Particles on the membrane are mobile and move due to surface diffusion or viscous drag of feed flow. (c) In the period without electric field, agglomerates are less strongly bound to the surface of the membrane and can be scoured more easily by permeate flow. (d). With electric field, grown agglomerates now experience an increased DEP force, which rises quadratically with particle size being elevated.

When the electric field is switched on again, the closing big particle together with the agglomerate of small particles presents pearl-chain effect and forms a new agglomerate, as shown in Figure 7 (d). The newly formed agglomerate is big enough to be moved away from the membrane by DEP effect at a quadratically increased velocity with the enlarged particle size, as presented in Figure 7 (d). The permeate flow is enhanced due to the removal of particle cake on the membrane. When the permeate flow is increased high enough to dominate DEP effect, the smaller particles will dispose on the membrane to form a particle cake again, which requires another electric-field-off step.

At the beginning of the process with continuous DEP, the permeate speed is higher than particle's DEP velocity, as presented in the particle trajectory simulation Figure 4 (b). Therefore, smaller particles such as 200 nm can not be moved away by DEP but stay on the membrane, until the permeate flow is reduced to be lower than particle's DEP velocity. The electric field in the process with continuous DEP is applied in the whole process so that the electrostatic adhesion of particle on the membrane and pearl-chain effect between particles collect and form a particle cake on the membrane. The formed particle cake together with the membrane and grid electrode works as an opposite electrode to the plate electrode, therefore, these particles on the membrane are not in the working region of DEP effect and can not be removed by DEP, as shown in Figure 7 (b). In the process with continuous DEP, the DEP effect can only work to move big particles and particles which are not sufficiently close to the membrane. Therefore, the permeate flow was increased compared to the process without DEP, but the increase of permeate flow is not very high and decreases much after a certain process time.

To alleviate the adhesion of particles on the surface of membrane caused by the electrostatic force or van der Waals binding, a pulsed DEP was carried out. The pulsed application of DEP was examined in two frequencies: pulsed DEP 10 -10 (10 min with electric field after 10 min without), and pulsed DEP 5 -15 (5 min with DEP after 15 min without). Two steps were involved in a pulsed DEP intensified cross-flow membrane filtration process: with DEP and without DEP, as shown in Figure 8 (a). In the step without DEP, no additional force was applied to levitate clay particles, therefore, more particles deposited on the surface of membrane and the permeate flux was reduced. After this step, the electric field was applied and DEP worked to move particles away from the membrane and drifted by the feed flow thereby cleaning the membrane and recovering the permeate flux. The recovery of permeate flux was very clear when comparing the permeate fluxes between with and without DEP in a pulsed DEP process, as shown in Figure 8. Although the permeate

flux was also reduced with time, the decrease of the permeate flux has been much slower compared to that in the process without DEP. The permeate fluxes in pulsed DEP membrane filtration processes were increased about 38% (pulsed DEP 10-10) and 44% (pulsed DEP 5-15) in average compared to the permeate flux without DEP respectively, which is higher than that in continuous DEP. When the performances of DEP function in anti-fouling are compared between with continuous DEP and with pulsed DEP 5-15, the recovery of permeate flux in process of pulsed DEP 5-15 was much more significant with much lower energy required, as shown in Figure 8 (b). In both cases of pulsed DEP processes, the pulsed DEP 5-15 presented better performance in recovering permeate flux compared to the pulsed DEP 10-10. It is because that the thinner particle cake adhered on the membrane in a shorter time application of electric field is easier to be removed.

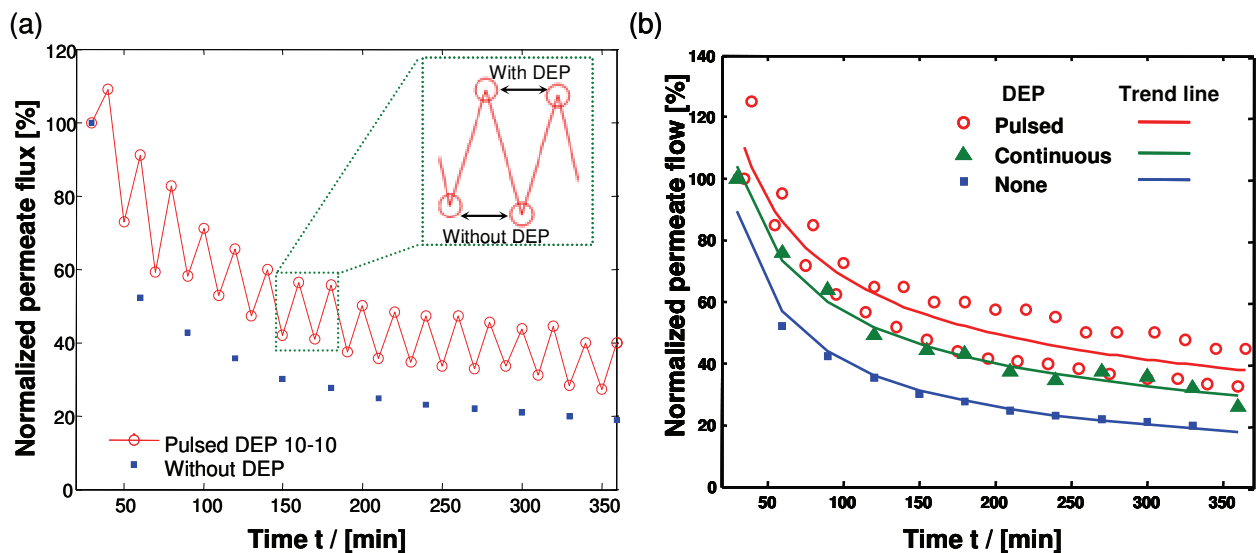


**Figure 8.** Normalized permeate fluxes comparison between without DEP, with continuous DEP and with (a) pulsed DEP 10-10 (on/off periods of 10 minutes) and (b) pulsed DEP 5-15 (on/off periods of 5 and 15 minutes respectively) in microfiltration ( $0.2 \mu\text{m}$ ) processes with supernatant of 5 g/L suspension (after overnight sedimentation).

The recovery of permeate flux caused by DEP can be presented with relative time for reaching 50% permeate flux of the initial compared to the cross-flow membrane filtration process without DEP. With continuous DEP, the 50% permeate flux of the initial was prolonged twice longer than that in a process without DEP, as shown in Figure 9. The process with pulsed DEP 5-15 presented much better performance by keeping 50% permeate flux of the initial 3.3 times longer than that in a process without DEP. The extended working time for membrane to produce 50% permeate flux in DEP intensified cross-flow membrane filtration processes not only improved the productivity of the process but also increased the working life of the membrane.

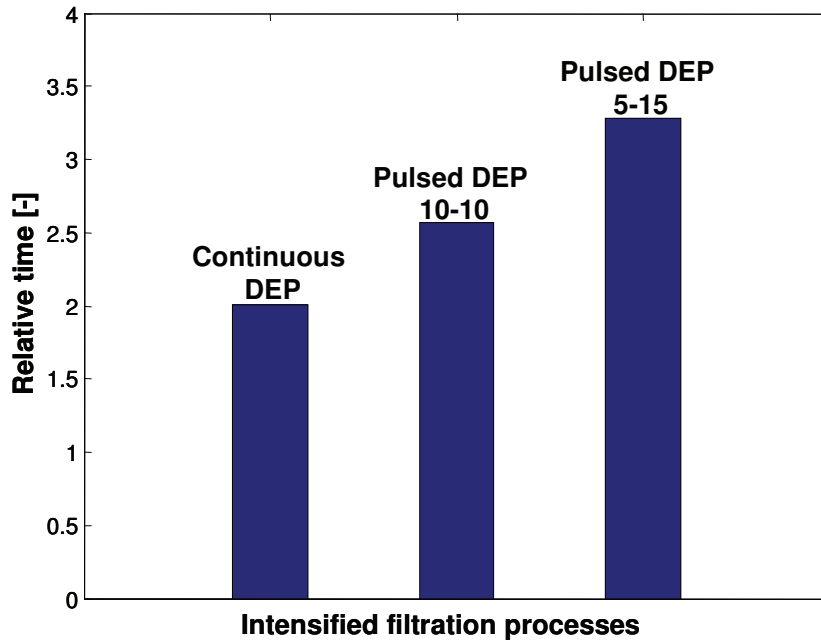


**Figure 9.** Relative time to reach 50% permeate flux of the initial during cross-flow membrane filtration; time of processes with DEP are shown relative to the standard case without DEP; pulsation was performed with on/off periods of 10 minutes (10-10) and with 5/15 minutes (5-15).

The energy consumed in the DEP intensified processes can be calculated with an assumption that all energy outputted by electric field is used to generate joule heat. This is because the input electric energy is converted into joule heating and the energy consumed by a capacitor composed of two opposite electrodes (grid and plate) and the liquid medium. The energy consumption of the capacitor is about  $2.6 \times 10^{-5}$  W, which is negligible compared to the joule heating. The temperatures of retentate were measured and compared between with and without electric field. The electric field increased the temperature of retentate up around 11 °C. Then the joule heat in a certain electric field application time can be given,

$$Q = C_p \rho \dot{V} \Delta T t \quad (6)$$

Where,  $Q$  is the joule heat generated by electric field,  $C_p$  is specific heat capacity of water (4.18 kJ/(kg K) at room temperature),  $\rho$  is the density of water,  $\dot{V}$  is average feed flow,  $\Delta T$  is temperature increment,  $t$  is the heating time in the whole process. In case of stationary system, both joule heating and energy loss of the system via heat flux are in equilibrium allowing for an estimate with about 10% uncertainty. The energy estimation is only valid in our system, which was designed to provide a severe fouling problem and thereby a poor permeate flux, instead of an optimized permeation. Based on Eq. 6, the most efficient DEP intensified process, the pulsed DEP 5-15, consumes the least energy 31.3 kJ, which is about

half of the pulsed DEP 10-10 (62.6 kJ) and about 1/4 of the process with continuous DEP (132.5 kJ). Therefore, the optimized DEP intensified cross-flow membrane filtration process by using pulsed DEP not only improved the intensification function of DEP but also saved energy.

## 6. Conclusion

In this work, a novel method based on dielectrophoresis (DEP) to intensify cross-flow membrane filtration is presented allowing for a higher performance at reduced energy consumption. Simulated particle trajectories in the feed chamber of the filtration cell demonstrate the strong influence of particle size and permeate flow rate on efficacy of DEP application. Comparison of the particle layers left on the membrane surface after a certain process time between of the two cases with and without DEP demonstrates the significance of DEP's potential in anti-fouling. Both ultrafiltration and microfiltration membranes were investigated in a cross-flow lab-scale setup. Since pore diameter of the latter was in the same range as particle size, in this case the observed DEP effect on permeate flux was much stronger. The initial permeate flow rate exceeded a threshold value, above which the small particles were moved to the membrane even in a process with DEP. Close enough to membrane surface, particles might undergo electrostatic or van der Waals binding with the surface of membrane. This adhesion reduced the permeate flow. However, in the case with continuous DEP there was a significant enhancement of permeate flow compared to the process without DEP.

Applying pulsed DEP we observed an improved permeate flow and prolonged membrane service time at a lower energy consumption compared to the process with continuous DEP. This could be explained by an agglomeration of particles on the membrane surface if no electric field is present. According to this hypothesis the agglomeration leads to an alleviation of the volume specific adhesion of particles on the membrane. Furthermore grown in size (radius  $a$ ) particles experience a stronger DEP force  $F_{\text{DEP}}$  with  $F_{\text{DEP}} \propto a^3$  and can be easily elevated. However, further experiments should be performed to deeply understand influences of parameters on functionality and energy consumption in order to optimize the DEP intensification function in cross-flow membrane filtration process.

## Acknowledgement

The authors wish to acknowledge German Research Foundation (DFG) for financial support to Dr. Alaa Hawari's research stay in Germany, and Dr. Norbert Riefler from Institut für Werkstofftechnik, University of Bremen for his help in measurement of particle size distribution.

## Nomenclature

a	particle radius (m)
C	parameter ( $\text{m}^4\text{s}^{-4}$ )
C <sub>p</sub>	specific heat capacity ( $\text{kJ kg}^{-1} \text{K}^{-1}$ )
E	electric field ( $\text{V m}^{-1}$ )
f	frequency (Hz)
F <sub>DEP</sub>	dielectrophoretic force (N)
h <sub>i</sub>	particle motion height (m)
K	Clausius-Mossotti factor (-)
Q	heat (kJ)
r <sub>1</sub>	thickness of grid electrode (m)
r <sub>2</sub>	distance between two electrodes (m)
S	displacement (m)
T	temperature ( $^{\circ}\text{C}$ )
t	time (s)
$\Delta t$	time interval (s)
U <sub>0</sub>	applied voltage (V)
U <sub>M</sub>	voltage cross medium (V)
v <sub>F</sub>	velocity of feed flow ( $\text{ms}^{-1}$ )
v <sub>P</sub>	velocity of permeate flow
$\dot{V}$	volume flow ( $\text{m}^3 \text{s}^{-1}$ )
W	energy (kJ)
$\epsilon_0$	permittivity of free space ( $8.854 \times 10^{-12} \text{F m}^{-1}$ )
$\epsilon_M$	relative permittivity of medium (-)
$\epsilon_P$	relative permittivity of particle (-)
$\eta$	dynamic viscosity (Pa s)



$\rho$	density ( $\text{kg m}^{-3}$ )
$\sigma$	electrical conductivity ( $\text{S m}^{-1}$ )
$\omega$	angular frequency ( $\text{rad s}^{-1}$ )

## Reference

- Baune, M., Du, F. and Thöming, J., Dielectrophoresis–Bridging the scale in modeling and application, in P.J. Plath and E. Hass (Ed.), *Vernetzte Wissenschaften*, Logos Verlag Berlin GmbH, Berlin, 2008, 47-64.
- Belfort, G., Davis, R.H. and Zydney, A.L., The behavior of suspensions and macromolecular solutions in crossflow microfiltration, *J. Membr. Sci.* 1994, 96 1-58.
- Benítez, F.J., Acero, J.L., Leal, A.I. and González, M., The use of ultrafiltration and nanofiltration membranes for the purification of cork processing wastewater, *J. Hazard. Mater.* 2009, 162 1438-1445.
- Chai, X., Kobayashi, T. and Fujii, N., Ultrasound-associated cleaning of polymeric membranes for water treatment, *Sep. Purif. Technol.* 1999, 15 139-146.
- Crozes, G.F., Jacangelo, J.G., Anselme C. and Laine, J.M., Impact of ultrafiltration operating conditions on membrane irreversible fouling, *J. Membr. Sci.* 1997, 124 63-76.
- Du, F., Baune, M., and Thöming, J., Insulator-based dielectrophoresis in viscous media – Simulation of particle and droplet velocity, *J. Electrostat.* 2007, 65 452-458.
- Du, F., Baune, M., Kück, A. and Thöming, J., Dielectrophoretic gold particle separation, *Sep. Sci. Technol.* 2008, 15 3842-3855.
- Henry, J.D.J., Lawler, L.F. and Kuo, C.H.A., A solid/liquid separation process based on cross flow and electrofiltration, *AIChE J.* 1977, 23 (6) 851-859.
- Kennedy, M., Kim, S.M., Muteryo, I., Broens, L. and Schippers, J., Intermittent crossflushing of hollow fiber ultrafiltration system. *Desalination* 1998, 118 175-188.
- Koh, C.N., Wingtgens, T., Melin, T. and Pronk, F., Microfiltration with silicon nitride microsieves and high frequency backpulsing, *Desalination* 2008, 224 88-97.
- Kyllönen, H.M., Pirkonen, P. and Nyström, M., Membrane filtration enhanced by ultrasound: a review, *Desalination* 2005, 181 319-335.
- Lamminen, M.O., Walker, H.W. and Weavers, L.K., Cleaning of particle-fouled membranes during cross-flow filtration using an embedded ultrasonic transducer system, *J. Membr. Sci.* 2006, 283 225-232.

- Li, J., Hallbauer, D.K. and Sanderson, R.D., Direct monitoring of membrane fouling and cleaning during ultrafiltration using a non-invasive ultrasonic technique, *J. Membr. Sci.* 2003, 215 33-52.
- Lin, Y.-T., Sung, M., Sanders, P.F., Marinucci, A. and Huang, C.P., Separation of nano-sized colloidal particles using cross-flow electro-filtration, *Sep. Purif. Technol.* 2007, 58 138-147.
- Maatens, A., Swart, P. and Jacobs, E.P., Feed water pretreatment: methods to reduce membrane fouling by natural organic matter, *J. Membr. Sci.* 1999, 163 51-62.
- Molla, S. and Bhattacharjee, S., Dielectrophoretic levitation in the presence of shear flow: implications for colloidal fouling of filtration membranes, *Langmuir* 2007, 23 10618-10627.
- Molla, S.H. and Bhattacharjee, S., Prevention of colloidal membrane fouling employing dielectrophoretic forces on a parallel electrode array, *J. Membr. Sci.* 2005, 255 187-199.
- Morgan, H. and Green, N.G., *AC Electrokinetics: Colloids and Nanoparticles*, Research Studies Press Ltd., Hertfordshire, 2002.
- Pethig, R. and Markx, G.H., Applications of dielectrophoresis in biotechnology. *TIBTECH* 1997 15 426.
- Pohl, H.A., *Dielectrophoresis*, Cambridge University Press, Cambridge, 1978.
- Redkar, S.G. and Davis, R.H., Enhancement of crossflow microfiltration performance using high frequency reverse filtration. *AIChE J.* 1995, 41 501-508.
- Sondhi, R., Lin, Y.S. and Alvarez, F., Crossflow filtration of chromium hydroxide suspension by ceramic membranes: fouling and its minimization by backpulsing, *J. Membr. Sci.* 2000, 174 111-122.
- Srijaroonrat, P., Julien, E. and Aurelle, Y., Unstable secondary oil/water emulsion treatment using ultrafiltration: fouling control by backflushing, *J. Membr. Sci.* 1999, 159 11-20.
- Thöming, J., Du, F. and Baune, M., Dielectrophoretic separation of oil-water-solid dispersions–Selectivity and particle velocity, *Fresenius Environ. Bull.* 2006, 15 (7) 687-691.
- Wakeman, R.J. and Tarleton, E.S., An experimental study of electroacoustic crossflow microfiltration, *Chem. Eng. Res. Des.* 1991, 69 387-397.

### 3.4. Paper No. 4

#### Dielectrophoresis – Bridging the scale in modeling and application

Michael Baune, Fei Du, Jorg Thöming

UFT, Section of Process Integrated Waste Minimization, University of Bremen,  
Leobener Str., D 28359 Bremen, Germany

*This paper was published in a book entitled “Vernetzte Wissenschaften”. The book “Vernetzte Wissenschaften” was edited by P.J. Plath and E. Haß for a general discussion collected and connected scientific works from interdisciplined subjects in physics, chemistry and social science.*

#### Abstract:

Dielectrophoresis (DEP) is an electro-kinetic separation process which is based on dielectric polarization effects in nonuniform electric field. DEP is currently used for analytical purposes of submicron particles, but it shows also high potential for separating and handling larger particles suspended in non-aqueous and even aqueous liquid. In this article, an overview of the theory of DEP is given as well as a demonstration of how DEP can be used for particle fractionation by adjusting the dielectric properties of materials and frequency and electric field strength of electric field. Additionally, two frequently occurring side effects, electrothermal and high-pass-filter effects, are introduced, demonstrated in case studies and discussed. Finally the potential experimental applications of DEP technique in scaled-up systems are prospected and discussed.

#### Introduction

Dielectrophoresis (DEP), which was firstly termed and defined by Pohl [Pohl 1978], describes the translational motion of neutral particles caused by dielectric polarization effects in nonuniform electric field. It must be distinguished from electrophoresis, which is a motion caused by free charges carried by the particle. Its direction depends upon the polarity of the free charge in a given electric field.

DEP technique has been developed and applied in separating [Pohl 1978, Thöming et al. 2006, Morgan & Green 2002, Castellanos et al. 2003], trapping [Chou et al. 2002, Green et al. 1997, Muller et al. 1996], and handling [Mueller et al. 1999] bioparticles principally in micron and sub-micron scale biotechnology. Besides, although DEP applications in preparative and large scale have not been developed yet, its potential in separating, trapping, fractionating, and handling particles is tremendous.

The physical principles of DEP are already well understood: particles are polarized when an electric field  $E$  is superimposed. The polarization of a spherical particle with free charge lying in an electric field, presents the deformation of double layers of the free charges (Figure 1 b), differently from dielectric polarization of neutral particle (Figure 1 a). The dipole moment  $P$  induced on particle caused by dielectric polarization can be represented by equal but opposite charges nonuniformly distributed on the particle boundary.

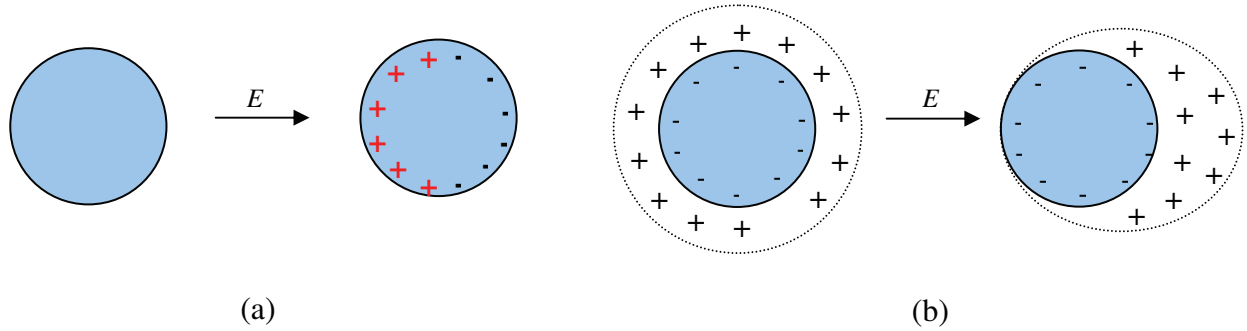


**Figure 1.** Polarization comparison between neutral (a) and charged (b) particles [Thöming et al. 2006].

If the electric field  $E$  is inhomogeneous, the local electric field and resulting forces on both sides of the particle will be different. A net force termed as dielectrophoretic force, will arise and is expressed to be [Morgan & Green 2002]:

$$F_{\text{DEP}} = (\mathbf{P} \cdot \nabla) \mathbf{E} \quad \text{Eq. 1}$$

From Eq. 1, the dielectrophoretic force is zero when the electric field is not inhomogeneous. For a spherical particle of radius  $r$  suspended in a dielectric medium, the dipole moment  $P$  depends upon the dielectric and electric properties of particle and medium and is given as [Morgan & Green 2002],

$$P = \frac{4}{3} \pi r^3 \alpha E \quad \text{Eq. 2}$$

where  $\alpha$  is effective polarization, which is a function of dielectric and electric properties of particle and medium given in Eq. 3,

$$\alpha = 3\epsilon_M \left( \frac{\tilde{\epsilon}_p - \tilde{\epsilon}_M}{\tilde{\epsilon}_p + 2\tilde{\epsilon}_M} \right) = 3\epsilon_M \tilde{f}_{\text{CM}} \quad \text{Eq. 3}$$

$$\tilde{\epsilon} = \epsilon - \frac{j\sigma}{\omega} \quad \text{Eq. 4}$$

where  $\epsilon_M$  is permittivity of medium,  $\tilde{\epsilon}$  is the complex permittivity of the particle ( $\tilde{\epsilon}_p$ ) and the medium ( $\tilde{\epsilon}_M$ ),  $\tilde{f}_{\text{CM}}$  is Clausius-Mossotti factor, which is a function of frequency of electric field and describes the effective permittivity of a particle with a relaxation time,  $\sigma$  is

the conductivity,  $\omega$  is the angular frequency of the applied electric field ( $\omega=2\pi f$ ) in which  $f$  is frequency,  $j = \sqrt{-1}$ .

Hence time averaged dielectrophoretic force can be expressed to be [Pohl 1978]:

$$F_{DEP} = 2\pi r^3 \epsilon_0 \epsilon_M \operatorname{re}[\tilde{f}_{CM}] |\nabla|E|^2 \quad \text{Eq. 5}$$

where  $\epsilon_0$  is the permittivity of free space with the value of  $8.854 \times 10^{-12} \text{ F m}^{-1}$ ,  $\operatorname{re}[\tilde{f}_{CM}]$  is the real part of Clausius-Mossotti factor varies between +1 and -0.5, and  $(E \cdot \nabla)E = |E|\nabla|E| = \frac{1}{2}\nabla|E|^2$ , in which  $\nabla|E|^2$  is the (geometric) gradient of the square of the field intensity, which was defined by Pohl [Pohl 1978] and generally applied in DEP with the assumption that the materials are linear isotropic dielectrics. The Eq. 5 can tell us that dielectrophoretic force is dependent upon the dielectric and electric properties of particle and medium, volume of particle and the electric field gradient. In addition, depending upon the polarizability difference between particle and medium, which is described in the real part of Clausius-Mossotti factor, the motion of particle suspended in a medium will be either be towards lower electric field (negative real part of Clausius-Mossotti factor), negative dielectrophoresis (nDEP) shown in the Figure 2 (a); or towards higher electric field (positive real part of Clausius-Mossotti factor), positive dielectrophoresis (pDEP) shown in the Figure 2 (b). As an example shown in Figure 2, a simple inhomogeneous electric field can be provided by a T-form electrode configuration.

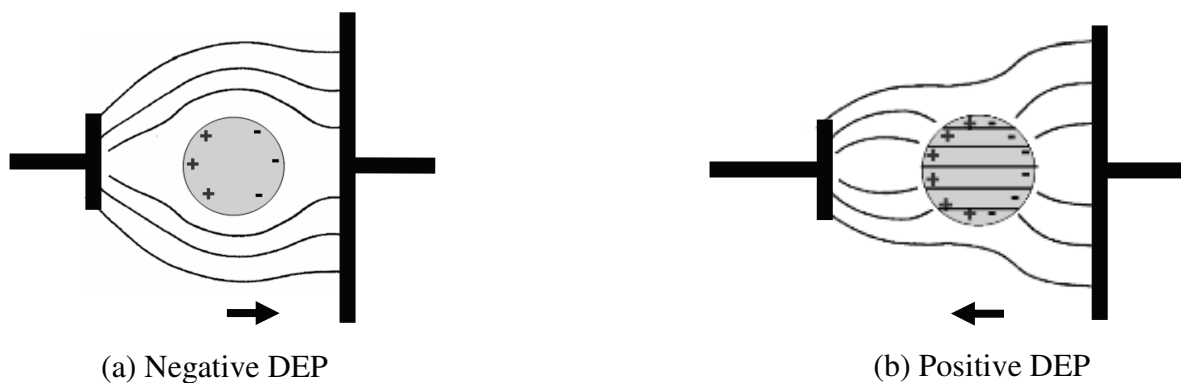


**Figure 2.** Principle of dielectrophoresis - motion of a polarized particle in an inhomogeneous electrical field towards low (a) and high (b) electric field region corresponds to negative DEP (nDEP) and positive DEP (pDEP), respectively.

A spherical particle suspended in a liquid medium will experience gravitational and buoyancy force in the direction vertical to the surface of the medium, and dielectrophoretic force and drag force in the direction horizontal to the surface of the medium, if the particle is

large enough to neglect the Brownian effect, which is proportional to the inverse of particle's radius. By ignoring the vertical forces on the particle and balancing the dielectrophoretic force and drag force, the dielectrophoretic velocity can be given,

$$v_{DEP} = \frac{r^2 \varepsilon_0 \varepsilon_M \operatorname{Re}[\tilde{f}_{CM}] \nabla |E|^2}{3\eta_M} \quad \text{Eq. 6}$$

where  $v_{DEP}$  is the dielectrophoretic velocity,  $\eta_M$  is the dynamic viscosity of the medium. In Eq. 6, the system is assumed to be steady, the medium is assumed to be static and the Reynolds number is assumed to be low enough to keep the motion of particle in the Stokes-regime. Hence the dielectrophoretic motion is dependent upon the Clausius-Mossotti factor, which is a function of frequency of the electric field and dielectric properties of particle and medium, the size of particle, the electric field, and the fluid properties. In comparison, the motion caused by electrophoresis  $v_{EP}$  is dependent upon the zeta-potential  $\zeta$ , electric field, electric property of medium and the fluid property of medium, as shown in Eq. 7,

$$v_{EP} = \frac{\varepsilon_0 \varepsilon_M \zeta E}{\eta_M} \quad \text{Eq. 7}$$

Nevertheless, many effects do influence the dielectrophoretic motion. For example, the high electric field gradient used to drive the dielectrophoresis will always generate thermal field thus initiating fluid motion [Castellanos et al. 2003], which was assumed to be static in the Eq. 6.

### Thermal effects in DEP

In principle, DEP is superimposed by the thermal effects that are always present. They are typically caused by both high electric field strength used to drive particle's motion, and external heat sources such as the incident light used for the observation of the micro-devices. It is possible to at most reduce the thermal effects caused by the latter reason by using a cold light source instead of the light on the microscope [Du et al. 2007]. The joule heating generated by the high electric field strength always forms a temperature field that depends on the boundary conditions within the system, thus initiating fluid flow. There are generally two types of joule heating induced fluid flow: electrothermal flow (EF) and electrothermal induced buoyancy (EB). Both the electrothermal effects (ETE) are always involved in a DEP system,

$$ETE = EF + EB \quad \text{Eq.}$$

8

In the considered systems, the ETE gives rise to electrical forces induced by the variation in the conductivity and permittivity of the suspending medium [Castellanos et al.

2003]. It is especially pronounced when the microelectrodes and microchannels are used, i.e. for a characteristic length below 1 mm [Du et al. 2007], the electrothermal flow is always dominant. With the assumption of negligible electrode polarization due to high enough frequency, the fluid flow velocity generated by electrothermal flow can be given as [Castellanos et al. 2003],

$$v_{Max} = 5.28 \times 10^{-4} \frac{|M| \varepsilon_M \sigma_M U^4}{T k \eta_M l} \quad \text{Eq. 9}$$

$$|M| = \frac{\left(\frac{T}{\sigma_M}\right)\left(\frac{\partial \sigma_M}{\partial T}\right) - \left(\frac{T}{\varepsilon_M}\right)\left(\frac{\partial \varepsilon_M}{\partial T}\right)}{1 + \left(\frac{\omega \varepsilon_M}{\sigma_M}\right)^2} + \frac{1}{2} \frac{T}{\varepsilon_M} \frac{\partial \varepsilon_M}{\partial T} \quad \text{Eq. 10}$$

where  $v_{Max}$  is the fluid flow caused by electrothermal,  $|M|$  is a dimensionless factor (between 0.6 and 6.6 when temperature is 300 K) [Castellanos et al. 2003],  $T$  is the temperature of environment,  $U$  is the voltage,  $k$  is the thermal conductivity of the medium,  $l$  is the characteristic length of the electrode configuration. From both equations 9 and 10, the fluid flow induced by electrothermal is a function of voltage applied in the system, the geometry of the system, temperature of the operation, the frequency of the electric field as well as electric, thermal and hydrodynamic properties of fluid.

When scaling up the process from micron to millimeter scale, i.e. with increasing the geometry of electrode setup, the power of joule heating increases, since joule heating is generated on the electrodes boundaries and more electric power is applied in a scaled-up DEP system. Additionally, the variation of permittivity and conductivity is much smaller compared to such largely increased magnitude of the geometry of electrode. Hence, when the order of magnitude of the system's characteristic length is above 1 mm, the buoyancy due to joule heating always dominates the fluid flow [Du et al. 2007]. The gravitational body force on a fluid generated by a temperature field is due to the local density change caused by the temperature difference. Hence the buoyancy force can be expressed to be [Du et al. 2007],

$$f_B = \frac{\partial \rho_M}{\partial T} \Delta T g \quad \text{Eq. 11}$$

where  $f_B$  is the buoyancy volume force,  $\rho_M$  is the density of medium and  $g$  is the gravitational acceleration.

The fluid flow  $u$  induced by buoyancy force can be given, by balancing the buoyancy force and drag force [Du et al. 2007],

$$u = U \sqrt{\frac{\alpha g l^3}{V C_p \eta_M R}} \quad \text{Eq. 12}$$

where  $\alpha$  is volume expansion coefficient,  $V$  is volume of medium,  $C_p$  is the specific heat capacity of the medium,  $R$  is the resistance of the whole system. Considering DEP and electrothermal effect (ETE) on a suspended particle, Eqs. 6 and 12 can be combined and the velocity  $v_{DEP}$  of the particles' motion can be expressed as [Du et al. 2007],

$$v_{DEP} = \frac{r^2 \epsilon_0 \epsilon_M \text{re}[\tilde{f}_{CM}]}{3\eta_M} \nabla |E|^2 \pm U \sqrt{\frac{\alpha g l^3}{V C_p \eta_M R}} \quad \text{Eq. 13}$$

In this equation, the first term on the right side represents the motion caused by DEP effects, while magnitude and algebraic signs of the second term represent the speed and the direction of the fluid respectively [Du et al. 2007].

Especially in a closed system, with a liquid volume above about 5 mL, the temperature difference  $\Delta T$  can be found to be above 1 K. Consequently, the fluid flow due to buoyancy will lead to a convective circulation, in which the fluid flow from the higher temperature region (close to the electrode) to the lower temperature region (far away from the electrode) in the upper plane of the liquid and then recirculates back on the lower plane of the liquid at the lower temperature level. Differently, the fluid flow due to electrothermal flow will lead the fluid flows from the lower temperature region (higher permittivity) to the higher temperature region (lower permittivity).

As an example, PVC particles suspended in silicone oil were simulated to indicate the effect from fluid flow caused by joule heating (buoyancy) on particle's motion in a millimeter-scale DEP system, as shown in Figure 3. A similar case was verified experimentally for water droplets as demonstrated elsewhere [Du et al. 2007]. In this case, the PVC particles move towards higher electric field region, a positive DEP effect due to the much higher permittivity of PVC particle than silicone oil. However, the fluid caused by buoyancy flows from higher electric field region to lower electric field region, in other words, the fluid flow is in an opposite direction to the particle's motion due to DEP. Therefore, when the electric field strength is not high enough to generate sufficiently high positive dielectrophoretic force to displace the PVC particles, the PVC particles will be moved in an identical direction to the fluid flow.

Conversely, in the case of negative DEP, the fluid flow increases the particle's velocity. For example, this effect on the polyethylene (PE) particle suspended in silicone oil is presented in Figure 4, by comparing the dielectrophoretic velocity of PE particle's motion



with and without the fluid flow caused by the joule heating effect as a function of particle's size.

In general, the fluid flow caused by joule heating does influence the dielectrophoretic effect and always exists in a DEP system in which very strong electric field is employed.

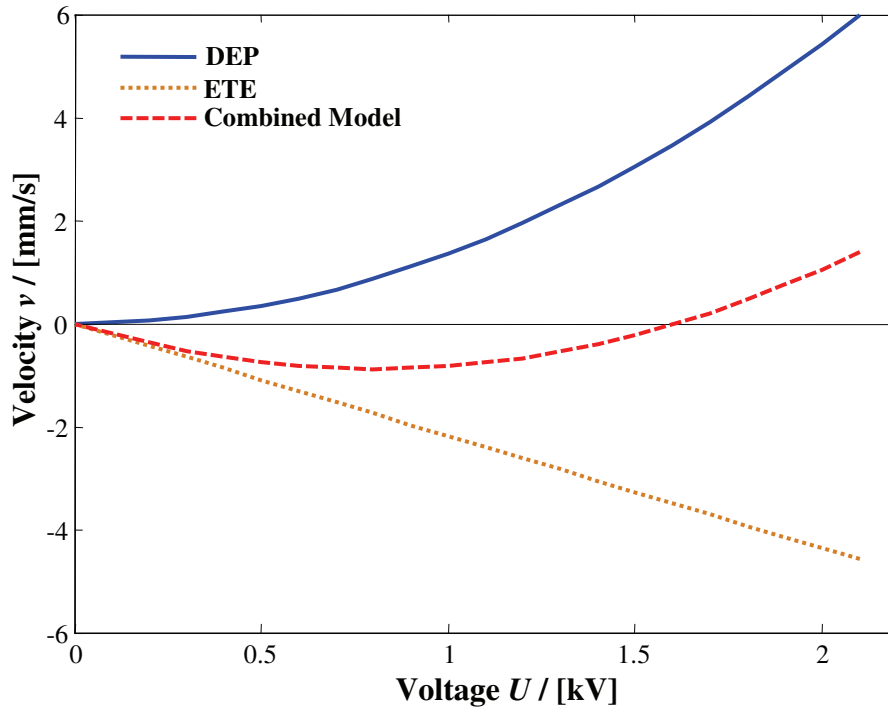


**Figure 3.** Electrothermal effect (ETE) influence on millimeter scale on pDEP. The calculations using Eqs. 6, 12 and 13 were performed for 0.25 mm diameter PVC particle in silicone oil ( $\eta = 20$  mPas,  $\rho_M = 0.96$  g/mL,  $\epsilon_M = 2.9$ ,  $\epsilon_P = 4.6$ ) in a spherical geometry of electrodes setup (characteristic length: 6mm).

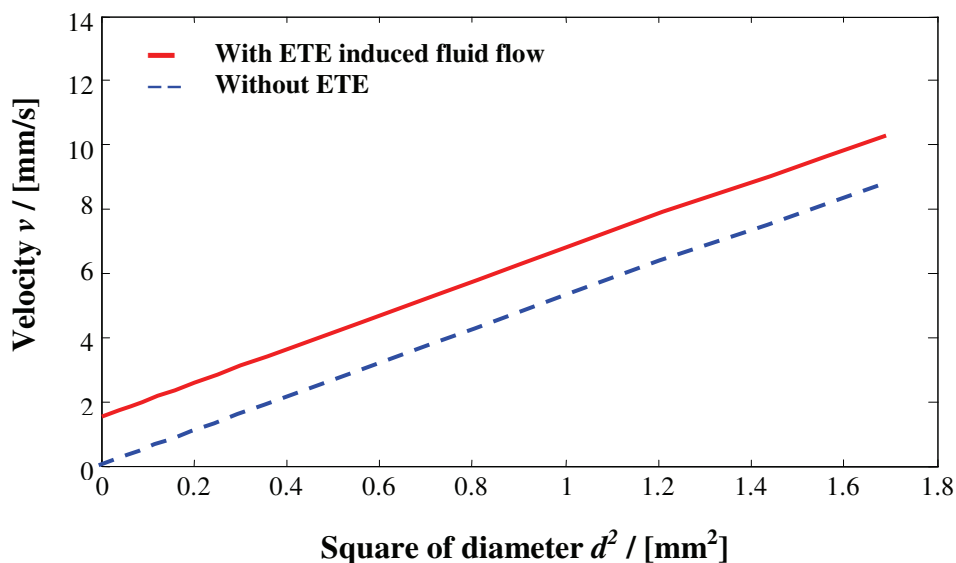


**Figure 4.** Influence of ETE in millimeter scale on nDEP. The calculations using Eqs. 6 and 13 were performed for PE particles of different sizes in silicone oil ( $\eta = 20$  mPas,  $\rho_M = 0.96$  g/mL,  $\varepsilon_M = 2.9$ ,  $\varepsilon_p=2.25$ ) under a certain electric field (applied voltage 700 V DC) in a spherical geometry of electrodes setup (characteristic length: 6 mm).

### High-pass-filter effect in DEP

Due to the strong electric field strength in DEP system, electrical insulation of electrodes can be necessary to avoid the short circuit and electrochemical reaction on electrodes (electrode fouling). This is especially true if a medium is used that shows electrolyte characteristics (like aqueous solutions) or contains such an electrolyte in case of emulsions. The whole DEP system including the insulation films and medium could be represented by an electrical circuit shown in Figure 5, in which two insulation films on the electrodes form capacitors  $C_{i1}$  and  $C_{i2}$  connected in series with a sub-circuit consisting of a resistor  $R_m$  and a capacitor  $C_m$  in parallel. This circuit can block low frequency signals, when the electric field is alternating, but offer a passage to high frequency signals - a typical high-pass-filter effect. In other words, the voltage drop across the medium  $U_m$ , which provides the electric field for DEP, will be too low to drive DEP if the frequency is not high enough. This high-pass-filter effect exists in both micron and millimeter scale DEP systems. Nevertheless, since the scale of the DEP applications drastically influences  $R_m$  and  $C_m$ , the difficulty to handle this effect increases with increasing scales of DEP system. Hence it is important to investigate the voltage fraction of  $U_m$  to the applied voltage from power source  $U_0$  as a function of frequency.

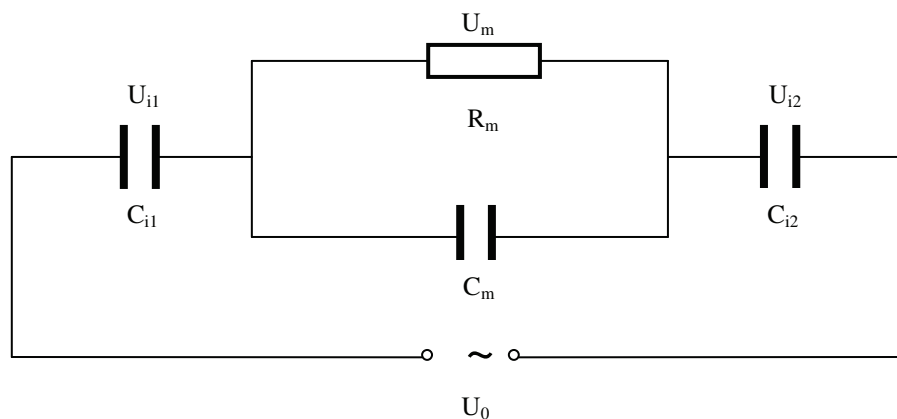


**Figure 5.** Electrical circuit analogy to the insulated DEP system.

Considering that the current across the insulation films  $Z_{i1}$  (impedance of capacitor  $C_{i1}$ ) and  $Z_{i2}$  (impedance of capacitor  $C_{i2}$ ) and the medium  $Z_m$  (impedance of the in parallel

connection of resistor  $R_m$  and capacitor  $C_m$ ) is equal in the ac (alternating current) circuit shown in Figure 5. The voltage fraction  $U_m/U_0$  can be given as,

$$\frac{U_m}{U_0} = \frac{Z_m}{(Z_{i1} + Z_{i2} + Z_m)} \quad \text{Eq. 14}$$

and the impedances as a function of frequency will be presented by,

$$Z_m = \frac{j\omega R_m C_m}{R_m + j\omega R_m C_m} \quad \text{Eq. 15}$$

$$Z_{i1} = \frac{1}{j\omega C_{i1}} \quad \text{Eq. 16}$$

$$Z_{i2} = \frac{1}{j\omega C_{i2}} \quad \text{Eq. 17}$$

Inserting equations Eqs. 15 to 17 into Eq. 14, the voltage fraction can be expressed as a function of frequency. By executing Eq. 14, it will result to function plots shown in Figure 6, which presents an example of high-pass-filter, in which case the voltage fraction increases with the increase of the frequency. The voltage fractions shown in Figure 6 influenced by either insulation material or insulation thickness will even be less than 1 in some cases, which is different from the usual high-pass-filter circuit.

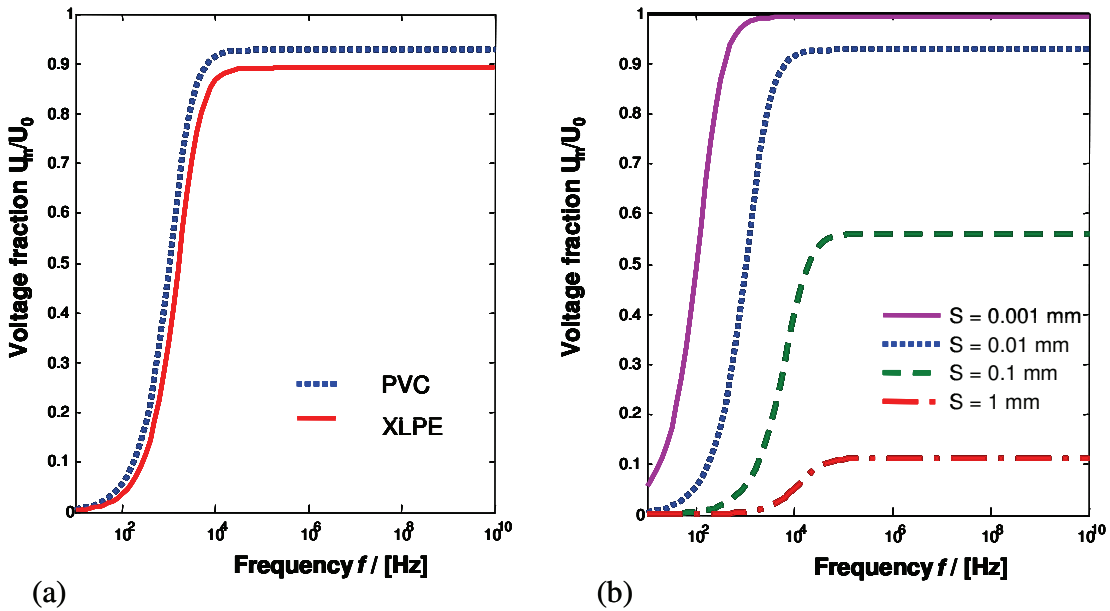


**Figure 6.** High-pass-filter effect in an insulated DEP system, in which the cylindrical electrode configuration is used (medium: pure water). In (a), the effect of materials of insulation (PVC and XLPE) on the voltage fraction is shown, which is effective with respect to DEP. In (b), high-pass-filter effect of PVC insulation material depending on the key factor, the thickness of the insulation,  $S$ .

Furthermore, the resistance and capacitances in the electric circuit shown in Figure 5 are dependent upon both the electrical properties (dielectric constant and conductivity) of insulation material and medium and geometries of electrode configuration and insulation. Therefore, in a given DEP system (with certain electrodes geometry and medium) the material and geometry of the insulation on the electrodes are critical factors to define the range of frequency being able to be applied for effective DEP, as shown in Figure 6.

Moreover, because of the high-pass-filter effect in an ac DEP system, the voltage applied by the power source has to be very high in low frequency range in order to provide high enough electric field to drive DEP. Additionally, in order to avoid the problem caused by high-pass-filter effect, very high frequency must be applied, this will nevertheless cause partial loss of DEP effect due to the dependence on frequency. Therefore, in order to solve the problems caused by high-pass-filter effect in DEP application in practice, the decision of material and geometry of the insulation is crucial.

### DEP potential applications

In biotechnology, the principle of DEP has been well developed and applied to handle bioparticles in microelectrodes setup and microchannels [1-8]. By bridging the DEP between micron and large scale applications, the millimeter scale DEP system was modeled and experimented [9]. In a millimeter scale DEP system, DEP can be applied to fractionate particles mixture (Case 1), separate particles by size (Case 2), separate particles by material characteristics (Case 3), trap particles (Case 4) and auxiliary function in mechanical separation techniques (Case 5).

#### **Case 1: fractionation of particles mixture**

As described above, the direction of particle's movement is dependent upon the real part of Clausius-Mossotti factor, which is a function of frequency and dielectric properties (permittivity and conductivity) of particle and medium. Hence, for a given particle or particle mixture, the particles' dielectrophoretic motion directions can be controlled by frequency of electric field and properties of medium. As an example, the DEP behaviours of a particles mixture composed of latex colloid, metal, and PE particles suspended in pure water are quite different as presented in Figure 7 with a function of frequency. With the difference in particles' dielectrophoretic motion directions corresponding to the signs of real part of Clausius-Mossotti factor, the particle mixture can be separated selectively by controlling the order parameter of frequency. As shown in Figure 7, when the frequency is lower than about 100 kHz, the metal and latex colloid particles present positive DEP behaviour due to their higher conductivity compared to pure water, instead of negative DEP as PE particle.

When the frequency is higher than about 3 MHz, the latex colloid and PE particles show negative DEP effect due to their lower permittivity compared to pure water, instead of positive DEP as metal particle. It means that when the frequency is lower than 100 kHz, the metal and latex colloid particles move towards higher electric field regions opposite direction to the motion direction of PE particle; similarly, when the frequency is higher than 3 MHz the metal particle will still keep their motion direction unchanged, while PE and latex colloid particles move towards weaker electric field. The different DEP behaviours in different frequency ranges grant the chance to selectively separate and fractionate particles mixture.

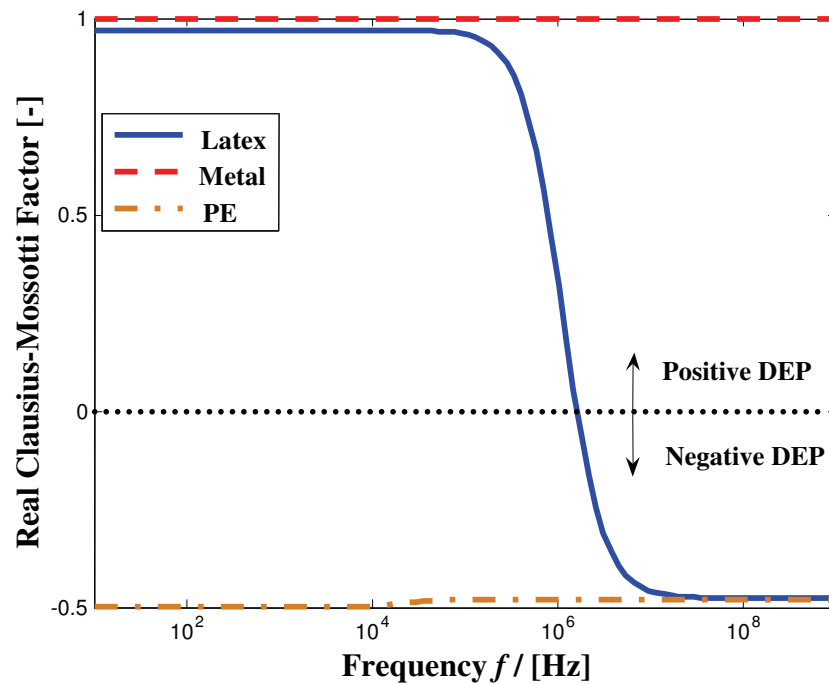


**Figure 7.** Different DEP behaviors of different particles (latex colloid, metal and PE) in pure water.

### Case 2: separation of particles by size

Similarly, since the dielectrophoretic velocity of particle is a square function of particle's size as presented in Eq. 6, the DEP can also be used to fractionate particles with identical properties but different sizes. This is because, together with the thermal effects, the particle's dielectrophoretic velocity varies very much with its size. For example, the water droplets suspended in silicone oil will exhibit a positive DEP due to much higher permittivity of water (78) than that of silicone oil. However, together with the thermal effect, some small water droplets will show a phenomenon of negative DEP, and the velocity difference between different sizes observed is shown in Figure 8. In the case shown in Figure 4, although the ETE effect does not increase the difference of velocity from different sizes, the velocity varies

greatly. In addition, even if the difference in size is minimal, the small difference in DEP velocity can be amplified by increasing electric field strength.

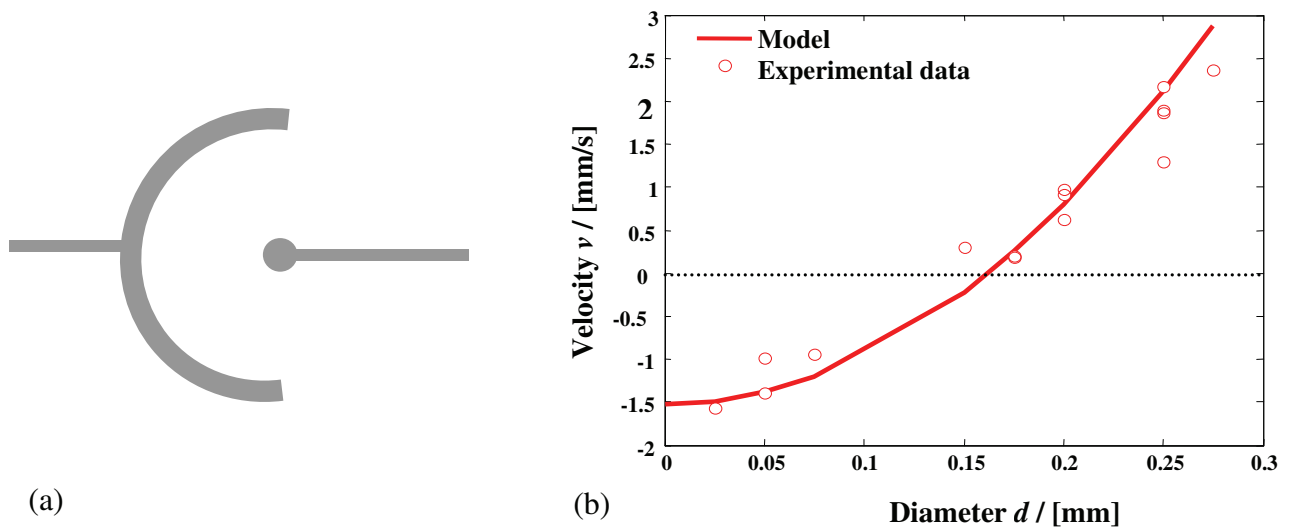


**Figure 8.** Experimental set-up, a spherical insulated electrode configuration (characteristic length 6 mm) (a), for determining the velocity of water droplets in silicone oil with a function of diameter at 0.7 kV DC (b). The model (Eq. 13) is a combination of DEP and ETE [9].

### Case 3: separation of particles by material characteristics

The difficulties in fractionation of particles that have nearly identical physical and chemical properties are well known. As an example, PVC and PE particles, have nearly the same appearance, density, electric conductivity and very close chemical properties, which make them very hard to be separated from each other with common separation techniques such as sedimentation, filtration, membrane, etc. but can be done satisfactorily using DEP due to the difference of dielectric constants between PVC (4.6) and PE (2.25). This implies that, if a fluid medium with a dielectric constant that lies between the two values can be found then the PVC and PE particles suspended in that medium will express different DEP behaviors, resulting to different motion directions. In Figure 9 (a), the results obtained from the suspension of PVC and PE in silicone oil (dielectric constant 2.9) is presented. However, as a comparison, the difference of DEP motion between PVC and PE in pure water (shown in Figure 9 (b)) is very small. From the results it can be deduced that the different directions of particle movement caused by different DEP behaviors can make them be fractionated.

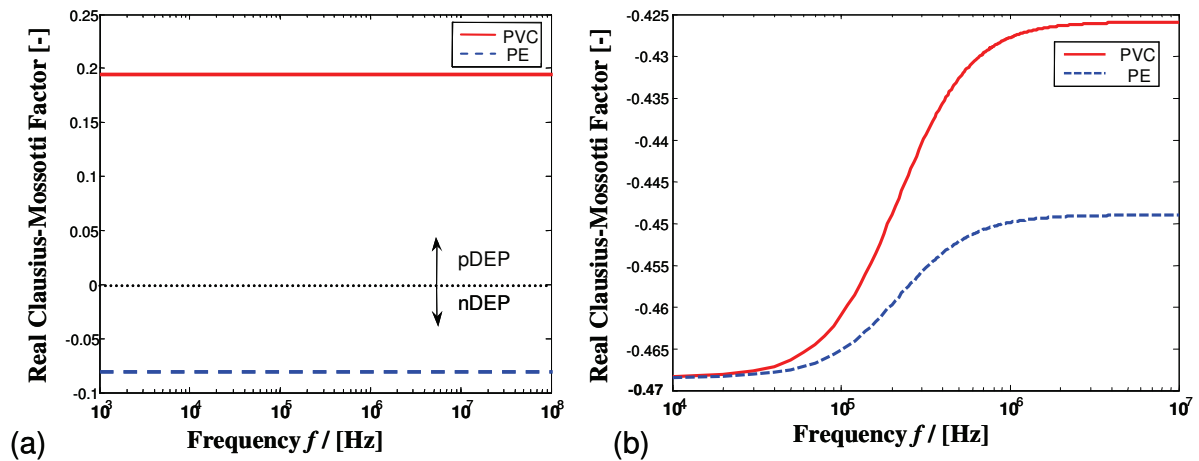
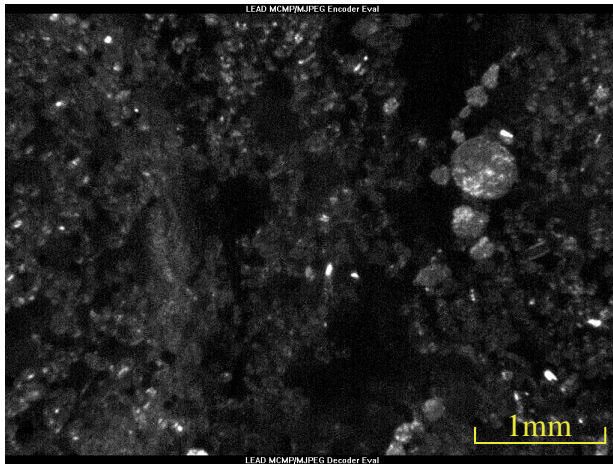


**Figure 9.** Feasibility of fractionation of similar particles (PVC and PE) by choosing the medium (a) (silicone oil), (b) (pure water).

#### Case 4: trapping particle

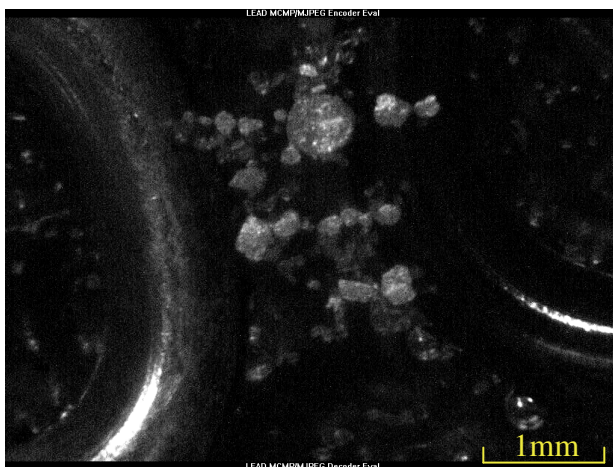
Apart from the properties of medium and frequency of electric field, the DEP effect is also dependent upon the electric field gradient as presented in Eq. 6, which is not only defined by the geometry and configuration of electrodes but also the applied voltage from the power source. The two important factors, notably the electrodes design and power source, can allow both DEP to occur, and concurrently offer many opportunities of handling particles. A well designed electrodes setup and power source can amplify very small difference of particles' electric properties, thus separating them. In addition, one of the opportunities the two factors offer is to trap particles. In order to separate gold particle from a particles mixture composed of gold, quartz, and zircon particles, for example, the DEP trapping was used, because the ultrathin gold plates of the tested samples cannot be separated by any other physical methods. This DEP gold-separation is a unique case because gold is chemically inert and exists as a free and pure metal in nature. Gold, which is characterized by an infinitely large permittivity [1], will consequently always move towards stronger electric field when suspended in any liquid, depicting a positive DEP. Therefore, the underlying concept here is to move and trap gold particle at the stronger electric field regions, which concurrently repel contained other particles in the mixture away from gold particles, as shown in Figure 10.



(a) without electric field



(b) gold trapped in 120 seconds with electric field



(c) gold concentrated in 210 seconds with electric field

**Figure 10.** Experimental phenomena for particles mixture of gold (light-scattered big particles), zircon and quartz (gray particles) in pure water with and without electric field (AC voltage output  $100 V_{\text{rms}}$ , frequency 220 kHz).

#### **Case 5: auxiliary function of DEP in mechanical separation techniques**

It worth noting that, DEP can also be applied in mechanical separation techniques to improve the separation efficiency hence leading to process intensification. The auxiliary function DEP in a sedimentation process was simulated and investigated in the lab-scale setup shown in Figure 11 (a). In the investigation, the particles not separated by sedimentation either with or without DEP effect respectively were collected and weighted. It was observed that the better the separation is, the less the particles were collected and measured. As shown in Figure 11 (b), the effect with and without DEP effect is divided clearly into two parts: with DEP, the particle collected and weighted less than 1g, rather without DEP the total mass of particle collected was more than 1g. This improvement in particle sedimentation was independent of the volume flow range investigated.



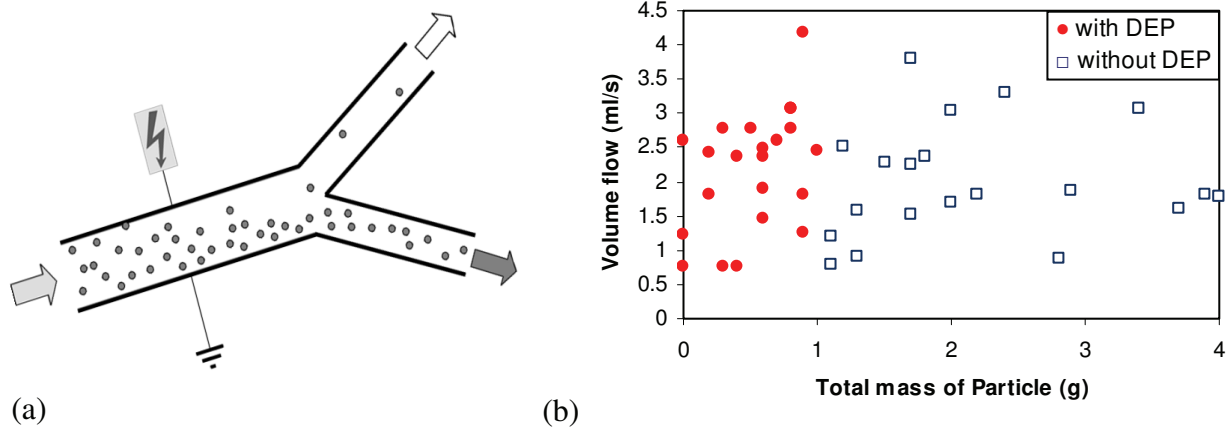


**Figure 11.** Experimental setup of a continuous clarifier with superimposed DEP (a) and (b) demonstration of the reduction of total PE particle mass in silicone oil due to DEP detected at the upper outlet (3 kV DC).

## Conclusion

Dielectrophoresis is a phenomenon of neutral particle's translational motion caused by dielectric polarization in an inhomogeneous electric field. DEP combined with side effects like ETE is a promising technique even for high-pass-filter systems. It can be applied in separation of different phases: solid from liquid, liquid from liquid, and solid from solid. All in all, the DEP can be used to separate, fractionate, and trap particles according to the different properties of particles and medium and deliberately designed electric field. Since the dielectrophoretic motion direction is always defined by the electric field, it gives the opportunity to control particle to move as designed. Although its application in large scale is not yet developed, the investigated millimeter-scale DEP systems, as a bridge, present prospect of the DEP application in separation technology.

## Acknowledgements

The authors wish to acknowledge Max-Buchner-Forschungstiftung for funding in dielectrophoretic gold separation project, and BIA GmbH/ BIG mbH of the Federal State of Bremen, Germany for funding in the investigation of dielectrophoretic auxiliary function in lamella sedimentation. The authors would like to thank Prof. Dr. P. J. Plath and his group at the University of Bremen for fruitful discussions.

## References

Castellanos, A., Ramos, A., González, A., Green, N.G. and Morgan, H., Electrohydrodynamics and dielectrophoresis in microsystems: scaling laws, *J. Phys. D: Appl. Phys.* 36 (2003) 2584-2597.

- Chou, C., Tegenfeldt, J., Bakajin, O., Chan, S., Cox, E., Darnton, N., Duke and Austin, T.R., Electrodeless dielectrophoresis of single- and double-stranded DNA, *Biophys. J.* 83 (2002) 2170-2179.
- Du, F., Baune, M. and Thöming, J., Insulator-based dielectrophoresis in viscous media – Simulation of particle and droplet velocity. *J. Electrostat.*, 65 (2007) 452-458.
- Green, N.G., Morgan, H. and Milner, J.J., Manipulation and trapping of sub-micron bioparticles using dielectrophoresis, *J. Biochem. Biophys. Methods* 35 (1997) 89-102.
- Morgan, H. and Green, N.G., *AC Electrokinetics: Colloids and Nanoparticles*, Research Studies Press Ltd., Hertfordshire, 2002.
- Mueller, T., Gradl, G., Howitz, S., Shirley, S., Schnelle, T. and Fuhr, G., A 3-D microelectrode system for handling and caging single cells and particles, *Biosensors & Bioelectronics* 14 (1999) 247-256.
- Muller, T., Gerardino, A., Schnelle, T., Shirley, S.G., Bordoni, F., DeGasperis, G., Leoni R. and Fuhr, G., Trapping of micrometer and sub-micrometer particles by high-frequency electric fields and hydrodynamic forces, *J.Phys.D: Appl. Phys.* 29 (1996) 340-349.
- Pohl, H.A., *Dielectrophoresis*, Cambridge University Press, Cambridge, 1978.
- Thöming, J., Du, F. and Baune, M., Dielectrophoretic separation of oil-water-solid dispersions–Selectivity and particle velocity, *Fresenius Environ. Bull.*, 15 (7) (2006) 687-691.

#### 4. Summarized discussion

The versatility of DEP force allows its application in separating, manipulating and fractionating particles in fluid suspensions. Its effect involves a wide range of particle characteristics through the frequency-dependent permittivity of particle materials and structures and can be modified by choosing different suspending media. Besides, the magnitude of DEP force is determined by the inhomogeneity and strength of electric field, which can easily be realized through configuration of electrodes and power input.

Despite its high selectivity and controllability as well as the ease of construction, a successful application of DEP does demand thought and awareness of a number of confounding factors, such as electrothermal effect, high-pass-filter effect, particle-particle interaction and other electrokinetic effects possibly involved such as electrophoresis and electroosmosis. These factors either disturb particles motion direction and velocity, as it is the case for electrothermal and other electrophoresis, or confine DEP application scope and waste more energy, like high-pass-filter effect. Although DEP technique has already been applied principally in micron and sub-micron scale biotechnology, its industrial application in larger scale requires further investigation.

In order to understand the fundamentals of DEP in process relevant scale that is, for  $Re > 1$  and characteristic electrode length above 1 mm, it is crucial to investigate and understand the influence of the mentioned parameters and side effects. This thesis therefore comprises three main aspects, firstly basic research of DEP mechanism, its side-effects and constraints, secondly a proof of principle for DEP application in particles' fractionation, and thirdly DEP as an aid in intensifying cross-flow membrane filtration.

The DEP effects on micro-particles suspended in viscous media were examined as a function of parameters such as particle size and potential. Particles' velocities in a spherical electric field [Pohl 1978] were measured to demonstrate the influence of electrothermal effect on particles' DEP effects. Evidently the convective fluid flow due to thermally induced buoyancy force in a DEP system with a characteristic length of 6 mm can determine particle's motion velocity. In the case of PE particles with negative DEP effect in silicone oil, velocity increased with internal temperature gradients, whereas water droplets suspended in silicone oil present a positive DEP effect, and velocity decreased with the internal temperature gradients. The identified model explicitly described the observed effects with excellent quantitative and quantitative agreement with the experimental results. Accordingly, the model allows for predicting particle trajectory and potential problems in a DEP system.

As a proof of principle, DEP for gold particle fractionation using a free flow cross current approach where electric field and fluid flow were orthogonal to each other was tested. Here, for the first time DEP was applied as the main separation mechanism for mixtures of particles in the micrometer and millimeter size range. Gold particles were separated from a mineral mixture with high efficiency. The ultra-thin gold particles in the raw mixture can not be fractionated by any other physical method. Compared to all other known techniques, namely amalgamation and cyanidation, this technique eliminates environmental pollution risks. An electrode configuration with one bare electrode and one insulated electrode was designed for solving the problem caused by the high-pass-filter effect. This electrode configuration provided a 56% increase of the voltage developed across the medium.

Due to the very short distance between electrodes and the closed channel in the separation chamber, the heat resulted from joule heating could not be removed from the system and resulting in a boiling after several minutes separation time. Both effects reduced the separation efficiency and increased the energy consumption and cost by interfering with movement of particles. Therefore, a cycling medium system was required to cool down the system. Although these problems resulted in a low throughput, the success of dielectrophoretic gold particles separation proved the feasibility of DEP application in separation and its main advantages - high selectivity and controllability.

Both high-pass-filter effect and electrothermal effect often occur in DEP systems due to the very high electric field strength. And both constrain DEP applications, waste energy and increase costs. The electrical energy demand for DEP with a cycling medium system increases with the decrease of distance between electrodes, because the joule heating increases with the increment of electric field caused by reducing distance between electrodes. In gold particle fractionation (volume flow 2.36 mL/s, applied voltage 190 V and 200 kHz and 7500 Ohm impedance of the system), it was calculated to be 5.06 Wh per gram fractionated gold particles and 5.9 Wh per liter of feed suspension (energy calculated using parameters and Eq. 4 described in Chapter 3.2). In addition, the short distance between electrodes (6 mm) for providing sufficient electric field gradient limited the throughput of the separator in the magnitude of milligram per second (mass flow of particles mixture 2.2 mg/s), thereby decreasing the separation yield.

To find a DEP application with drastically reduced energy demand, an integration of DEP in unit operations was investigated focusing on cross-flow ultrafiltration and microfiltration as case study. In membrane filtration fouling is inevitable, although flow rate can reduce contact between particles and membrane so as to prolong the membrane service

time. Many methods have already been applied to reduce the fouling problems, such as backpulsing, backwashing, and chemical cleaning. The drawbacks of these methods are: interrupted process, additional equipment cost, additional energy and usage of chemicals. Integrated ultrasonic fields, as a measure for reducing fouling, is hard to be applied in industry due to the control of erosion and possible damage of the membrane as well as the bulky ultrasound system with its difficulty in installation.

Here, DEP was for the first time applied in a cross-flow membrane filtration process to enhance the permeate flow and increase the work life of membrane. Due to the lower permittivity of clay particle compared to that of pure water, the negative DEP force worked to move clay particles away from the membrane independent of the charge on particles so as to realize alleviating particle fouling and concentration polarization, thereby intensifying the filtration process. Based on the experience of high-pass-filter effect in the work of gold particle fractionation, the electrode configuration with a characteristic length of 1 mm was a combination of a bare stainless steel grid electrode and a stainless steel plate insulated by a plastic film. Despite relative low characteristic length a high throughput (specific permeate volume flow  $470 \text{ mL}/(\text{min m}^2)$ ) can be realized in this case of an integrated DEP system.

Comparisons of the particle layers left on the membrane surface and the permeate flux after a certain process time with and without DEP demonstrated the significance of the DEP's potential in enhancing the membrane filtration process. The enhancement of permeate flux with continuously applied DEP can be further increased by means of pulsed application of DEP with a much lower energy consumption. This is because smaller particles could be bound to the membrane surface due to electrostatic or van der Waals force when they are close enough to the membrane, and not be able to be removed by DEP force. Especially, the initial permeate flux was so high to exceed a threshold value, which dominated the DEP force and move smaller particles to close to the membrane surface. When the pulsed DEP was applied, due to pearl-chain effect small particles adhering to the membrane surface agglomerate, and hence increase the specific size. The increment of particles' specific size thereby increases the DEP force, which can more easily move particle agglomerate away from the membrane surface. The electric energy demand for a 5-15 pulsed DEP (on/off periods of 5 and 15 min, respectively) intensified cross-flow membrane filtration, for instance, presents a 8.7 Wh for maintaining a 50 % initial permeate flow in a 6 hours process time resulting in 45.5 Wh per liter feed suspension. The experiments were performed under high solid concentration condition to represent a serious fouling situation. Accordingly the concentration of clay suspension was 5g/L, which is about 168 folds higher than that in a reference case

described in work of Bourgeois et al. [Bourgeois et al. 2001]. There a similar cross-flow filtration process and a typical process cycle consisting of a production period, a backwash period, and a fast flush period were applied. The efficacies of both cross-flow membrane filtration processes can be compared with the ratio of time-averaged permeate flow to feed flow. In a 6 hour 5-15 pulsed DEP filtration, the ratio of time-averaged permeate flow to feed flow is about 3.6 times higher with a 172.4 times lower energy consumption of DEP compared with the energy demand for backwash in the filtration process presented in the work of Bourgeois et al..

Compared to the DEP enhanced filtration, the DEP fractionation presented higher energy demand for treating one liter suspension. This is because the electrodes are much longer than those in DEP enhanced filtration, thereby cause a longer heating time and lower impedance. As an example, in the DEP gold fractionation process with a cycling water cooling system, a process yields 1g/h of gold particles. The energy consumption is 54.57 Wh/g gold particles. A multi-channel system could increase the separation yield but will definitely largely increase the specific energy demand. However, the optimised DEP intensified filtration process demonstrated lower energy consumption with a higher enhanced performance. This result is crucial in opening a new door in anti-fouling in cross-flow membrane filtration and prolonging membrane service life with non-stopped process and less energy.

## 5. Outlook

Over 3 decades after DEP was explored and defined, it has already been successfully applied in separating, trapping, and handling bioparticles in micro and sub-micro scale biotechnology. However, nearly all of DEP applications are concentrated on the analysis and manipulation of particles in sub-micron and micron scaled systems with flow rates below milliliters per minute. So far, almost none is known in process engineering for DEP in a scaled up application at flow rates of liters or even cubic meters per minute. The research described in this Ph D thesis is the first that attempts to scale up DEP application. With the research results described above, the feasibility of the DEP technique application in separation is verified. The proved high selectivity and controllability of DEP technique in separation application grand DEP a very promising prospect in separating, trapping, handling and manipulating particles.

However, there are still some challenges for a further scaling up and an improved energy efficiency. For example, the electrothermal side-effect interferes with particle's DEP motion. The constraint from high-pass-filter effect requires much higher frequency, thereby much more energy input, and limits the application range of DEP effect. Although both problems have already been investigated before, they need further work for a better understanding. In the case of the electrothermal effect, the model in predicting the fluid flow was established under a specific condition, i.e. particle suspended in a **dielectric** medium under a **dc** electric field. The open question is how parameters, such as frequency, electric properties of liquid medium and electrode configuration, influence the temperature gradient and fluid flow, in an ac DEP system with conductive (conductivity higher than  $10^{-4}$  S/m) medium. In addition, although the high-pass-filter effect has already been observed, a theoretical model together with responding experiments on the influences of the main parameters (thickness and electric properties of insulation material) requires further investigation. An integration of the high-pass-filter effect into DEP force and electrothermal model could provide a more precise prediction of DEP effect.

In addition, another side effect, pearl-chain-effect, often occurs in DEP system especially when the particle's concentration is high. The pearl-chain-effect is caused by the interaction between two closed particles. The local electric field between two closed electric field will result in a much higher DEP force on both particles and thereby attract them to move toward each other because of the increased inhomogeneity of electric field. With carefully controlling the parameters (concentration of particle, electrode configuration, voltage, and frequency), the pear-chain-effect should allow improving the separation

efficiency. This is because the increased size of agglomerated particles due to pearl-chain-effect results in a cubically increased DEP force, thereby presents a much faster DEP movement of particles and reducing possible disturbances caused by fluid flow and electrothermal effect. A factor based on the relationship between particle concentration and distance between electrodes could demonstrate the influence of these parameters on the pearl-chain effect and help in designing a DEP separation process.

During this thesis work, a dilemma of the relationship between particle size and characteristic length of electrode configuration was found to be a key problem in scaling up DEP applications in industry. DEP velocity is a function of squared particle size, but of an inversed cubic of distance between electrodes. This dilemma is immanent because both parameters influencing the DEP force most, particle size and electrode distance, are opposing. If the distance between electrodes for scaling up DEP application is increased, the DEP force on small particles will become too weak to move them and thereby reduce both separation and energy efficiency. However, if the distance between electrodes is decreased, due to the decreased distance between electrodes, the DEP force on large particles will become too strong to avoid intense interaction between them inducing particle agglomeration as well as adherence of particles on the surface of electrodes and consecutive pearl-chain formation between electrodes, which endangers electric short-circuit and damage of insulation films. This dilemma also concerns operability at high flow rates. The reason is that high throughput requires a channel cross section large enough to avoid high pressure drops and therefore a large electrode distance, since the electric field has to cover the entire channel. On the other hand, a certain field strength drops with increasing electrode distance. Therefore, it is crucial to find out first the interplay of the two parameters – particle size and the characteristic length of electrode configuration. A model of this relationship between two parameters can help in predicting the particle trajectory and design electrode configuration. Further, this dilemma becomes more serious when the mass flow direction is perpendicular to the arrangement of electrodes, which means that suspension passes through between two electrodes. If the electrodes are not installed orthogonally but along the direction of the mass flow, with which suspension flows over/below electrodes, the distance between electrodes could be decreased without reducing mass flow.

Theoretically, the electric current in an insulated DEP system is very low as in the magnitude of miliampere. The electric current density (current per area of membrane) in the DEP intensified cross-flow filtration process, for instance, is about  $13.39 \text{ A/m}^2$ . However, the voltage applied in a DEP system, especially in order to scale up DEP application, must be



high enough to produce sufficient electric field intensity for a better DEP efficacy, which causes an increased energy demand. The aim for high efficacy and low energy consumption in DEP system can be reached by optimizing electrode configuration design to increase electric field gradient with unchanging or decreasing voltage application. The electrodes arranged along the direction of mass flow are hint in providing good DEP effect with a lower energy input.

Together with the improved understanding of DEP, a scaling bridge approach is proposed to solve the dilemma of scaling up DEP application by bridging the gap between particle size and characteristic length of electrode configuration with the electrode configuration scale in millimeter and centimeter. In that case, an optimized design of electrode configuration is crucial to solve or alleviate the problems.

## 6. Reference

- Arnold, W.M., Positioning and levitation media for the separation of biological cells *IEEE Trans. Ind. Appl.* 37 (2001)1468-75.
- Bahrami A., Hosseini M.R., Razmi K., An investigation on reusing process water in gold cyanidation. *Mine water environ.*, 26 (2007) 191.
- Baune, M., Du, F. and Thöming, J., Dielectrophoresis–Bridging the scale in modeling and application, in P.J. Plath and E. Hass (Ed.), *Vernetzte Wissenschaften*, Logos Verlag Berlin GmbH, Berlin, 2008, 47-64.
- Belfort, G., Davis, R.H. and Zydney, A.L., The behavior of suspensions and macromolecular solutions in crossflow microfiltration, *J. Membr. Sci.* 1994, 96 1-58.
- Benítez, F.J., Acero, J.L., Leal, A.I. and González, M., The use of ultrafiltration and nanofiltration membranes for the purification of cork processing wastewater, *J. Hazard. Mater.* 2009, 162 1438-1445.
- Bourgeois, N.K., Darby, J.L. and Tchobanoglous, G., Ultrafiltration of wastewater: effects of particles, mode of operation, and backwash effectiveness, *Water Res.*, 35 (2001) 77-90.
- Boussinesq, J., *Theorie analytique de la chaleur*, Vol.2, Gauthier-Villars, Paris, 1903.
- Castellanos, A., Ramos, A., González, A., Green, N.G. and Morgan, H., Electrohydrodynamics and dielectrophoresis in microsystems: scaling laws, *J. Phys. D: Appl. Phys.* 36 (2003) 2584-2597.
- Chai, X., Kobayashi, T. and Fujii, N., Ultrasound-associated cleaning of polymeric membranes for water treatment, *Sep. Purif. Technol.* 1999, 15 139-146.
- Chou, C., Tegenfeldt, J., Bakajin, O., Chan, S., Cox, E., Darnton, N., Duke and Austin, T.R., Electrodeless dielectrophoresis of single- and double-stranded DNA, *Biophys. J.* 83 (2002) 2170-2179.
- Crozes, G.F., Jacangelo, J.G., Anselme C. and Laine, J.M., Impact of ultrafiltration operating conditions on membrane irreversible fouling, *J. Membr. Sci.*, 124 (1997) 63-76.
- Cummings, E. and Singh, A., Dielectrophoresis in Microchips Containing Arrays of Insulating Posts: Theoretical and Experimental Results, *Anal. Chem.* 75 (2003) 4724-4731.
- Du, F., Baune, M., and Thöming, J., Insulator-based dielectrophoresis in viscous media – Simulation of particle and droplet velocity, *J. Electrostat.*, 65 (2007) 452-458.
- Du, F., Baune, M., Kück, A. and Thöming, J., Dielectrophoretic gold particle separation, *Sep. Sci. Technol.* 15 (2008) 3842-3855.
- Du, F., Hawari, A., Baune, M. and Thöming, J., Dielectrophoretically intensified cross-flow membrane filtration, *Journal of Membrane Science*, 336 (2009) 71-78.

- Eow, J.S., Ghadiri, M., Sharif, A.O. and Williams, T.J., Electrostatic enhancement of coalescence of water droplets in oil: a review of the current understanding, *Chemical Engineering Journal*, 84 (2001) 173-192.
- Gascoyne, P.R.C. and Vykokal, J., Particle separation by dielectrophoresis, *Electrophoresis*, 23 (2002) 1973-1983.
- Green, N.G., Morgan, H. and Milner, J.J., Manipulation and trapping of sub-micron bioparticles using dielectrophoresis, *J. Biochem. Biophys. Methods* 35 (1997) 89-102.
- Henry, J.D.J., Lawler, L.F. and Kuo, C.H.A., A solid/liquid separation process based on cross flow and electrofiltration, *AIChE J.*, 23 (6) (1977) 851-859.
- Hughes, M.P., Strategies for dielectrophoretic separation in laboratory-on-a-chip systems, *Electrophoresis*, 23 (2002) 2569-2582.
- Hylander, D.L., Plath, D., Miranda, R.C., Lücke, S., Öhlander, J. and Rivera, A.T.F., Comparison of different gold recovery methods with regards to pollution control and efficiency. *Clean*, 35 (1) (2007) 52.
- Jones, T.B., *Electromechanics of particles*, Cambridge University Press, USA, 1995.
- Kennedy, M., Kim, S.M., Muteryo, I., Broens, L. and Schippers, J., Intermittent crossflushing of hollow fiber ultrafiltration system. *Desalination*, 118 (1998) 175-188.
- Koh, C.N., Wingtens, T., Melin, T. and Pronk, F., Microfiltration with silicon nitride microsieves and high frequency backpulsing, *Desalination*, 224 (2008) 88-97.
- Kumar, S, Yoon, S.H., Kim, G.H., Bridging the nanogap electrodes with gold nanoparticles using dielectrophoresis technique. *Current Applied Physics*, (2008), doi:10.1010/j.cap.2007.12.001.
- Kyllönen, H.M., Pirkonen, P. and Nyström, M., Membrane filtration enhanced by ultrasound: a review, *Desalination*, 181 (2005) 319-335.
- Lamminen, M.O., Walker, H.W. and Weavers, L.K., Cleaning of particle-fouled membranes during cross-flow filtration using an embedded ultrasonic transducer system, *J. Membr. Sci.*, 283 (2006) 225-232.
- Lapizco-Encinas, B.H., Simmons, A.B., Cummings, B.E. and Fintschenko, Y., Insulator-based dielectrophoresis for the selective concentration and separation of live bacteria in water, *Electrophoresis*, 25 (2004) 1695-1704.
- Li, J., Hallbauer, D.K. and Sanderson, R.D., Direct monitoring of membrane fouling and cleaning during ultrafiltration using a non-invasive ultrasonic technique, *J. Membr. Sci.*, 215 (2003) 33-52.

- Li, Y., Kaler, K.V.I.S., Dielectrophoretic fluidic cell fractionation system, *Analytic Chimica Acta*. 507 (2004) 151-161.
- Lin, Y.-T., Sung, M., Sanders, P.F., Marinucci, A. and Huang, C.P., Separation of nano-sized colloidal particles using cross-flow electro-filtration, *Sep. Purif. Technol.* 2007, 58 138-147.
- Loewen, W.W., Method of gold separation and gold separation device. U.S. Patent 7,012,209 B2, March 14, 2006.
- Maatens, A., Swart, P. and Jacobs, E.P., Feed water pretreatment: methods to reduce membrane fouling by natural organic matter, *J. Membr. Sci.*, 163 (1999) 51-62.
- Molla, S. and Bhattacharjee, S., Dielectrophoretic levitation in the presence of shear flow: implications for colloidal fouling of filtration membranes, *Langmuir*, 23 (2007) 10618-10627.
- Molla, S.H. and Bhattacharjee, S., Prevention of colloidal membrane fouling employing dielectrophoretic forces on a parallel electrode array, *J. Membr. Sci.*, 255 (2005) 187-199.
- Morgan, H. and Green, N.G., *AC Electrokinetics: Colloids and Nanoparticles*, Research Studies Press Ltd., Hertfordshire, 2002.
- Muller, T., Gerardino, A., Schnelle, T., Shirley, S.G., Bordoni, F., DeGasperis, G., Leoni R. and Fuhr, G., Trapping of micrometer and sub-micrometer particles by high-frequency electric fields and hydrodynamic forces, *J. Phy.D: Appl. Phys.* 29 (1996) 340-349.
- Mueller, T., Gradl, G., Howitz, S., Shirley, S., Schnelle, T. and Fuhr, G., A 3-D microelectrode system for handling and caging single cells and particles, *Biosensors & Bioelectronics* 14 (1999) 247-256.
- Pethig, R. and Markx, G.H., Applications of dielectrophoresis in biotechnology. *TIBTECH*, 15 (1997) 426.
- Pohl, H.A., *Dielectrophoresis*, Cambridge University Press, Cambridge, 1978.
- Ramadan, Q., Samper, V., Poenar, D., Liang, Z., Yu, C., and Lim, T.M., Simultaneous cell lysis and bead trapping in a continuous flow microfluidic device. *Sensors and Actuators, B* (2006) 113-944.
- Redkar, S.G. and Davis, R.H., Enhancement of crossflow microfiltration performance using high frequency reverse filtration. *AIChE J.*, 41 (1995) 501-508.
- Sommerfeld, M., *Theoretical and experimental modeling of particulate flows*, Martin-Luther University Halle-Wittenberg, Germany, 2000.
- Sondhi, R., Lin, Y.S. and Alvarez, F., Crossflow filtration of chromium hydroxide suspension by ceramic membranes: fouling and its minimization by backpulsing, *J. Membr. Sci.*, 174 (2000) 111-122.

- Srijaroonrat, P., Julien, E. and Aurelle, Y., Unstable secondary oil/water emulsion treatment using ultrafiltration: fouling control by backflushing, *J. Membr. Sci.*, 159 (1999) 11-20.
- Thöming, J., Du, F. and Baune, M., Dielectrophoretic separation of oil-water-solid dispersions—Selectivity and particle velocity, *Fresenius Environ. Bull.*, 15 (7) (2006) 687-691.
- Wakeman, R.J. and Tarleton, E.S., An experimental study of electroacoustic crossflow microfiltration, *Chem. Eng. Res. Des.*, 69 (1991) 387-397.
- Wakizaka, Y., Hakoda, M. and Shiragami, N., Effect of electrode geometry on dielectrophoretic separation of cells, *Biochem. J.* 20 (2004) 13-19.

## 7. Acknowledgement

I would like to express my sincere gratitude to my supervisors Prof. P. J. Plath, Prof. J. Thöming and Dr. M. Baune for giving me the opportunity to register as a Ph D student in University of Bremen. Especially, I would like to thank Prof. J. Thöming very much, who gave me the chance to work in his work group, patiently instructed me and taught me the secrets of scientific thinking, working, writing and speaking.

Special and many thanks to Dr. M. Baune for many creative, helpful and nice discussion, suggestions, and instructions.

I would also like to thank my co-writers and co-workers who have helped me with my research work and colleagues: A. Al Hawari, A. Kück, B. Jürgen, C. Nelson, C. Evgenia, F. José Francisco, M. Hencken, J. Hüppmeier, G. Okoth, R. Waldemar, D. Waterkamp, M. Weinhold, Y. Ahmed Ibrahim Salem, S. Steudte, S. Stolte, D. Bobenhausen, D. Grotheer, A. Nienstedt, G. Pesch, A. Bludau, A. Geier, P. Erol, V. Linke-Wiennemann, T. Pressler, J. Sauvageau, S. Ziegert, and many more...

This work had not been possible without my family!

## 8. Appendix

### 8.1. Paper No. 5

#### Dielectrophoretic separation of oil-water-solid dispersions – selectivity and particle velocity

J. Thöming, F. Du, M. Baune

UFT, Section of Process Integrated Waste Minimization, University of Bremen, Leobener Str., D 28359 Bremen, Germany

#### Abstract

Dielectrophoresis (DEP) is an electro-kinetic method that allows to direct even uncharged particles in suspension. In this paper, the high potential of DEP for separating oil-and-water dispersions as well as fine solid particles from oil is shown and discussed. The mechanisms occurring during DEP are modeled, simulated, and examined experimentally. It is demonstrated how the particle velocity depends on particle size, the gradient of the electrical field, and on the viscosity of the continuous phase. Furthermore, it is shown that the selectivity of the separation of different particles depends on their permittivity relative to that of the continuous phase. However, since the permittivity is frequency-dependent, the selectivity can be controlled in technical applications by adjusting the electrical field.

**Keywords:** Selectivity, particle velocity, oil purification, permittivity

#### Introduction

Oily separation problems are considered as a challenge in environmental technology [1]. Although a couple of technologies have been suggested and developed (Tab. 1), there is still a demand for efficient, robust and non-expensive methods.

Among the techniques that are already applied is electro- coalescence [4]. It has been used for decades to separate w/o-emulsions, but the mechanism was understood only recently [5]. Following this understanding, the mechanism of droplet formation and separation appears to be independent from any electro-kinetic phenomenon.

The common electro-kinetic phenomena are based on electrostatic forces in (usually homogeneous) electrical fields, which are induced by electrodes that are connected to direct current (DC). The application of these phenomena in environmental technology is widespread: Electro-migration (ions migrate towards oppositely charged electrodes) is used e.g. in electro-dialysis [9], electrophoresis (migration of charged colloidal particles towards oppositely

charged electrodes) is used e.g. in electro-membrane-filtration, and electro-osmosis (migration of water in porous media) is used e.g. in electro-remediation [10].

**Table 1. Dispersions of oil, water and solids as a challenge for environmental technology.**

System	Environmental problem	Separation method	Ref.
Oil-in-water	Reuse of process water	Coagulation Membrane- filtration	[1] [2, 3]
Water-in-oil	Recycling of waste oil	Electro-coalescence Hydrocyclone	[4, 5] [6]
Solid-in-oil	Recycling of waste oil	Filtration	[7, 8]

An additional but in environmental technology not yet investigated, electro-kinetic approach is dielectrophoresis (DEP), which allows moving particles in suspension even if they are uncharged. The motion of charged or uncharged colloids, microparticles and droplets is based on dielectric forces in inhomogeneous electrical fields caused by alternating current (AC) or by DC. The theory of DEP was firstly developed by Pohl [11] to describe the translational motion of neutral matter caused by polarization effects in a non-uniform electric field. It is a technique that has been used in separating, concentrating, and trapping particles in biotechnological applications [12]. But it has not been investigated for the purpose of a destruction of unwanted but stable (colloidal) dispersions like the breaking of oil emulsions.

The physical properties of colloids and their suspensions are strongly dependent on the nature of the particle-liquid interface. As it is especially true for aqueous dispersions, the stability of colloidal suspensions is intimately related to the electrical double layer that characterizes the interface. Interparticle repulsion due to the overlap of similarly charged electric double layers is an important stabilizing mechanism in oil-in-water emulsions. With polarization due to an external electrical field (Fig. 1 b) the stabilizing effect is reversed.



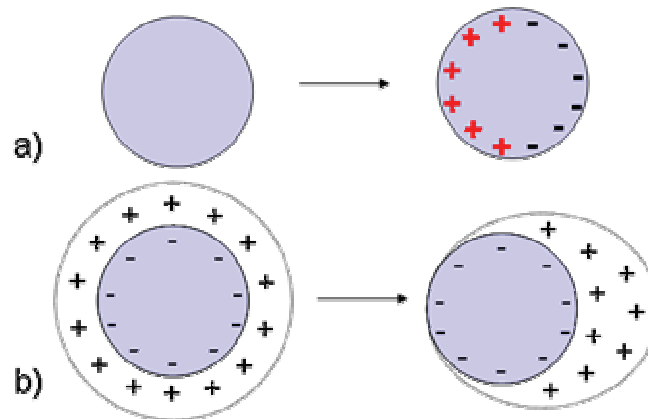


**Figure 1.** Polarisation of an uncharged (a) and charged (b) particle within an external electrical field.

The dipole moment induced in the particle can be represented by two equal and opposite charges at the particle boundary. These two induced charges are not uniformly distributed over the surface of the particle, but create a macroscopic dipole (Fig. 1 a). When the dipole is located in a non-uniform electric field, a net dielectrophoretic force arises (Fig. 2). Depending upon the different polarizations of particle and medium, the particle will be induced to move towards stronger electric field region (positive DEP) or to move towards weaker electric field region (negative DEP). This force is due to the fact that the local field strength on each side of the particle is different, and a replacement of the dipole allows minimizing the total permittivity, which leads to a minimization of the systems' total energy.

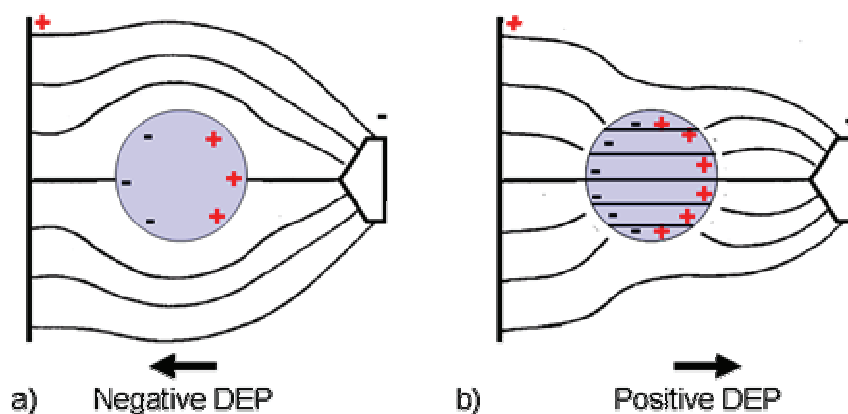


**Figure 2.** Dielectrophoresis (DEP) of a polarized particle in a non-uniform external electrical field with (a) high and (b) low relative dielectric permeability of the particle. DEP is called positive if it occurs in the direction of the positive field gradient.

In this research work, the particle's motion was investigated in low conductivity medium with AC (theoretical) and DC electric fields and discussed to validate the reasonability of separation of liquid droplets as well as solid particles from oil using DEP.

## Materials and methods

Two Pt electrodes of spherical geometry were insulated by a thin layer of glass. The radius of the central sphere electrode was 1.4 mm, and the outer concentric shell had a radius of 6 mm. The two electrodes were integrated into a glass reservoir (Fig. 3) filled with silicone oil DC200 (Fluka).

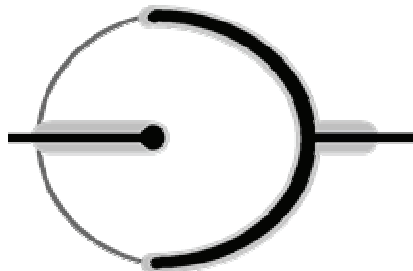


**Figure 3.** Investigated DEP-cell system

The electrodes were polarized using a high stability power supply (KNOTT ELECTRONIK), which could provide voltages from DC 0.2 kV to 2.4 kV. A microscope with a scaled lens and a timer were used to observe and measure the diameter and the velocity of the particles during the experiments. Instead of using the light source from microscope, a cold light source (KL2500LCD, SCHOTT) was used to decrease the external heat influence. The cell resistance was measured by electrochemical impedance analysis (EG&G Instruments). In the experiments, water droplets and PE (polyethylene) spherical particles (diameter range from 100  $\mu\text{m}$  to 2 mm) were suspended in the silicone oil that had a viscosity of 20 mPa s.

## Theoretical model

In the case of a spherical particle (radius  $a$ ) suspended in a medium with a relative dielectric constant  $\epsilon_M$ , the dielectrophoretic force is given in Eq. 1:

$$F_{\text{DEP}} = 2\pi a^3 \cdot \epsilon_0 \epsilon_M \cdot \Psi \cdot \nabla |E|^2 \quad (1)$$

where  $\nabla |E|^2$  is electric field gradient,  $\Psi$  is the Clausius-Mossotti factor and  $\epsilon_0$  is permittivity of free space equal to  $8.854 \cdot 10^{-12}$  [11]. This parameter defines the effective dielectric polarizability of the particle; it is a function of frequency of the electric field, depending upon the particle and medium's dielectric properties (dielectric constant and conductivity). The Clausius-Mossotti factor  $\Psi$  is given as the real part  $re$  of the complex dielectric constants  $\tilde{\epsilon}$ :

$$\Psi = \text{re} \left( \frac{\tilde{\epsilon}_p - \tilde{\epsilon}_m}{\tilde{\epsilon}_p + 2\tilde{\epsilon}_m} \right) \quad (2)$$

$$\text{with } \tilde{\epsilon} = \epsilon - \frac{i\kappa}{\omega} \quad (3)$$

where  $\kappa$  is the conductivity,  $\omega$  is angular frequency of the applied electric field ( $\omega=2\pi f$ ) in which  $f$  is frequency, and  $i = \sqrt{-1}$ . When DC electric fields are applied, the imaginary part of the complex dielectric constant can generally be neglected. This is not the case for an AC application, for which the conductivities become high importance. The particle conductivity is a sum of inner material conductivity  $\kappa_I$  and a term that is proportional to the surface conductivity  $\lambda$ .

$$\kappa_P = \kappa_I + \left( \frac{2 \cdot \lambda}{a} \right) \quad (4)$$

The motion of a particle suspended in a liquid is often simply assumed to be a steady state by balancing the dielectrophoretic force and the drag force. Thus, the DEP-velocity of a particle  $v_{DEP}$  can be given as Eq. 5:

$$v_{DEP} = \frac{a^2 \cdot \epsilon_0 \epsilon_M \cdot \Psi \cdot \nabla |E|^2}{3\eta_M} \quad (5)$$

where  $\eta_M$  is the dynamic viscosity of the medium. In comparison, for electrophoresis the velocity, which is proportional to the zeta-potential  $\zeta$ , is described by the Helmholtz-Smoluchowski equation (6):

$$v_{EP} = \frac{\epsilon_0 \epsilon_M \cdot \zeta \cdot E}{\eta_M} \quad (6)$$

In the Eq. 5, the liquid was assumed to be static. However, the high strength electric fields that are used in DEP can generate fluid motion [12]. As a consequence of Joule heating and local temperature gradients, spatial variations of electrical conductivity and permittivity occur, leading to an electro-thermal force. This electro-thermal force can play an equally important role in the motion of the suspended and polarized devices, when compared to the role of the DEP forces [13, 14]. When Joule heating is intensive enough, it gives rise to buoyancy forces. In addition, when the order of magnitude of diameter of particle is in the millimetre range, the stokes' law used in the theoretical calculation equation has to be added a convective correction due to the larger Reynolds number caused by much higher particle's velocity.

## Results and discussion

Results of simulation calculations that are based on the model equations (1)-(3) are shown in Figure 4. It can be clearly seen that in w/o emulsions (4 a) dielectrophoresis of water droplets is positively independent of the frequency of the applied field and of the conductivity of the particles. A switch to negative DEP occurs at low frequencies, or at DC only for a

conductivity of the particles lower than that of the continuous phase. In contrary, in o/w emulsions (4 b) dielectrophoresis of oil droplets is negatively independent of the dielectricity of the continuous aqueous phase, as long as its values are higher as they are for the medium.

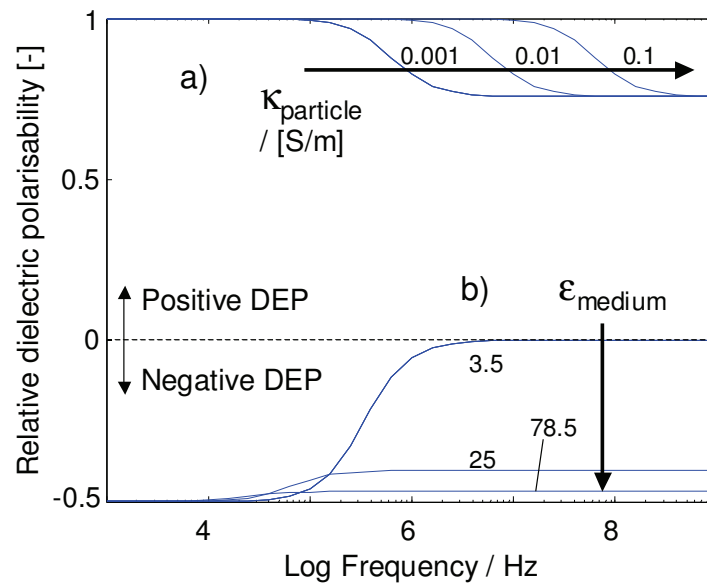


**Figure 4.** Relative dielectric polarizability of (a) w/o emulsions ( $\epsilon_P = 25.2$ ,  $\epsilon_M = 3.5$ ,  $\kappa_M = 10^{-12}$  S/m) and (b) o/w emulsions ( $\epsilon_P = 3.5$ ,  $\kappa_P = 10^{-12}$  S/m,  $\kappa_M = 10^{-4}$  S/m) depending on conductivity  $\kappa$  and dielectricity  $\epsilon$  of the continuous phase (medium).

The influence of surface characteristics of solid particles on separation selectivity is demonstrated in Fig. 5. With increasing fraction of polar functionalized groups, the change from pDEP to nDEP and, thus, the direction of the motion shifts to lower frequencies.

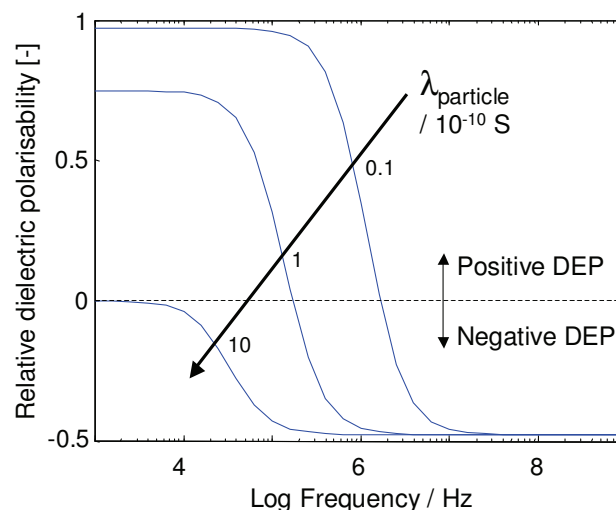


**Figure 5.** Influence of surface conductivity  $\lambda$  of 400 nm Latex-colloids on frequency-dependent DEP in distilled water ( $\epsilon_M = 78.5$ ,  $\kappa = 0.0001$  S/m).

Calculations of the relative dielectric polarizability of plastic particles in oil and water (Fig. 6 a) show that the selectivity to separate PE from PVC is only in the case of oil as

continuous phase high enough to collect each material at different electrodes. In water, the situation is completely different. Figure 6 b shows a frequency-depending relative dielectric polarizability of the plastic materials. Even if there might occur also a DEP force (according to equation 1, the force  $F$  is proportional to the relative dielectric polarizability  $\Psi$ ) in water high enough to separate the particles efficiently from the medium, the selectivity appears not to be significant enough to separate PE from PVC in water.

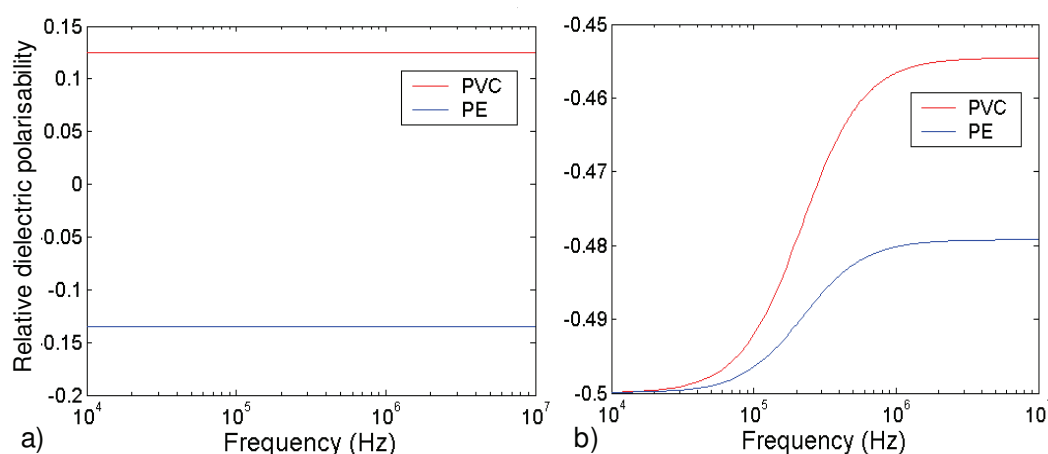


**Figure 6.** Relative dielectric polarizability of plastic particles in (a) silicon oil ( $\epsilon_M = 2.9$ ,  $\kappa = 10^{-12}$  S/m) and (b) water resulting in a frequency-depending selectivity with respect to the plastic material.

Consider that in the case of electrophoresis electrodes must not be isolated. At voltages one order of magnitude higher as illustrated in Fig. 7, the dielectrophoretic plane is completely located above the other one, resulting in a much better separation potential, independent from the zeta-potential of the particles.

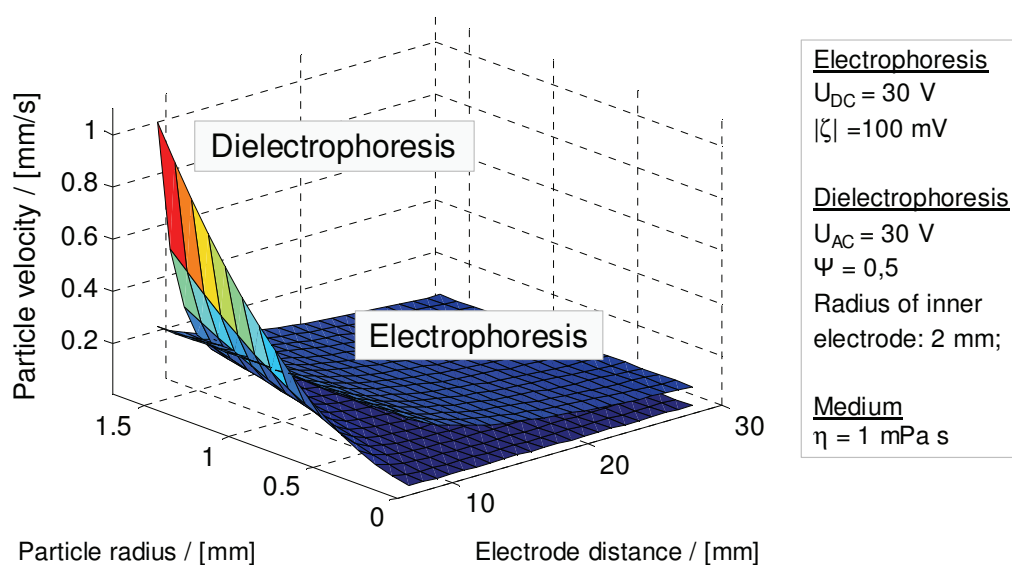


**Figure 7.** Comparison of particle velocity caused by dielectrophoresis and electrophoresis at low voltage according to equations 5 and 6, respectively.

In the experiments, the PE particles in silicone oil moved immediately towards the outer concentric shell, where the electric field strength was weaker (negative DEP), since the polarizability of PE (relative dielectric constant 2.25) is lower than that of silicone oil (relative dielectric constant 2.9). The PE particles movement could be speeded up or slowed down by increasing or decreasing the voltage of power supplier. Once the particles reached the outer concentric shell, they would retain there, even if the magnitude or/and sign of voltage were changed.

In contrast to PE particles, water droplets moved towards the inner electrode (positive DEP). Both observations, the contrary direction of PE and water motion, are congruent with the theoretical prediction shown in Figures 4, 6, and 8.

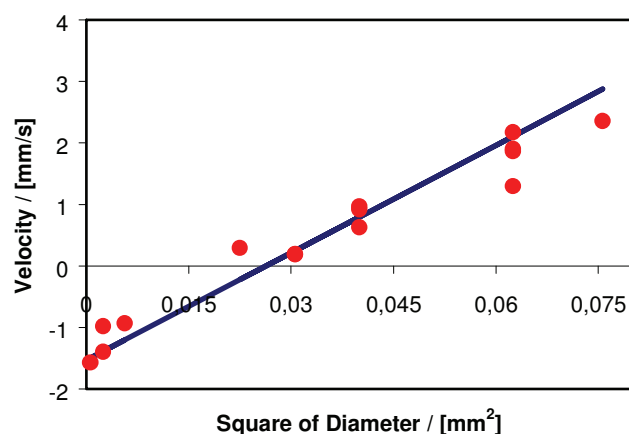


**Figure 8.** Experimental particle velocity vs. square of diameter for water droplets in silicone oil. The solid line represents the simulated velocity taking electrothermal effects into account. This simulation is based on a model we described elsewhere [15].

Even though the phenomena are understood, it is still a long way to end up with an efficient design of a new type of separator that is based on this technique.

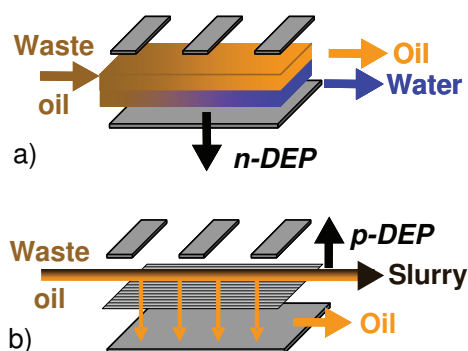


**Figure 9.** Potential Applications in Environmental Technology a) DEP-separator for splitting emulsions, b) DEP-supported filtration of oily slurry

Reference

- 
- [1] Shin, S.H. and Kim, D.S. (2001) Studies on the interfacial characterization of O/W emulsion for the optimization of its treatment. ENVIRONMENTAL SCIENCE & TECHNOLOGY 35 (14): 3040-3047
- [2] El-Shafey, E.I., Correia, P.F.M. and de Carvalho, J.M.R. (2005) An integrated process of olive mill wastewater treatment. SEPARATION SCIENCE AND TECHNOLOGY 40 (14): 2841-2869
- [3] Benito JM, Rios G, Ortea E, Fernandez E, Cambiella A, Pazos C and Coca J (2002) Design and construction of a modular pilot plant for the treatment of oil-containing wastewaters. DESALINATION 147 (1-3): 5-10
- [4] J. Drelich, G. Bryll, J. Kapczyński, J. Hupka, J.D. and Miller, F.J. Hanson (1992) The effect of electric field pulsation frequency on breaking water-in-oil emulsion. FUEL PROCESSING TECHNOLOGY., 31, 105-113.
- [5] Eowa, J.S., Ghadiri, M., Sharif, A.O. and Williams, T.J. (2001) Electrostatic enhancement of coalescence of water droplets in oil: a review of the current understanding. CHEMICAL ENGINEERING JOURNAL. 84 173–192
- [6] Hashmi K.A. and Hamza, H.A. (2005) Integration of the CANMET hydrocyclone in a conventional heavy oil treatment facility. JOURNAL OF CANADIAN PETROLEUM TECHNOLOGY. 44 (7): 12-15
- [7] Mendonca, M.B., Cammarota, M.C., Freire, D.D.C., Ehrlich A. Newman AP, Puehmeier T, Kwok V, Lam M, Coupe SJ, Shuttleworth A, (2004) A new procedure for treatment of oily slurry using geotextile filters. JOURNAL OF HAZARDOUS MATERIALS. 110 (1-3): 113-118
- [8] Phair, B., Bensch, L., Duchowski, J., Khazan, M. and Tsalyuk, V. (2005) Overcoming the electrostatic discharge in hydraulic, lubricating and fuel-filtration applications by incorporating novel synthetic filter media. TRIBOLOGY TRANSACTIONS. 48 (3): 343-351
- [9] Nystroem, G.M., Ottosen L.M. and Villumsen A. (2005) Electrodialytic Removal of Cu, Zn, Pb and Cd from Harbour Sediment: Influences of Changing Experimental Conditions. ENVIRONMENTAL SCIENCE & TECHNOLOGY. 39, 2906-2911.
- [10] Hansen, H.K., Ottosen, L.M., Kliem, B.K. and Villumsen, A. (1997) Electrokinetic Remediation of Soils Polluted with Cu, Cr, Hg, Pb and Zn. JOURNAL OF CHEMICAL TECHNOLOGY & BIOTECHNOLOGY. 70, 67-73.
- [11] Pohl H.A. (1978) Dielectrophoresis. Cambridge University Press.

- 
- [12] Castellanos, A., Ramos, A., González, A., Green, N.G. and Morgan, H. (2003) Electrohydrodynamics and dielectrophoresis in microsystems: scaling laws, JOURNAL OF PHYSICS D: APPLIED PHYSICS. 36, 2584-2597
- [13] Muller, T., Gerardino, A., Schnelle, T., Shirley, SG, Bordoni, F., DeGasperis, G., Leoni, R. and Fuhr, G. (1996) Trapping of micrometer and sub-micrometer particles by high-frequency electric fields and hydrodynamic forces JOURNAL OF PHYSICS D: APPLIED PHYSICS. 29 340-9
- [14] Ramos, A, Morgan, H., Green, N.G. and Castellanos, A. (1998) AC electrokinetics: a review of forces in microelectrode structures JOURNAL OF PHYSICS D: APPLIED PHYSICS. 31 2338-53
- [15] Du, F., Baune, M. and Thöming, J. (2005) Insulator-based dielectrophoresis in viscous media – Simulation of particle and droplet velocity. JOURNAL OF ELECTROSTATICS. (subm.)
- [16] Drelich, J., Bryll, G., Kapczyński, J., Hupka, J., Miller, J.D. and Hanson, F.J. (1992) The effect of electric field pulsation frequency on breaking water-in-oil emulsion, FUEL PROCESSING TECHNOLOGY. 31, 105-113
- [17] Eow, J.S., Ghadiri, M., Sharif, A.O. and Williams, T.J. (2001) Electrostatic enhancement of coalescence of water droplets in oil: a review of the current understanding. CHEMICAL ENGINEERING JOURNAL. 84, 173–192



## 8.2. Curriculum Vitae

- 25.06.1974      Born in Dalian, P.R. China
- 09/1990-07/1993 Dalian No. 1 Senior Middle School, P.R. China
- 09/1993-07/1997 Huazhong University of Science and Technology, Wuhan, P.R. China  
Major: Internal Combustion Engine  
Degree: Bachelor of Engineering
- 10/2001-05/2004 Hochschule Bremerhaven, Germany  
Major: Process Engineering and Energy Technology  
Degree: Master of Science
- 10/2004-present University of Bremen, Bremen, Germany  
Major: Physical Chemistry  
Degree (expected): Ph. D in Science  
Thesis topic: Separation of solid-liquid and liquid-liquid phases using dielectrophoresis
- 10/2006-present Associate member in DFG Graduiertenkolleg PoreNet